Teresa Gonçalves Carreira Maia

Licenciatura em Biologia Celular e Molecular

Comparative immunological analyses of whole-sporozoite malaria vaccines

Dissertação para obtenção do Grau de Mestre em

Genética Molecular e Biomedicina

Orientador: António M. Mendes, Post-Doctoral Fellow, Prudêncio Lab, Instituto de Medicina Molecular João Lobo Antunes

Co-orientador: Miguel Prudêncio, Head of Laboratory, Prudêncio Lab, Instituto de Medicina Molecular João Lobo Antunes

FACULDADE DE CIÊNCIAS E TECNOLOGIA
UNIVERSIDADE NOVA DE LISBOA

Setembro de 2019

Teresa Gonçalves Carreira Maia

Licenciatura em Biologia Celular e Molecular

Comparative immunological analyses of whole-sporozoite malaria vaccines

Dissertação para obtenção do Grau de Mestre em

Genética Molecular e Biomedicina

Orientador: António M. Mendes, Post-Doctoral Fellow, Prudêncio Lab, Instituto de Medicina Molecular João Lobo Antunes

Co-orientador: Miguel Prudêncio, Head of Laboratory, Prudêncio Lab, Instituto de Medicina Molecular João Lobo Antunes

Júri:

Presidente: Prof. Doutora Margarida Casal Ribeiro Castro Caldas Braga
Arguente: Doutora Cristina Fernández Arias
Vogal: Doutor António Manuel Barbeiro Mendes

FACULDADE DE CIÊNCIAS E TECNOLOGIA
UNIVERSIDADE NOVA DE LISBOA

Setembro de 2019

Comparative immunological analyses of whole-sporozoite malaria vaccines

Acknowledgments

Para começar, quero agradecer-te Miguel, por me teres dado a oportunidade e depositado em mim a tua confiança para trabalhar na tua equipa, por me tratares como igual e por estares sempre disposto a ouvir a minha opinião e a responder a todas as minhas questões. Obrigada por me teres mostrado que um verdadeiro líder também lá está nos momentos mais difíceis e extenuantes, a trabalhar ao nosso lado, e por nunca deixares de ter uma palavra amiga para mim.

Ao António, quero agradecer o quanto me fizeste crescer como pessoa e como aluna, por teres sempre exigido de mim rigor e dedicação, o que me permitiu atingir os meus objectivos e chegar ao fim desta etapa. A tua orientação permitiu-me não só ganhar independência, mas também estar segura por saber que estavas a meu lado para qualquer dificuldade que eu enfrentasse. Obrigada por me teres ensinado que há sempre uma história para contar mesmo quando não sabemos o final. Obrigada por um ano entusiasmante, cheio de aprendizagens e aventuras.

Helena, quero agradecer toda a ajuda que me deste, essencial para a conclusão desta tese, não só cientificamente, mas também todas as palavras queridas de motivação. Ensinaste-me muito durante este ano, mostraste-me o quão importante é questionarmos o que fazemos e os resultados obtidos e incentivaste-me sempre a ser melhor. À Patrícia, com quem trabalhei pouco tempo mas intensivamente, quero agradecer toda a paciência que tens em ensinar uma inexperiente aluna de mestrado a ser rigorosa, precisa e corrceta. Estiveste sempre disponível para me ajudar e sempre com um sorriso, mesmo quando o cansaço já pesava. Filipa, muito obrigada pela tua enorme vontade de criar um ambiente divertido e um bom espírito de grupo entre todos nós e por me incluíres sempre em todos os planos. Margarida, obrigada por estares sempre disponível para nos ajudar, fosse a que horas fosse. Fontinha, obrigada por me ajudares quando precisei, sempre com muita calma e paciência. Adriana, trazes uma alegria especial ao laboratório, obrigada por me teres ensinado com tanta paciência, obrigada por todas as palavras divertidas e pela tua boa-disposição contagiante. Raquel, obrigada por me teres sempre recebido bem e por teres organizado uma mega aula de surf! À Isabel e ao Gonçalo desejo um excelente ano, boa sorte para a vossa jornada e tenho a certeza que daqui a um ano estarão também a festejar.

À Andreia, Denise, Diana e Rafael um obrigada gigante por terem estado sempre a meu lado durante este ano. Andreia, obrigada por todos os momentos de "não faço ideia do que estou a fazer" que partilhámos, por nunca me deixares sozinha e por todas as andreiazices que nos animavam o dia. Denise, obrigada por nunca faltar uma palavra simpática do teu lado, por todas as vezes que perguntaste se estava tudo bem ou se precisava de ajuda e por toda a companhia.

Rafael, obrigada por todos os momentos em que nos fizeste rir, por todas as opiniões controversas que tens e que nos fazem a todas discordar de ti e trazem sempre discussões animadas, por toda a tua ajuda ao longo de todas as experiências e todos os teus conselhos de moda. Diana, agradeço-te em último (desculpa Rafael), porque foste sem dúvida a melhor lab partner que poderia ter pedido. Para além de te agradecer pelo óbvio, toda a tua ajuda incansável e por me guiares ao longo de muitas experiências, quero agradecer-te por seres minha amiga e nunca me deixares sem resposta. Quando estava mais atarefada com algo, sempre que saías ouvia um "Qualquer coisa que precises, é só dizeres" e, sempre que precisei e disse, tu respondeste. Obrigada por fazeres com que até time-points até à uma da manhã fossem divertidos e por todas as conversas e ideias que partilhámos. Tenho a certeza que vais fazer um doutoramento espectacular e que todos os que aprenderão contigo terão a maior sorte do mundo.

Um obrigada também aos Figueiredos que sempre me trataram bem e foram uns vizinhos excelentes e um obrigada a todos com quem pude contar no restante iMM que tornaram este ano mais fácil.

Agradeço também a todos os meus amigos que estiveram sempre a meu lado, mas em especial a ti Ana, que me acompanhaste durante todo o meu percurso universitário e mesmo este ano, já sem nos vermos todos os dias (tive muitas saudades), sempre me ajudaste com um sorriso.

A ti, Luís, um obrigada gigante por me aturares sempre que estava estafada e sem paciência para nada, por fazeres tua missão colocar um sorriso na minha cara, por acreditares sempre que eu consigo tudo e por seres o meu apoio constante. Obrigada por tornares a minha vida mais feliz todos os dias.

Para os meus pais, Catarina, Leonor e Inês um grande obrigado por me terem levado até onde estou hoje e por me apoiarem sempre. Obrigada em especial a ti, pai, por todas a boleias a horas menos próprias e por todas as vezes que me perguntaste se precisava de ajuda, e a ti, mãe, por todas as comidinhas boas que deixavas feitas à filha e por todo o carinho. Obrigada por acreditarem sempre e por todo o amor que me dão.

A todos os que de algum modo me ajudaram a chegar aqui, um grande obrigada.

Abstract

Malaria, a mosquito-borne infectious disease, affects hundreds of millions of people yearly. Although an effective malaria vaccine has not yet been found, whole-sporozoite vaccines are the most promising approaches available.

In this work, several types of whole-sporozoite vaccines were studied: radiation attenuated sporozoites (RAS), genetically attenuated parasites (GAP) and immunization with sporozoites under chemoprophylaxis (CPS). This thesis aims to broaden the current knowledge about immune responses elicited by whole-sporozoite vaccines *via* quantitative real time-PCR and flow-cytometry and compare their efficacy against a sporozoite challenge.

The parasites studied have different liver stage developments, inducing distinct immune responses. In the CPS approach, parasites are only eliminated in the blood, inducing a strong two-wave type I IFN response, as occurs upon infection with *P. berghei* parasites. *PbΔmei2Δlisp2,* a late-arresting GAP induces a weaker type I IFN response, also in two waves. Early-arresting parasites, the GAP *PbΔb9Δslarp* and RAS, lead to one wave of induction and to the absence of a type I IFN response, respectively.

The protection conferred by each parasite studied correlates with its liver stage development: the longer the development, the more effective an immunization is, as long as the parasite is not released to the blood - this seems to negatively affect the immunization efficacy. Also, type I IFN response seems to have a dual effect in whole-sporozoite vaccines, being essential for protection conferred by *PbΔb9Δslarp* and RAS but deleterious for the protection conferred by CPS.

Frequency analysis of mouse liver leucocytes upon immunization revealed, most interestingly, different NKT dynamics depending on the vaccination approach. Further experiments should be performed to elucidate their role in the establishment of protection.

This exploratory work represents a contribution for the understanding of mechanisms by which whole-sporozoite immunizations act, allowing for the rising of questions and providing valuable insight to pursue in future studies.

Keywords: Malaria, *Plasmodium*, Whole-sporozoite vaccines, Genetically attenuated parasites (GAP), Radiation Attenuated Sporozoites (RAS), Chemoprophylaxis and sporozoites (CPS)

Resumo

A malária, doença infecciosa transmitida por mosquitos, afecta centenas de milhões de pessoas anualmente. Embora ainda não haja uma vacina eficaz contra a malária, as de organismo-inteiro são a abordagem mais promissora.

Nesta dissertação, foram estudados vários tipos destas vacinas: parasitas atenuados por radiação (RAS), parasitas geneticamente modificados (GAP) e imunização com parasitas e quimioprofilaxia (CPS). Pretende-se, nesta tese, alargar o conhecimento sobre as respostas imunes despoletadas por estas vacinas através de PCR quantitativo em tempo real e citometria de fluxo, e comparar a sua eficácia.

Os parasitas estudados apresentam diferentes desenvolvimentos no fígado, induzindo respostas imunitárias díspares. Na imunização com CPS, os parasitas só são eliminados após a saída para o sangue, induzindo uma forte resposta de IFN tipo I com dois picos, semelhante ao que acontece após a infecção por *P. berghei. PbΔmei2Δlisp2*, um GAP que termina o seu desenvolvimento tardiamente no fígado, induz uma resposta de IFN tipo I mais fraca, apresentando também dois picos de indução. Parasitas que terminam o seu desenvolvimento mais cedo, como o GAP *PbΔb9Δslarp* ou parasitas irradiados, conduzem apenas a um pico de indução e à ausência de uma resposta de IFN tipo I, respectivamente.

A protecção conferida por estes parasitas está relacionada com o seu desenvolvimento no fígado: a maior extensão corresponde imunização mais eficaz, desde que o parasita não seja libertado para o sangue - tal aparenta ser negativo para a eficácia da imunização. A resposta de IFN tipo I parece ter um efeito duplo nas vacinas de organismo inteiro, sendo essencial para a protecção conferida por *PbΔb9Δslarp*, mas prejudicial para a protecção conferida por CPS.

A análise da frequência de leucócitos no fígado de ratinhos imunizados revelou diferentes dinâmicas de frequência de NKT dependendo da vacina usada. É de elucidar melhor, noutras experiências, o papel desta família celular na protecção conferida por vacinas de organismo inteiro.

Este trabalho, de cariz exploratório, representa uma contribuição para a compreensão dos mecanismos imunes através dos quais as vacinas de organismo inteiro actuam, levando ao surgimento de novas questões e novos caminhos a explorar.

Palavras-chave: Malaria, *Plasmodium*, Vacinas de organismo inteiro, Parasitas geneticamente atenuados (GAP), Parasitas atenuados por radiação (RAS), Esporozoítos e quimioprofilaxia (CPS)

Index of Contents

Index of figures

Index of tables

Abbreviations

ACK	ammonium-chloride-potassium
ACT	artemisinin based combination therapies
cDNA	complementary DNA
CPS	chemoprophylaxis and sporozoites
CSP	circum-sporozoite protein
ct	cycle threshold
DC	dendritic cell
EA	early-arresting
EEF	exo-erythrocytic form
FBS	foetal bovine serum
GAP	genetically attenuated parasites
hpi	hours post immunization/infection
hprt	hypoxanthine guanine phosphoribosyl transferase
HSPGs	heparan sulphate proteoglycans
IFN	interferon
IFNAR	IFN-α receptor
IFNLR	IFN-λ receptor
IFNGR	IFN-γ receptor
IRF3	IFN regulatory factor 3
IRF7	IFN regulatory factor 7
IRS	indoor residual spraying
ISG	IFN-stimulated genes
ITN	insecticide treated net
JAK	Janus kinase
LA	late-arresting
LISP2	liver-specific protein 2
MAVS	mitochondrial antiviral signalling protein
MDA5	melanoma differentiation-associated gene
MEI2	meiosis inhibited 2 - like RNA binding protein
Myd88	myeloid differentiation primary response 88
NKT	natural killer T cells
PCR	polymerase chain reaction

pDC	plasmacytoid dendritic cell
RAS	radiation attenuated sporozoites
RBC	red blood cell
RDTs	rapid diagnostic tests
RPMI 1640	Roswell Park Memorial Institute 1640 medium
SLARP	Sporozoite and Liver stage Asparagine-Rich Protein
STAT	signal transducer and activator of transcription
SPZ	sporozoite
TCR	T cell receptor
TLR	Toll-like receptor
WHO	World Health Organization
WT	wild-type

1. Introduction

1.1. Malaria: essential facts

Malaria, a mosquito-borne infectious disease, affected an estimated 219 million people worldwide in 2017 (95% confidence interval, 203–262 million), resulting in 435 000 deaths, 61% of which of children aged less than five years old. Although this disease is endemic in 80 countries, 93% of malaria-related deaths in 2017 occurred in the Sub-Saharan African region. Unfortunately, after over 20 years of continuous reduction in global malaria incidence, progress has stalled since 2015, and renewed efforts are necessary to continue tackling this disease[1].

Malaria imposes a high economic burden on affected populations, especially due to high productivity losses, lower capacity to work and a higher number of absent days from work in infected individuals. These factors result in a significant loss of income for the household, and therefore malaria and poverty are always closely correlated, strongly contributing to the delay in socio-economic development in observed malaria-endemic countries[2,3].

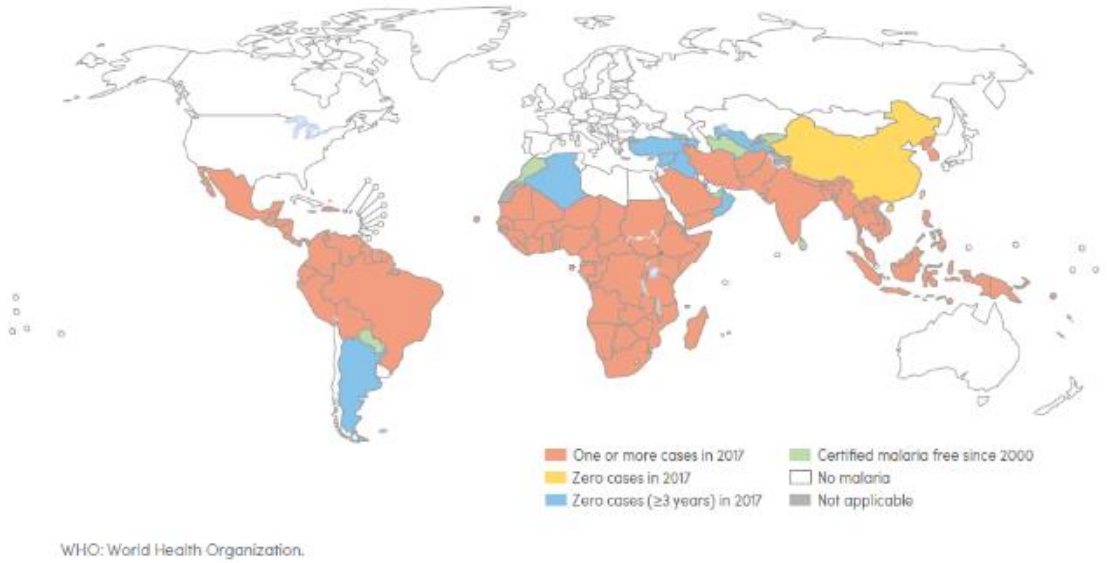

Figure 1.1 Incidence of malaria in 2017. World map representing with different colours the countries that had cases of malaria in 2000 and their status by 2017. Countries in orange had at least one case of malaria in 2017, countries in yellow did not have any malaria cases in 2017 and countries with zero cases in the past three consecutive years are considered to be malaria free (represented in blue, green and white). Adapted from: World Malaria Report 2018[1].

1.2. *Plasmodium* life cycle

Apicomplexan *Plasmodium* parasites are the infectious agents of malaria, *Plasmodium falciparum, P. vivax, P. ovale, P. malariae and P. knowlesi* being the five *Plasmodium* species that infect humans. *P. berghei* and *P. yoelii*, are the most commonly rodent-infective parasites employed for *in vivo* and *in vitro* laboratory studies[4].

Plasmodium parasites have a complex life cycle, alternating between female *Anopheles* mosquitoes and vertebrate hosts. Infection begins when *Plasmodium* parasites are transmitted to their host through the bite of an infected female *Anopheles* mosquito. Inside the mammalian host, the parasite's life cycle is composed by three different stages: an obligatory and asymptomatic pre-erythrocytic stage which occurs in the liver (Figure 1.2.(A)); an asexual symptomatic blood-stage and a sexual stage that allows the formation of male and female gametocytes (Figure 1.2 (B)) which can then be taken up by mosquitoes upon a blood meal[5].

When an infected mosquito takes a blood meal, an average of 15 to 123 sporozoites, the liver-infective form of the parasite, are injected into to the host's skin. Then, the sporozoites move through the dermis, employing gliding motility, until they encounter a blood vessel. About 30% of the sporozoites never reach blood vessels, being trapped and then degraded inside lymph nodes[6]. Once in the circulatory system, sporozoites travel to the liver as they can efficiently target this organ by interacting with heparan sulphate proteoglycans (HSPGs), the major receptors of *Plasmodium* sporozoites, which are not exclusively present in the liver but display a superior degree of sulphation in this organ. The circumsporozoite protein (CSP) is the most abundant protein in *Plasmodium* sporozoite surface and appears to have a central role in interacting with the liver HSPGs, resulting in the arrest of the parasites at the liver sinusoids (small and fenestrated blood vessels located in the periphery of the liver)[7].

In the liver, sporozoites invade hepatocytes after crossing the cells that line liver sinusoids: endothelial and Kupffer cells (macrophage or monocytic liver cells). It has been suggested that sporozoites can use more than one cellular pathway to traverse these cells, such as the formation of a parasitophorous vacuole or disruption of plasma membranes[8].

The sporozoites' journey through the liver does not stop upon the encounter with a hepatocyte. These parasites migrate through several hepatocytes, employing gliding motility, until they reach a final hepatocyte that they productively invade with the formation of a parasitophorous vacuole, where they reside until the end of the liver stage of development. During this process, the sporozoites differentiate into exo-erythrocytic forms (EEF), which then undergo a phase of asexual reproduction, schizogony (nuclear division in the absence of cell division), leading to intense DNA replication and parasite growth. Thousands of merozoites are then formed, filling merosomes (merozoite-filled vesicles). *P. vivax* and *P. ovale* can also form dormant liver stages

(hypnozoites) which persist in the liver for long periods of time, responsible for relapses if left untreated. The liver stage of development ends with the budding of merosomes from the hepatocyte plasma membrane to the liver sinusoids, resulting in the release of up to 40 000 parasites per hepatocyte[5,8]. Since merosome membranes are derived from the host cell plasma membrane, they are not recognized by Kupffer or dendritic cells (DCs), safely escaping to the bloodstream. Depending on the *Plasmodium* species, the duration of the liver stage of development varies. For human-infective *Plasmodium* parasites it can last between six days in *P. falciparum* to sixteen days in *P. malariae*[9]. For the rodent-infective *P. berghei,* it lasts about 52 hours[10]. The liver stage is an obligatory and immunogenic but asymptomatic stage of infection, which qualifies it as an ideal target for vaccination[11].

Following their release into the bloodstream, merozoites invade erythrocytes (red blood cells – RBCs), where successive cycles of invasion, intracellular growth, proliferation and re-invasion occur. Invasion starts with a first attachment and reorientation so that the apical end of the merozoite faces the RBC, allowing a tight attachment and a tight junction formation. The parasite then creates a parasitophorous vacuole to invade the RBC[12]. Inside erythrocytes, merozoites go through different stages with distinct morphologies. First, the ring stage, acquiring a biconcave disc form, followed by rounding up to a trophozoite form, and then the schizont stage where nuclear division occurs, with the formation of about 16-32 merozoites. Newly formed merozoites egress in a coordinated way, resulting in the destruction of the RBCs membrane and explosive release of parasites to the blood. New rounds of invasion and schizogony follow, but some of the asexually reproducing parasites are reprogrammed and commit to sexual development, forming male (microgametocytes) and female gametocytes (macrogametocytes) which can be taken up by mosquitoes on a blood meal. Malaria-associated symptoms and pathogenesis appear during the blood stage of infection[5].

Plasmodium life cycle continues as a female *Anopheles* mosquito ingests male and female gametocytes upon a blood meal from an infected host (Figure 1.2.(C)). Due to environmental and mosquito-specific factors, gametocytes develop into gametes. Fusion of female and male gametes in the mosquito midgut originates a zygote, which will then form an ookinete through meiosis and genetic recombination. Ookinetes travel to the mosquito's epithelium and develop into oocysts. Asexual sporogonic replication occurs, oocysts burst and thousands of sporozoites are released. Sporozoites actively travel to mosquito's salivary glands and are ready to be injected into a new host when the mosquito takes a blood meal, completing the parasite's life cycle[13].

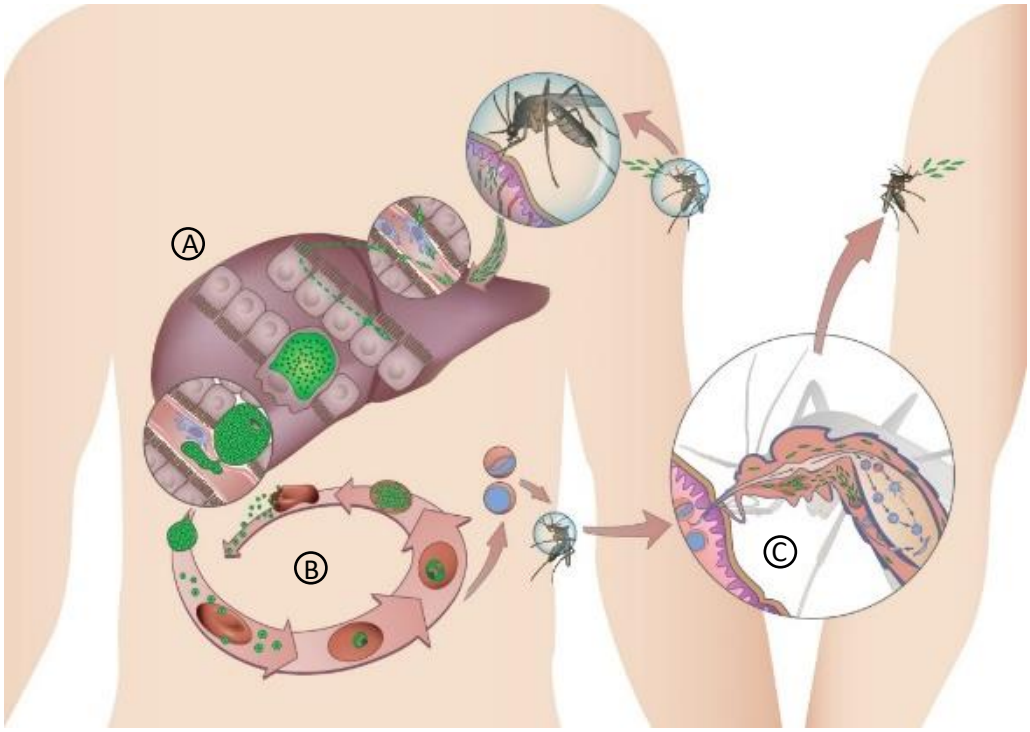

Figure 1.2 *Plasmodium* spp. life cycle. The bite of an infected female *Anopheles* mosquito injects sporozoites into the skin of the human host. Sporozoites travel to the blood stream and eventually reach the liver, where the liver-stage of development starts (A). In the liver, sporozoite transverse several liver cells until establishing the infection in one final hepatocyte. A period of differentiation and intense asexual reproduction occurs, ending with the release of thousands of merozoites to the blood stream, initiating the blood stage of infection (B). In the blood, merozoites continuously invade RBCs, undergoing intracellular growth and proliferation and causing the disease. Some merozoites differentiate into gametocytes that can be ingested by a mosquito upon a blood meal, leading to the mosquito stage of development (C). Gametocytes undergo sexual reproduction and differentiation processes inside the mosquito that culminate in the formation of liver-infective sporozoites, completing *Plasmodium* spp. life's cycle.

1.3. Diagnosis, pathogenesis and treatment

Diagnosis of malaria by light microscopy of stained thin and thick blood smears has been the gold standard for over a century. Thick smears present higher sensitivity than thin smears but the latter allow the identification of *Plasmodium* species, the diagnosis of mixed infections, and quantification of parasitaemia[14]. Although these methods are rapid and relatively sensitive, the lack of experienced personnel to analyse data may lead to an overdiagnosis of malaria. Rapid diagnostic tests (RDTs) are an alternative to blood smears and consist in detecting specific parasite proteins in the blood. These tests rely on immunochromatographic kits composed by strips of nitro-cellulose with bands of bound antibody for the antigen to detect. RDTs are easy to perform and do not require equipment, such as microscopes, electricity or trained professionals[15]. Other methods to diagnose malaria include the staining of parasite DNA with fluorescent dyes followed by its detection using flow cytometry or fluorescence microscopy and amplification of *Plasmodium's* DNA by polymerase chain reaction (PCR). These methods may offer better sensitivity and accuracy but have a higher cost and need to be performed in a laboratory, making them currently inappropriate for point-of-care settings[15,16].

Malaria symptoms appear during the blood stage of *Plasmodium* infection, as a consequence of the repeated invasion and destruction of RBCs. Most malaria cases are uncomplicated. In naive individuals, malaria infection almost always results in febrile illness, with flu-like symptoms that include headaches, nausea, muscle pains and rigors[5].

Severe malaria symptoms may include severe malarial anaemia (SMA) (particularly common in the first 2 years of life in high transmission areas), acute respiratory distress, acidosis, hypoglycaemia and severe jaundice. Cerebral malaria, which results in seizures and might lead to coma, and placental malaria, that leads to low birthweight and increased infant mortality, are associated with *P. falciparum* infections[5,17].

The first line of treatment from 1940 to 1980 was chloroquine, a drug that interferes with the parasite's free haem detoxification mechanism. Artemisinin was also a drug developed in the 20th century and acts against the ring and late trophozoite stages, leading to oxidative damage and alkylation inside the parasite[18]. Due to *P. falciparum* resistance mechanisms, the need to combine and develop new drugs has increased[5]. Artemisinin-based combination therapies (ACTs), a combination of artemisinin derivatives with drugs that possess a longer half-life, are indicated as therapy for uncomplicated malaria by the WHO. Since *P. vivax* and *P. ovale* form dormant liver stages (hypnozoites) responsible for relapses, these infections should also be treated with primaquine, a drug that acts against pre-erythrocytic stages of the parasite[1,18,19].

1.4. Malaria prevention

To prevent malaria, the WHO recommends vector control to avoid mosquito bites and chemoprevention by providing drugs that inhibit infection. Vector control measures consist mainly in insecticide-treated mosquito nets (ITNs) and in indoor residual spraying (IRS) with insecticides[1].

ITNs are placed over beds and offer not only a physical barrier between the human and the mosquitoes but also a lethal effect due to the insecticide impregnated in the ITNs. IRS consist on the application of insecticides to indoor walls and surfaces that may serve as resting places for mosquitoes. These measures alone cannot eliminate malaria, but vector control remains the most effective measure to prevent transmission[20]. In recent years, the number of malaria vector populations resistant to all classes of insecticides used in ITNs and IRS has increased, following the enhanced implementation of such vector control measures. These resistance mechanisms compromise the performance of ITNs and IRS[21].

The need for a highly efficacious and long-lasting malaria vaccine to control and eliminate the disease has become evident with the increasing drug and insecticide resistance[11,22,23].

1.5. Malaria vaccines

Malaria vaccination strategies are grouped depending on the parasite life stage they target: pre-erythrocytic vaccines aim to block sporozoites and/or work against infected hepatocytes preventing initial infection, illness and transmission; blood stage vaccines target merozoites or infected RBCs preventing replication, illness and reducing malaria transmission; transmission-blocking vaccines target gametocytes and ookinetes preventing mosquito infection[22].

Pre-erythrocytic vaccines have been the main focus of malaria vaccine investigation. Liver infection being asymptomatic and obligatory, illness is avoided if parasites are blocked at this stage. Another advantage of pre-erythrocytic vaccines is that the number of sporozoites in the skin and liver is much lower when compared to the number of parasites in the blood stage. Hence, pre-erythrocytic vaccines are the most attractive strategy to vaccinate against malaria[8,11].

1.5.1. Pre-erythrocytic vaccines

There are two main approaches to pre-erythrocytic vaccines against malaria: subunit vaccines and whole-sporozoite vaccines[11].

Subunit vaccines are usually built as peptides, multi-peptide constructs or recombinant proteins. Typically, the formulation of these vaccines contains adjuvants and can be based on one parasitic antigen or in a combination of different antigens. The most common target of subunit vaccines is the CSP[11]. RTS,S AS01 is a recombinant protein malaria vaccine in which part of the C-terminal end of *P. falciparum* CSP sequence is co-expressed and fused within a hepatitis B surface antigen and adjuvanted with AS01, an oil-in-water emulsion with liposomes, monophosphoryl lipid A and QS21[24]. RTS,S AS01 is the most advanced subunit malaria vaccine candidate so far, with an estimated efficacy of 36% against severe malaria for 48 months (end of the study), determined in a phase 3 clinical trial with children aged between 5 and 17 months who received 3 doses of the vaccine and an additional boost at 18 months of age and encompassing individuals from 11 different sites in Africa[24]. Although subunit vaccines have several advantages, such as being easy to produce and to administer, the lack of superior efficacy demonstrated in studies such as that mentioned above, reinforce the need for the development of a long lasting and more effective vaccine[23].

Whole-sporozoite vaccines are the gold standard for malaria immunization and consist in the administration of live *Plasmodium* sporozoites[25]. This type of vaccines have been considered the most successful approach as they contain all parasitic antigens and elicit strong immune responses[11]. This dissertation will focus on whole-sporozoite vaccines and immunological responses elicited by this type of vaccination approach.

1.5.1.1. Whole-sporozoite vaccines

As mentioned above, whole-sporozoite vaccines consist in the administration of live sporozoites to elicit an immune response that prevents parasite's progression to the blood stages of infection. Whole-sporozoite immunization can be achieved using several strategies, such as radiation-attenuated sporozoites (RAS), genetically attenuated parasites (GAP), sporozoite administration under chemoprophylaxis (CPS) and *P. berghei* sporozoite-based vaccines that express human *Plasmodium* antigens, a novel vaccination approach developed by IMM's PrudêncioLab[25,26].

The use of RAS as an immunization strategy was first demonstrated in the 1960s, when mice immunized with live sporozoites that were subjected to X-irradiation showed protective immunity against a subsequent sporozoite challenge[27]. This was later demonstrated in humans, where immunization with irradiated sporozoites delivered *via* infected mosquito bites protected 92% of the volunteers from later challenge[28,29]. Despite logistical problems such as the need to deliver the vaccine through more than 1000 mosquito bites to achieve this result, these findings established that it is possible to develop a highly efficacious malaria vaccine using a whole-sporozoite immunization approach[28,29]. When irradiated, sporozoites can enter liver cells and undergo partial development that stops before achieving a mature late stage schizont, preventing nuclear division, due to DNA damages induced by radiation[30]. It is essential that an accurate dose of radiation is applied to the sporozoites, as a higher dose can kill the parasites preventing them from infecting liver cells, whereas a lower dose might not result in a proper attenuation[30].

More recently, PfSPZ, a human vaccine based on purified, irradiated and cryopreserved *P. falciparum* sporozoites has been developed. This vaccine is delivered by direct intravenous inoculation with needle and syringe, and shown to be well tolerated and to provide homologous and heterologous protection[31]. In recent human trials, this vaccine achieved sterile protection rates up to 100% after homologous challenge and up to 83% of protection after heterologous challenge[32,33]. Although presenting very promising positive results, PfSPZ still faces some problems such as the challenge to scale-up its production (being the vaccine based in live sporozoites which need to be collected through the dissection of *Anopheles* mosquitoes) and the need to cryopreserve and transport the vaccine in liquid nitrogen[23].

GAPs are parasites in which one or more genes essential for liver development are knocked-out to arrest parasite development before entering the blood stage, not affecting its viability, mosquito infectivity or sporozoite production[34]. Firstly, a single knock-out GAP was generated by deletion of *UIS3* (upregulated in sporozoites gene 3), resulting in malaria parasites totally attenuated at the liver stage[35]. After immunizing mice with *uis3(-)* sporozoites and challenging them with infective sporozoites, sterile protection was observed. This proved that it is possible to create a genetically modified malaria vaccine[35]. As GAPs are generated by targeted gene deletion, depending on the genes deleted, the resulting GAP may either arrest its development at earlier or later stages of liver development, constituting an early-arresting (EA) or

a late-arresting (LA) GAP, respectively[34]. A triple knock-out parasite, PfGAP3KO, lacking the genes *p52, p36* and *sap1*, was administered to humans *via* mosquito bites and shown to be safe[36]. Efficacy using this vaccination strategy remains to be demonstrated in humans[11].

Another vaccination strategy is CPS, in which wild-type sporozoites are used for vaccination alongside the administration of a drug that eliminates blood stage parasites, preventing the disease. This results in complete sporozoite development, with full progression of the liver stage until the release of merozoites to the blood[11]. Using chloroquine as the selected antimalarial drug, this strategy has been demonstrated to lead to complete protection in healthy human volunteers upon sporozoite challenge[37]. However, several challenges are posed when using this approach, such large scale sporozoite production and the correct administration of the selected anti-malarial drug to arrest parasite development in the blood[11].

Finally, *P. berghei* sporozoite-based vaccines were developed by the Prudêncio Lab and consist in genetically modified rodent *Plasmodium* parasites that express and present antigens of human-infective *Plasmodium* parasites[25]. *P. berghei* parasites can infect and develop in human hepatocytes while being unable to cause a blood stage infection in humans[38]. These parasites are a naturally attenuated vaccine platform that can elicit cross-species immune responses and, when genetically engineered to express antigens of human-infective parasites, antigen-targeted responses. *Pb*Vac is a *P. berghei* parasite that expresses *P. falciparum* CSP under the control of the *P. berghei* UIS4 (upregulated in sporozoites 4) promoter[38], which has been shown to induce a strong immune response in humans capable of significantly reducing the liver infection load of *P. falciparum* sporozoites, but not inducing sterile protection[38].

1.6. Malaria-related immunity

Naive humans almost always develop a febrile illness with symptoms, as previously described, when infected with *Plasmodium* parasites. A proportion of malaria cases may become severe and eventually lead to death. However, with recurring exposure to the parasite, older children and adults are capable of developing partial protection against severe malaria and death[39]. Nevertheless, sterile immunity is probably never achieved. *Plasmodium* parasites' life cycle is complex, being composed of various stages during which the parasite presents several antigens. Immunity mechanisms can be triggered against any of the parasite life stages inside the human host[39]. Understanding which immune mechanisms can be correlated with protection is essential for the development of a successful vaccine.

1.6.1. Immunity to liver stage *Plasmodium* parasites

With the liver stage of infection being clinically silent, it was thought that the infection and replication of *Plasmodium* parasites inside hepatocytes was undetected by the immune system. However, generalized hepatic inflammation and formation of granulomas rich in neutrophils, eosinophils and macrophages following live sporozoite injection in naive mice was already observed in 1992[40]. Innate immune responses elicited by *Plasmodium* blood stage parasites were known to exist and to be mostly mediated by IFN-γ, tumour necrosis factor α (TNFα) and interleukin-12 (IL-12) but innate immune responses elicited by liver stage parasites remained undefined until recently. Studying and understanding such mechanisms is of extreme importance to create an effective vaccine that can enhance the immune response and inhibit the establishment of the disease[41].

1.6.1.1. Interferon-mediated immunity

IFNs were the first cytokines to be discovered, in 1957, and consist of polypeptides that are secreted by cells in response to a variety of stimuli[42–44]. There are four types of IFNs, type I IFN, type II IFN, type III IFN and IFN-like cytokines.

Type I IFNs are composed of seven different classes: IFN-α, IFN-β, IFN-ε, IFN-κ, IFN-ω, IFN-δ and IFN-τ (the latter two are not found in humans), IFN-α and IFN-β being the most well-defined type I IFNs. Type I IFNs have three major functions: 1) induce cell-intrinsic antimicrobial mechanisms in infected and adjacent cells; 2) modulate innate immune responses to promote antigen presentation, natural killer cells functions and restrain pro-inflammatory pathways; and 3) enhance the development of antigen specific B and T cells and immunological memory, thus activating/modulating the adaptive immune system[43,44]. Haematopoietic cells, especially plasmacytoid dendritic cells are the major producers of IFN-α, whereas IFN-β can be produced by most cell types[44]. IFN-α and IFN-β bind IFN-α receptor (IFNAR), which is a heterodimeric transmembrane receptor constituted by two subunits, IFNAR1 and IFNAR2. Engagement of IFNAR leads to the activation of the Janus kinase (JAK)-signal transducer and activator of transcription (STAT) pathway (JAK-STAT pathway), and consequently to the transcription of IFN-stimulated genes (ISGs)[44]. ISGs' products have several functions at resisting and controlling pathogens, being best known for mediating functional antiviral responses[45].

Type II IFN is solely composed of IFN-γ and signals through the IFN-γ receptor complex (IFNGR). Although, IFN-γ is mainly produced by leukocytes, especially T cells and natural killer cells (NK), almost all types of cells express IFNGR and are therefore able to respond to IFN-γ. IFN-γ signalling is essential for the establishment of cellular immunity, for defence against intracellular pathogens and to regulate the cross-talk between innate and adaptative responses. IFN-γ signalling gene products are capable of priming type I IFN response and vice-versa[43,45].

Type III IFN is the most recently discovered type of IFN and includes IFN-λ. IFN-λ signals through IFN-λ receptor (IFNLR) and induces a response similar to that of type IFN I signalling, inducing several of the same ISGs[45].

The hypothesis that IFNs could control *Plasmodium* liver stage infection was confirmed in 1970, when mice infected with *P. berghei* sporozoites became protected after the administration of exogenous mice serum IFN[46]. More recently, in 2014, a study conducted by Liehl *et al* presented the results of a transcriptomic analysis that compared liver transcriptomes of mice injected with *P. berghei* sporozoites versus mice injected with non-infected *Anopheles* salivary glands. Differences in 1088 transcripts were found, 89 of them being at least two-fold induced. All these 89 transcripts were interferon-stimulated genes (ISGs) linked to the type I interferon (IFN) signalling pathway, indicating that a type I IFN response was triggered in the liver of mice after the infection with *P. berghei* sporozoites. Liehl *et al* also showed that this response is neither restricted to a *Plasmodium* species nor to a mouse host strain. The results of a time-course analysis suggested that hepatocytes are the main source of ISGs expression, already evident at 36 hours post infection (hpi) and reaching a peak at 42 hpi[47]. In the same year, Miller *et al* published the results of a similar analysis using livers of mice infected with *P. yoleii* sporozoites, also revealing the induction of an innate immune response mediated by type I IFN and IFN-γ[48].

Type I IFN responses are well known for their efficacy against viral and bacterial infections, but little was known about its effect against parasitic infections. These two studies helped to uncover some characteristics of the innate immune response to pre-erythrocytic infection with *Plasmodium* parasites, such as which pattern recognition receptors (PRRs) initiate the type I IFN response; which pathogen-associated molecular pattern (PAMP) is recognized by the host PRRs; how does innate immune response impact infection; and which cells act as mediators of this response. They revealed that *Plasmodium* infections in the absence of type I IFN[47] or in the absence of IFN-γ[48] response resulted in higher numbers of liver-stage parasites and that type I IFN response generated in infected hepatocytes can be initiated by several PRRs that recognize PAMPs, such as Toll-like receptors (TLRs) and cytosolic RNA and DNA sensors. After testing the involvement of several PRRs in the immune response to *P. berghei* sporozoite infection, Liehl *et al* suggested that the recognition of *Plasmodium* RNA as a PAMP by a cytoplasmic PRR named melanoma differentiation-associated gene 5 (MDA5) induced a type I IFN response through the mitochondrial antiviral signalling protein (MAVS) and transcription factors interferon-regulatory factor 3 and 7 (IRF3;IRF7) leading to the induction of type I IFN and then, ISGs expression[47]. Furthermore, the study found that hepatocytes alone are not capable of eliminating parasites. Instead, the propagation of type I IFN response generated in these cells recruits and induces a type I IFN response in leukocytes that then eliminate liver-stage parasites (Figure 1.3)[47]. Miller *et al* proposed that an IFN-γ response was the one accountable for reducing liver stage infection instead. Infected hepatocytes would detect sporozoites, possibly sensing its RNA, trigger a type I IFN response that would recruit IFN-γ secreting lymphocytes, in particular

CD8+ T cells, natural killer (NK) and natural killer T cells (NKT; cells that possess a T cell receptor (TCR) and NK receptors), that would control the liver infection, possibly *via* IFN-γ production[48].

IFN-γ can be responsible for mediating the reduction in parasite liver load through several mechanisms such as enhancing the parasite killing potential of CD8+ T cells, increasing the phagocytic capacities of immune cells and inducing antibody production[48].

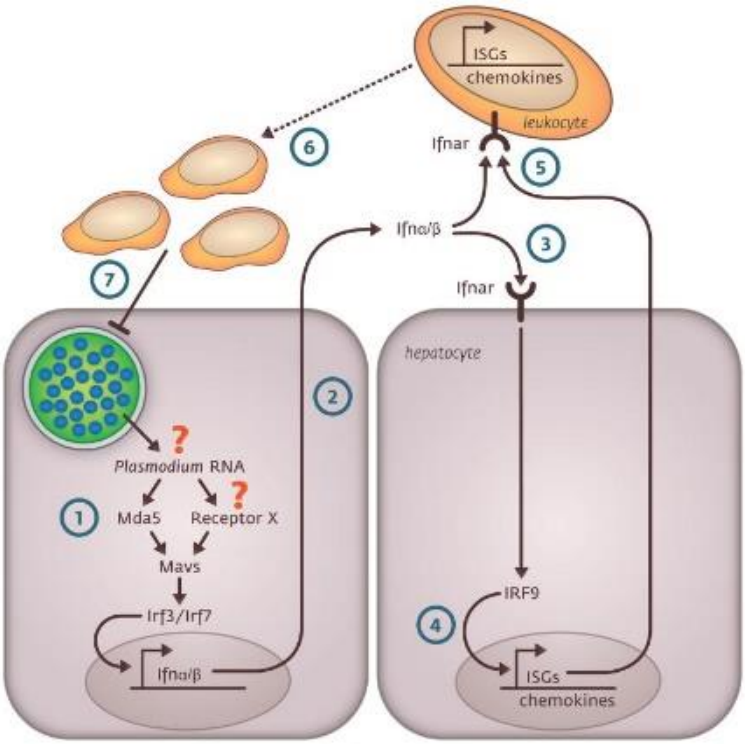

Figure 1.3 Representation of the events leading to a type I IFN response upon the infection with *Plasmodium* parasites. When *Plasmodium* parasites are inside hepatocytes, their RNA is recognized by the cytoplasmic receptor Mda5 or other unknown receptors leading to a type I IFN response *via* Mavs and the transcription factors Irf3 and Irf7 (1). Type I IFNs are released to the outside of the cell (2) and can bind to the Ifnar receptor in hepatocytes propagating the signal in an autocrine and paracrine way (3). The induced type I IFN response leads to the transcription of several ISGs inside the hepatocytes and to the propagation of the response throughout the liver (4). IFNs can also engage to Ifnar receptors in leukocytes, activating (5) and recruiting them (6) to the site of infection to eliminate parasites and infected cells (7). From "Host-cell sensors for Plasmodium activate innate immunity against liver-stage infection." by P. Liehl et al., 2014, Nature Medicine, 20, 47-53.

The innate immune response is not able to prevent disease, since not all parasites in the liver are eliminated upon the induction of the mechanisms described above. However, Liehl *et al* and Miller *et al,* also investigated the effect of the innate immune response upon a reinfection and found that, upon an ongoing malaria infection, the liver stage-induced type I IFN and IFN-γ responses constitute a host defence mechanism, inhibiting malaria reinfections[48,49]. There is a decrease in liver parasite load but also a delay in parasitaemia. This phenomenon contributes to the pre-erythrocytic resistance observed in humans of regions of malaria hyperendemicity[48,49].

Overall, the characterization of IFN mediated immune responses will be crucial for the development and enhancement of pre-erythrocytic malaria vaccines.

1.6.1.2. Innate cellular immunity

Following the activation of a type I IFN response by hepatocytes, these cells produce chemokines that recruit macrophages, neutrophils, lymphocytes, NK and NKT cells to the liver, leading to the killing of liver stage parasites by NKT cells[47,49]. NK cells can also inhibit the development of liver stage parasites and are important for priming $CD4^+$ T cells, linking innate and adaptive immunity[11].

γδ T cells induced by vaccination with RAS demonstrated to be essential for protection - in a mouse model with no γδ T cells, protective $CD8^+$ T cell responses were impaired resulting in absence of protection[50]. These cells, like NKT cells, play an essential role in priming $CD8^+$ and $CD4^+$ T cells, bridging between innate and adaptive cellular immune responses. They can recognize malarial antigens and proliferate in response to infection and impact cytokine production, being a potential correlate of protection[11].

CD8α DCs are important for the uptake of sporozoites that migrate to lymph nodes (after being injected into the skin of the host), conferring protection upon a RAS immunization and splenic CD8α DCs are involved in the priming of parasite-specific T cells[11].

1.6.1.3. Adaptive immunity

Adaptive immunity is what leads to efficacious and long-lasting immunity. Protective immunity in malaria is mainly due to the action of $CD8^+$ T cells that target parasites in the liver[51].

$CD8^+$ T cells are known to be crucial in the establishment of sterile immunity upon RAS vaccination in mice, as its depletion results in lack of protection[52]. Studies showed that $CD8^+$ T cells are responsible for the release of perforin and granzyme leading to the death of infected hepatocytes and parasite elimination, but most importantly that these cells mediate protection through IFN-γ production. Nonetheless, the presence of higher amounts of $CD8^+$ T cells not always correlates with protection and depending on the vaccination regimens employed and on the methods used to quantify the presence of $CD8^+$ T cells, results vary[11].

When present in large quantities (>1% of $CD8^+$ T cells in peripheral blood), $CD8^+$ effector T cells have been linked with sterile protection in mice[53] and $CD8^+$ tissue-resident T cells were deemed essential upon immunization with RAS[54].

Although the role of $CD4^+$ T cells in protection against malaria is not thoroughly understood, these cells have been shown to be important in several contexts such as a) support of $CD8^+$ T cell activation and are required to prime effector cells; b) CSP specific $CD4^+$ T cells are associated with natural protection in humans; and c) $CD4^+$ T cells are crucial for B cell development and antibody production[11].

Antibodies against pre-erythrocytic stages of *Plasmodium* infection, especially against CSP, can have various functions, such as mediating cytotoxic responses against sporozoites in the skin; inhibiting sporozoite gliding motility; opsonizing parasites; inhibiting invasion and development inside hepatocytes and mediate antibody-dependent cell mechanisms[11]. However, although antibody production are potential correlates of protection, their quality and not only their titers, needs to be taken into account, which requires their evaluation with functional assays[11].

1.6.2. Immunity to blood stage *Plasmodium* parasites – type I IFN response

When *Plasmodium* parasites exit the liver to the blood stream, the host is also capable of recognizing them and inducing an immune response. Through the recognition of certain PAMPs such as GPI anchors, AT-rich DNA or haemozoin by PRRs located in host cells' surface or cytoplasm, a type I IFN response is induced[55]. It is not thoroughly known which cells are the source of type I IFN response elicited during the erythrocytic stage of the parasites, although some studies identified plasmacytoid dendritic cells (pDCs) as one of the producers after an activation of a TLR7-mediatied signalling cascade, a myeloid differentiation primary response 88 (Myd88) or IRF7[56,57].

Although it is apparent that a type I IFN response is elicited when parasites are in the blood stream, it is not yet clear which are all the cells and pathways involved in it. Also, the effect of this response in the outcome of infection is also not totally understood, as it can have a positive or negative effect depending on the parasite's genetic background, the host's genetic background or even on whether it is induced exogenously or endogenously[46].

1.7. Malaria vaccination-related immunity

Understanding the immune mechanisms elicited by the different types of malaria vaccine candidates will allow the improvement of their efficacy. Some of these mechanisms have already been mentioned in the previous chapter. In particular, anti-CSP antibodies, $CD8^+$ T cells and IFN-γ seem to be essential for sterile protection in RAS, GAP and CPS immunizations[27]. Although there are some insights about the immune mechanisms behind whole-sporozoite vaccination, a clear correlate of protection has not yet been found[11,25].

Comparing different types of whole-sporozoite immunization approaches is useful to clarify which is the most efficacious approach, which immune mechanisms are behind each vaccination mode of action and outcome, and what can be done to improve such outcomes[25]. The different methods used to attenuate parasites mentioned in chapter 1.5.1.1 result in parasites that develop to different extents (Figure 1.4), which, in turn, results in different immune responses. RAS are metabolically active and can invade hepatocytes but are not capable of replicating inside

them. GAPs have genetically defined arrest time-points according to the genes deleted in their genome, which can be earlier or later in the liver stage (EA or LA-GAP, Figure 1.5). In CPS approaches, sporozoites develop fully in the liver, exit to the blood, and are then killed by the anti-malarial drug in circulation[58,59].

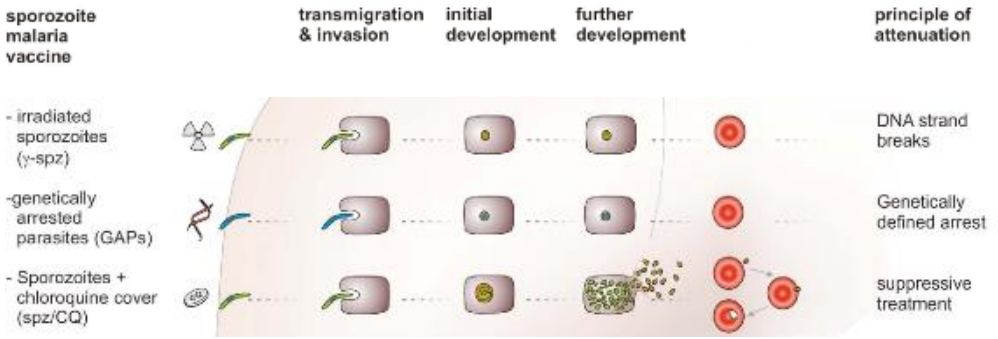

Figure 1.4. Different extent of liver stage development according to the type of attenuation strategy used in the design of whole-sporozoite vaccines. According to the type of attenuation used, parasites can develop to different extents in the liver. Irradiated sporozoites arrest their development early in the liver stage as DNA strand breaks induced by radiation interfere with the parasite replication process. Genetically attenuated parasites can have a genetically defined arrest, which can be earlier or later in the liver stage according to the genes knock-out of their genome. When sporozoites are administered concomitantly with chloroquine (CPS approach), their development in the liver is completed and soon after their release into the blood stream, the parasites are eliminated by the circulating drug. Adapted from "Arrested Plasmodium liver stages as experimental anti-malaria vaccines" by Matuschewski, K *et al, Human Vaccines* 7, 16–21 (2011).

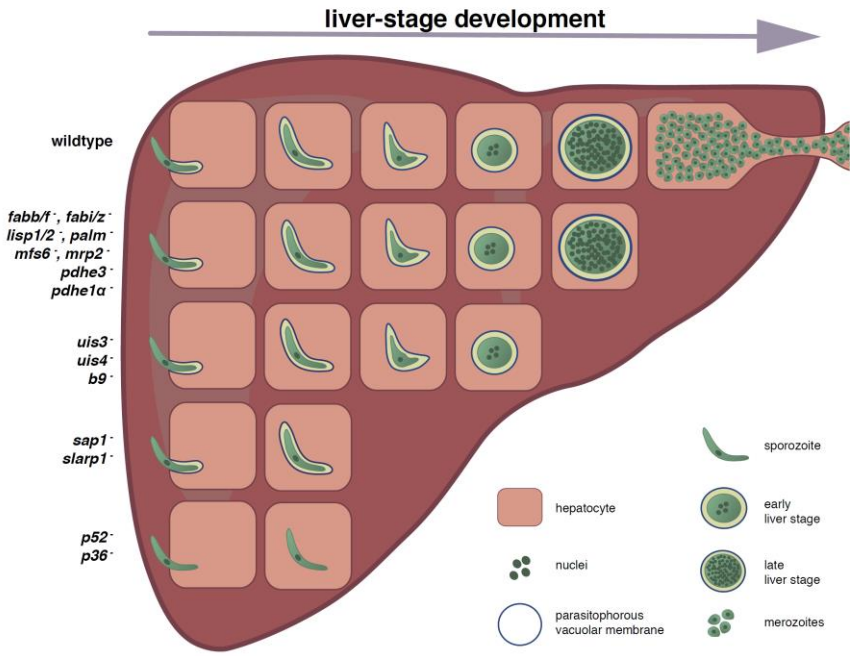

Figure 1.5 Liver stage developmental arrest of EA and LA-GAPs in rodent malaria models. Depending on the genes knock-out to attenuate different GAPs, the arrest of parasite development in the liver occurs sooner or later**.** Adapted from: "Genetically engineered, attenuated whole-cell vaccine approaches for malaria" by Vaughan, A. M. *et al*, *Human Vaccines* 6 (2010).

By comparing the efficacy of RAS, GAP, and CPS immunizations in mice, Friesen *et al* concluded that superior protection is achieved when mice are vaccinated with late liver stage arresting parasites, such as sporozoites under azithromycin cover[59]. This result may be explained by the display of late liver stage antigens that enhance the protection conferred by whole-sporozoite vaccines[59]. Butler *et al* also conducted a comparison between the performance of different whole-sporozoite immunizations, comparing the efficacy of an EA-GAP (*sap1-)* with a LA-GAP (*fabb/f-)* parasite. This showed that immunizing with a LA parasite conferred superior antimalarial protection and also suggested that this effect was due to a presentation of a more diverse set of antigens and possibly multi-stage antigens to the immune system[60]. These observations suggested that the longer the parasite develops in the liver, the stronger the protective efficacy of the vaccine is.

Although some studies, such as those mentioned above, have been performed to elucidate the immune response that supports a whole-sporozoite immunization, a lot remains to be uncovered. In particular, the influence of type I IFN responses on whole-sporozoite vaccination is not known, regardless of its importance in the mounting of an innate immune response against *Plasmodium* parasites (mentioned in detail in chapter 1.6.1.1).

2. Aims

Whole-sporozoite immunization approaches are the most promising and efficacious methods of immunization against malaria currently available.

Nonetheless, there is an urgent need to increase our understanding of the immune mechanisms behind each type of whole-sporozoite immunization and how they correlate with the different levels of protection observed.

Such understanding is key for the development of new and improved whole-sporozoite vaccine candidates and is at the basis of this thesis dissertation, which has the following aims:

- To unravel the dynamics of immune responses elicited by whole-sporozoite vaccination, including innate type I IFN responses as well as innate and adaptive cellular immune responses.
- To assess the contribution of innate type I IFN response to the establishment of sterile protection upon whole-sporozoite immunization.

To achieve these aims, a variety of experimental methodologies will be employed, including bioluminescence, quantitative real time-PCR and multiparameter flow-cytometry, to well-established and newly developed laboratory models of whole-sporozoite immunization and infection.

3. Materials and Methods

3.1. Parasite lines and sporozoite collection

To perform all the experiments that constitute this master's project, several rodent *P. berghei* strains were used:

- ***P. berghei*** ANKA luciferase-expressing parasites, *P. berghei* parasites that express the gene encoding for luciferase, an oxidative enzyme that produces bioluminescence allowing for the detection of this parasite by bioluminescence assays.
- ***PbΔb9Δslarp****,* an early-arresting double knock-out genetically attenuated (EA-GAP) *P. berghei* parasite created by deletion of the genes encoding for B9 and sporozoite and liver stage asparagine-rich protein (SLARP), two proteins essential for liver stage development. B9 has a critical role in the maintenance of a parasitophorous vacuole and SLARP is involved in the regulation of transcription in sporozoites and early liver stage parasites. Consequently, the deletion of both *b9* and *slarp* genes leads to a safe and completely attenuated parasite that successfully invades hepatocytes and arrests its development soon after[61].
- ***PbΔmei2Δlisp2****,* a late-arresting double knock-out genetically attenuated parasite (LA-GAP) *P. berghei* parasite created by deletion of the genes encoding for the meiosis inhibited 2 - like RNA binding protein (MEI2) and liver-specific protein 2 (LISP2). MEI2 affects parasite nuclear division and merozoite formation and LISP2 is specifically expressed during parasite liver-stages and in the parasitophorous vacuole. The deletion of both *mei2* and *lisp2* genes lead to a late liver stage arresting parasite.
- ***PbΔmei2***, a single knock-out genetically attenuated late-arresting parasite, from which the *mei2* gene was knocked-out.
- ***PbΔmei2* flagellin expressing parasites (thereafter referred as FLAG) -** *PbΔmei2* parasites in which the gene encoding for the *Salmonella typhimurium* flagellin was inserted under the control of the lisp2 promoter.

All the genetically attenuated parasites also express the luciferase gene, which allows their detection in the blood by bioluminescence.

Female *Anopheles stephensi* mosquitos were infected with the different parasite strains, bred and kept at the Instituto de Medicina Molecular João Lobo Antunes (Lisbon, Portugal). Sporozoites from different strains were obtained through the dissection of salivary glands of infected female mosquitoes in Roswell Park Memorial Institute 1640 (RPMI 1640; Gibco) medium. To free the sporozoites from the mosquitoes' salivary glands, the suspension obtained after

dissection was mechanically homogenized and filtered using a 40µm strainer. Sporozoites were counted using an Olympus CKX41 inverted microscope and a Neubauer chamber.

3.2. Sporozoite Irradiation

Freshly dissected *P. berghei* ANKA sporozoites were exposed to 16000 rad of γ-radiation, on a Gammacell 3000 ELAN Irradiator localized in Instituto de Medicina Molecular João Lobo Antunes, prior to its injection into mice.

3.3. Mice

All *in vivo* experiments were performed using either WT C57BL/6J mice or C57BL/6J *Ifnar1*$^{-/-}$ mice housed in the animal house of Instituto de Medicina Molecular João Lobo Antunes in specific pathogen-free conditions. C57BL/6J WT mice were purchased from Charles River Laboratories International, with ages ranging from 6 to 8 weeks upon arrival. C57BL/6J *Ifnar1*$^{-/-}$ were bred in the animal house of Instituto de Medicina Molecular João Lobo Antunes, also in specific-pathogen free conditions. *In vivo* experiments conducted in this work were performed in compliance with national and European Union regulations and approved by ORBEA (Órgão Responsável pelo Bem-Estar Animal) of iMM.

3.4. Infection of mice with *P. berghei* sporozoites

Mice were anaesthetised with isoflurane (IsoFlo, Zoetis), a volatile anaesthetic, and infected intravenously with sporozoites diluted RPMI 1640, *via* retro-orbital injection.

3.5. Monitoring of parasitaemia

Monitoring of parasitaemia followed the modified version of the protocol established by Zuzarte-Luis V et al (**Simple, sensitive and quantitative bioluminescence assay for determination of malaria pre-patent period).** Briefly, a small incision in the tip of each mouse's tail was made, to allow the collection of 5µl of blood from the tail vein daily (1, 3, 4, 5, 6, 7, 8, 9 days post-challenge). Blood was collected into 45µl of lysis buffer and preserved at -20ºC. To perform the bioluminescence assay, 50µl of D-Luciferin dissolved in luciferase assay buffer was added to 15µl of blood lysate and promptly measured in a microplate reader (Tecan M200, Switzerland)[62].

3.6. Sample collection from mice

At specific time-points post immunization – 12, 24, 42, 48, 60, 68, 72, 84 and 96 h post-immunization – mice were sacrificed using an overdose of isoflurane. Total blood collection was performed by cardiac puncture with a heparinized syringe (100U/ml sodic heparin; Braun) and then, mice were perfused with 20ml of 1x PBS. Livers were harvested and divided into several aleatory pieces to serve different purposes. About one third of the liver was flash frozen in liquid nitrogen to later serve as material for RNA extraction and the rest was used for liver leukocytes isolation.

3.7. Cell isolation

Liver leukocytes were isolated by grinding the perfused livers in a 1x PBS solution containing DNase (2U/ml), filtering through a 100µm filter and centrifuging at 2000 rpm during 5 min. The resultant pellet was resuspended in 10ml of 35% Percoll (Sigma) and centrifuged for 20 min at 2600 rpm, no brake, at RT. To lyse RBCs, the pellet was then resuspended in 3ml of Ammonium-Chloride-Potassium (ACK) buffer during 3 min at RT. To stop the reaction, FACS buffer (1x PBS containing 2% (v/v) fetal bovine serum (FBS)) was added and a 5 min centrifugation at 2000 rpm, RT was performed.

3.8. Flow Cytometry

To obtain liver leucocytes for flow cytometry analysis, the protocol described previously (3.7) was followed. One million liver cells from each mouse were placed in a well of a round-bottom plate and centrifuged 5 min at 1600 rpm, RT. PBS 1x was added to the cells, followed by 15 µl of Fc block (1:50). After 15 min incubation at 4ºC, the reaction was stopped with PBS and the cells were centrifuged as before. To each well was added 15 µl of antibody mixture, detailed in table 3.1, followed by an incubation of 20 min at 4ºC. Then, cells were incubated with Fixation/Permeabilization buffer (eBioscience) for 30 min at 4ºC to allow intracellular staining with anti-IFNγ antibody (1:400). Samples were run in on a BD LSRFortessa X-20 and analysed using the 10.6 version of FlowJo software. All the antibodies mentioned in table 3.1 are from the brand Biolengend.

Table 3.1 List of antibodies and respective concentrations employed in mice liver leukocytes flow cytometry analyses.

FACS Conjugated Antibody (fluorochrome – cell marker)	Dilution Factor
FITC-CD11b	1:100
PerCP-Cy5.5-CD3	1:100
eF450-TCRγδ	1:100
V500-CD4	1:400
BV605-Ly6C	1:400
BV711-CD8	1:200
BV785-MHC II	1:200
AF647-CD69	1:500
AF700-CD45	1:500
eF780-FVD	1:60
PE-Dazzle594-CD127	1:100
PE-Cy5-NK1.1	1:1000
PE-Cy7-Ly6G	1:300

3.9. RNA extraction and quantification

For RNA extraction, livers were mechanically homogenized in 3ml of denaturing solution (4 M of guanidine thiocyanite; 25 mM of sodium citrate pH 7; 0.5% (v/v) N- lauroylsarcosine and 0.7% (v/v) β-mercaptoethanol in DEPC-treated water). RNA was extracted from liver homogenates using the TripleXtractor direct RNA kit (Grisp) according to the manufacturer's instructions. To measure the RNA concentration after extraction, each sample was assessed in a NanoDrop 2000 (Thermo Sientific) spectophotometer, absorbance readings were performed at 260nm.

3.10. cDNA synthesis and qRT-PCR

Using NZYTech First-Strand cDNA synthesis kit, according to the instructions provided, complementary DNA (cDNA) was synthetized from 1µg of RNA, in a total volume of 20µl. A Biometra Personal thermocycler was used, employing the following conditions: 25ºC for 10 min, 55º for 30 min and 85º for 5 min.

qRT-PCR reactions were performed using the SYBR® Green (BioRad) reagent and the primers listed in table 3.2. Reactions were carried out in a Viia7 Applied Biosystems real-time thermal cycler. The program followed in the reactions was:

1. 50ºC for 2 min
2. 95ºC for 10 min
3. 40 cycles of 15 sec at 95ºC and 1 min at 60ºC
4. 95ºC for 15 sec (melting stage)
5. 60ºC for 1 min
6. 95ºC for 30 sec

Hypoxanthine guanine phosphoribosyltransferase gene (*Hprt)* was used as a housekeeping gene. The expression levels of all target genes were normalized against the value of expression of *Hprt* using the comparative threshold cycle (Ct) and calculated employing the ΔΔCt method[63], using the mean of the control group as a calibrator.

Table 3.2. List of primers used in qRT-PCR analyses of mice livers homogenates

Gene	Species	Forward primer (5'→3')	Reverse primer (5'→3')
18S	*P. berghei*	AAGCATTAAATAAAGCGAATACATCCTTAC	GGAGATTGGTTTTGACGTTTATGTG
Hprt	*Mus musculus*	TTTGCTGACCTGCTGGATTAC	A CAAGACATTCTTTCCAGTTAAAGTTG
Ifit-1		CCTTTACAGCAACCATGGGAGA	GCAGCTTCCATGTGAAGTGAC
Ifit-3		CTGAACTGCTCAGCCCACAC	TGGACATACTTCCTTCCCTGA
Usp18		CGTGCTTGAGAGGGTCATTTG	GGTCGGGAGTCCACAACTTC
Ifi44		TCGATTCCATGAAACCAATCAC	CAAATGCAGAATGCCATGTTTT
Irf7		CAGCGAGTGCTGTTTGGAGAC	AAGTTCGTACACCTTATGCGG
Viperin		CTTCAACGTGGACGAAGACA	GACGCTCCAAGAATGTTTCA

3.11. Statistical Analysis

Mann-Whitney test was used to analyse statistically significant differences between two experimental groups. Significances are depicted in the figures as follows: ns – not significant, **P* <0,05, ***P* <0,01, ****P* <0,001 and *****P* <0,0001. *P*-values less than 0,05 were considered significant.

4. Results and Discussion

4.1. Characterization of the immune responses elicited by different whole-sporozoite malaria vaccination approaches

To understand the differences between each type of whole-sporozoite immunization approach, a time-course analysis was performed (two independent experiments), employing 6-8 week old C57BL/6J mice immunized with either: a) 30 000 *P. berghei* wild-type sporozoites (WT-control group); b) 30 000 EA-GAP sporozoites (early-arresting genetically attenuated *P. berghei* parasite in which both the *b9* and the *slarp* genes were deleted); c) 30 000 irradiated *P. berghei* sporozoites (irradiated group); d) 30 000 LA-GAP sporozoites (late-arresting genetically attenuated *P. berghei* parasite in which both the *mei2* and the *lisp2* gene were deleted) or e) 30 000 *P. berghei* WT sporozoites administered under chloroquine prophylaxis (CPS group). Mice were then sacrificed at specific time-points post immunization in order to collect their livers for qRT-PCR and flow-cytometry analyses (Figure 4.1).

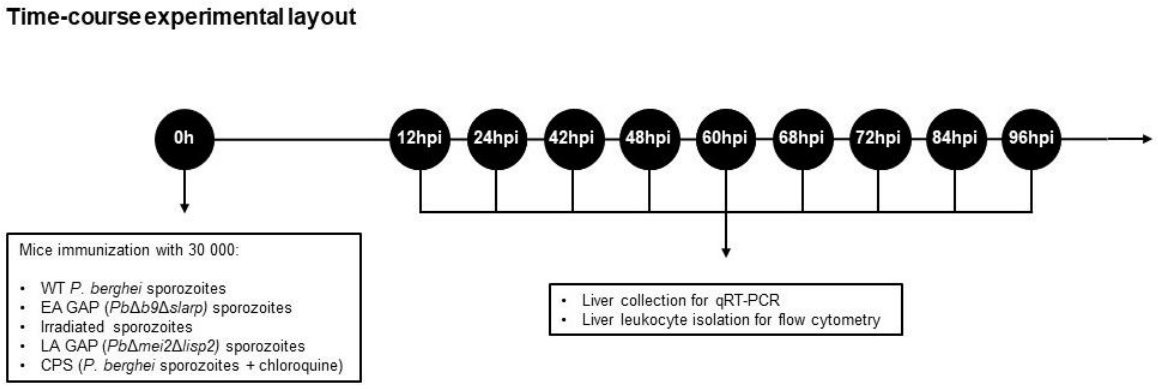

Figure 4.1 Time-course experimental layout. Mice were immunized with either wild-type *P. berghei* parasites, EA-GAP parasites, Irradiated parasites, LA-GAP parasites or with CPS (*P. berghei* parasites under the daily administration of 700 ug of chloroquine through intraperitoneal injection). Mice were sacrificed at 12, 24, 42, 48, 60, 68, 72, 84 and 96 h post immunization, their livers collected and analysed by qRT-PCR and liver leukocytes isolated and analysed by flow cytometry.

4.1.1. Wild-type *P. berghei* parasite development in mouse livers

We started by employing the experimental layout described in Fig. 4.1 to assess the dynamics of liver stage development for the wild-type *Plasmodium* parasites and parasites from each immunization approach. qRT-PCR analysis of the relative expression of *Plasmodium* ribosomal RNA 18S revealed that when mice are infected with WT *P. berghei* sporozoites, parasites can be easily detected in the liver at 12 hpi, with the 18S RNA copy number increasing exponentially thereafter, reaching a peak at 48 hpi (Figure 4.2.), which is followed by a decrease in parasite liver load corresponding to the exit of parasites to the blood, reaching a plateau at approximately 72 hpi, and increasing again at 96 hpi. This development pattern was expected as it was already reported to be the characteristic evolution of the liver burden upon an infection with *P. berghei* sporozoites[64].

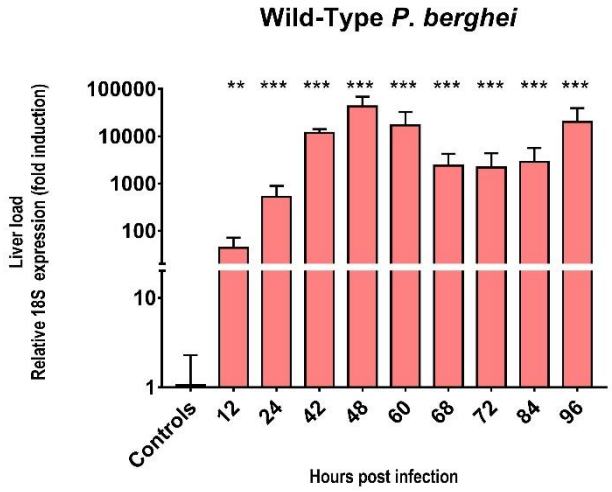

Figure 4.2 Liver stage development of wild-type *P. berghei* parasites. Parasite liver load at different times post infection in mice immunized with 30 000 *P. berghei* wild-type sporozoites. The relative expression of *P.berghei* 18S gene in whole-liver extracts was quantified via qRT-PCR to determine the liver load in the immunized mice at different times post immunization. Non-immunized mice were used as controls, data are expressed as means ±SD of two independent experiments (Controls, n=10; 12h, n=3; 24h, n=6; 42h, n=6; 48h, n=6; 60h, n=6; 68h, n=6; 72h, n=6; 84h, n=6; 96h, n=6).

Upon assessing liver stage parasite development dynamics, we also analysed the activation and induction of type I IFN responses elicited by the infection with wild-type *P. berghei* parasites and by each of the immunization protocols studied. To achieve this, mRNA expression of six ISGs, *Ifit-1, Ifit-3, Usp18, Irf7, Ifi44* and *Viperin,* was quantified by qRT-PCR at all the selected time-points as a surrogate for type I IFN response activation. The results obtained for the mice infected with live wild-type *P. berghei* parasites (Figure 4.3) indicate the presence of two distinct waves of ISGs induction, in agreement with what was previously described by Liehl *et al* in 2015[49]. A first wave of ISGs induction which occurs at ~42 hpi (1.635±1.073-fold induction of the averaged genes) and coincides with the intense asexual replication of the parasite in the liver[64], followed by a second wave of type I IFN induction which peaks at ~84 hpi, after parasite exit from the liver to the blood, with an averaged ~20-fold induction. Of note, in Liehl *et al*[49], the second wave of type I IFN induction occurred some hours earlier, between 68 hpi and 72 hpi, which we hypothesize to be due to the difference in the number of sporozoites used to infect the mice, which was smaller in our experimental *(*30 000 and 50 000 sporozoites, respectively).

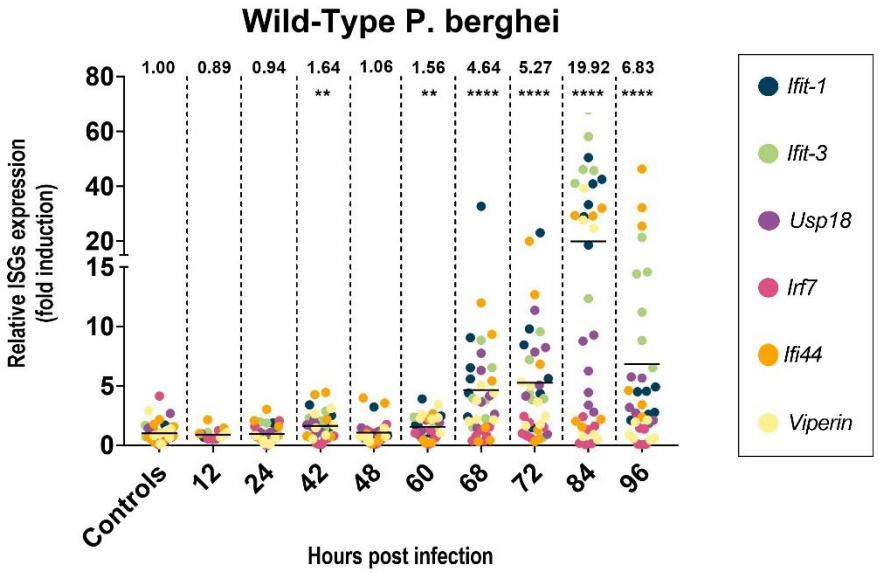

Figure 4.3 Infection with wild-type *P. berghei* parasites induces a type I IFN response leading to ISGs expression. ISGs (*Ifit-1, Ifit-3, Usp18, Irf7, Ifi44* and *Viperin)* expression was quantified in whole-liver extracts via qRT-PCR to determine the liver load in mice infected with 30 000 *P. berghei* wild-type sporozoites at different times post infection. Non-immunized mice were used as controls, data are expressed as individual values of expression of each ISG and means of the cumulative expression of all ISGs at each time-point, of two independent experiments (Controls, n=10; 12h, n=3; 24h, n=6; 42h, n=6; 48h, n=6; 60h, n=6; 68h, n=6; 72h, n=6; 84h, n=6; 96h, n=6).

4.1.2. Characterization of liver development upon immunization with different whole-sporozoite immunization approaches

To understand how the parasite development differs between wild-type parasites and the parasites used in different whole-sporozoite immunization approaches, the liver development was assessed also in mice immunized with each of the different immunization approaches. In mice immunized with EA-GAP parasites, such as *PbΔb9Δslarp* parasites or irradiated sporozoites, parasite infection of the liver is expected to be limited to the earliest time-points, 12 hpi and 24 hpi, as these EA parasites undergo only a few cycles of replication or do not undergo replication at all[58]. In fact, EA-GAP and irradiated parasites were detected in small quantities in the liver of immunized mice at 12 hpi and 24 hpi, respectively (Figure 4.4 (A,B)). When mice were immunized with LA-GAP parasites, the parasite liver load was similar to that of mice immunized with WT sporozoites (Figure 4.1), up to 48 hpi. From 48 hpi onwards, liver load decreased and very few parasites were detected at 84 hpi and 96 hpi (Figure 4.4 (C)). Finally, the results for the CPS group present a liver development dynamics similar to that of infection with WT parasites until 72 hpi, followed by a significant decrease in liver load at 84 hpi and 96 hpi, indicative of parasite elimination in the blood (Figure 4.4 (D)).

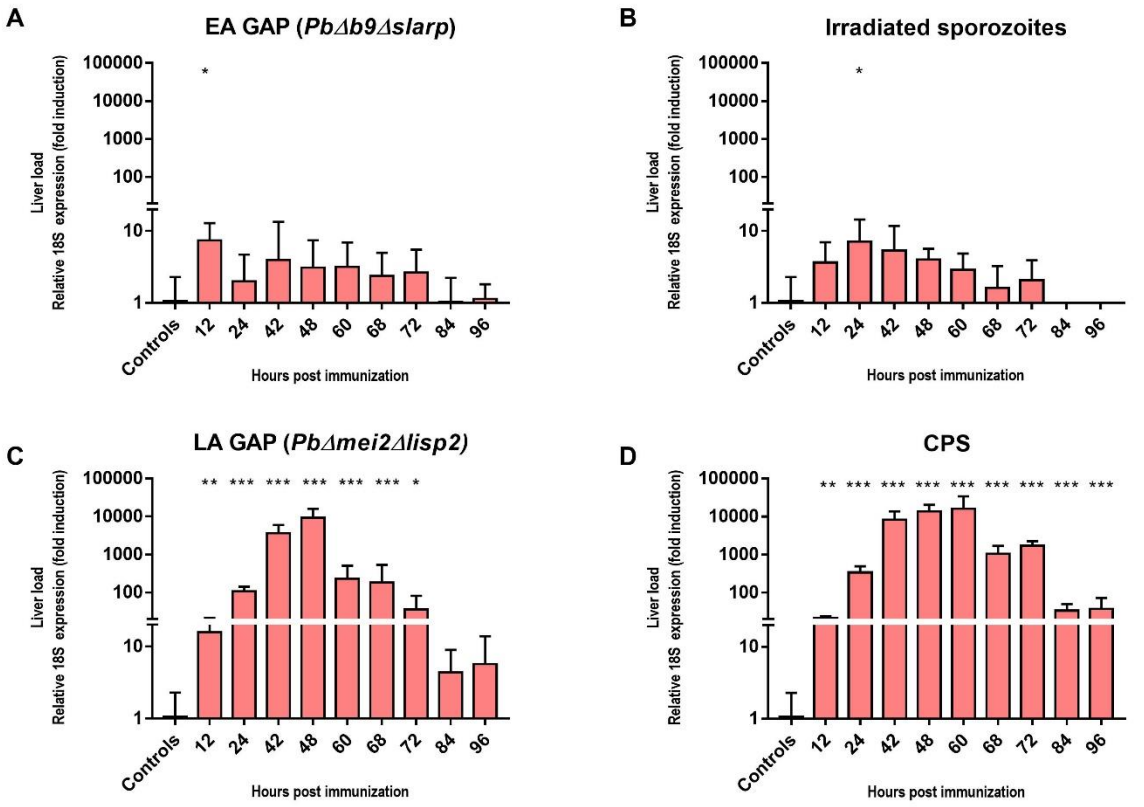

Figure 4.4 Different whole-sporozoite immunization approaches use *Plasmodium* parasites with different liver stage developments and arrest time-points. Parasite liver load at different times post immunization in mice immunized 30 000 EA-GAP (*PbΔb9Δslarp)* sporozoites (A), 30 000 Irradiated sporozoites (B), 30 000 LA-GAP (*PbΔmei2Δlisp2*) sporozoites (C) and 30 000 *P. berghei* sporozoites concomitantly with the administration of chloroquine (D). The relative expression of *P.berghei* 18S gene in whole-liver extracts was quantified via qRT-PCR to determine the liver load in the immunized mice at different times post immunization. Non-immunized mice were used as controls, data are expressed as means ±SD of two independent experiments (Controls, n=10; 12h, n=3; 24h, n=6; 42h, n=6; 48h, n=6; 60h, n=6; 68h, n=6; 72h, n=6; 84h, n=6; 96h, n=6).

Substantially different patterns of ISG induction in the liver were observed for the different immunization approaches assessed. Results obtained for immunization with EA-GAP parasites indicate a relatively small ~2-fold induction of the averaged ISGs at 12 hpi that subsequently returns to basal non-infected levels of expression for the remaining time-points, while in the livers of mice immunized with irradiated parasites, no significant induction of ISGs can be detected at any time-point post immunization (Figure 4.5 (A and B)). As both the EA-GAP and irradiated groups employ parasites that terminate their development in the liver without any or after only a few cycles of replication occur, it is possible that these parasites do not subsist long enough in the liver to induce the activation of IFN responses, explaining the absence of ISG induction observed.

Results obtained for the LA-GAP group (Figure 4.5 (C)) indicate the presence of a first wave of ISG induction similar to that observed for the control group, with a peak at 42 hpi (1.966±1.462-fold induction of the averaged genes) without, however, the presence of a second wave peaking at 84 hpi. Because *PbΔmei2Δlisp2* parasites arrest their development late in the

liver-stage, as indicated by our parasite liver stage development analysis, we hypothesize that the lack of merozoite release to the blood may explain the absence of the strong second wave of ISG induction observed for wild-type parasites. Nonetheless, a small increase in ISG expression could be detected between 68 hpi and 72 hpi (3.350±2.683 and 2.334±1.506- fold induction of the averaged genes respectively).

Finally, mice subjected to immunization with live WT parasites under chloroquine prophylaxis show two waves of ISG induction similarly to what can be observed in mice infected with WT parasites (Figure 4.5 (D)). However, the maximum induction is observed at 72 hpi with 9.116±7.145-fold induction of the averaged genes and is significantly lower than that observed for the control group (Figure 4.2), which peaks at 84 hpi with a ~19-fold magnitude of induction. The exiting of the parasites to the bloodstream, as opposed to what happens in the LA-GAP group, may account for the presence of a second wave of ISG induction, while the immediate killing of blood stage parasites by chloroquine is potentially the reason to why the magnitude of the second wave of induction is not as high as that observed in the WT group, where parasites develop normally in the blood.

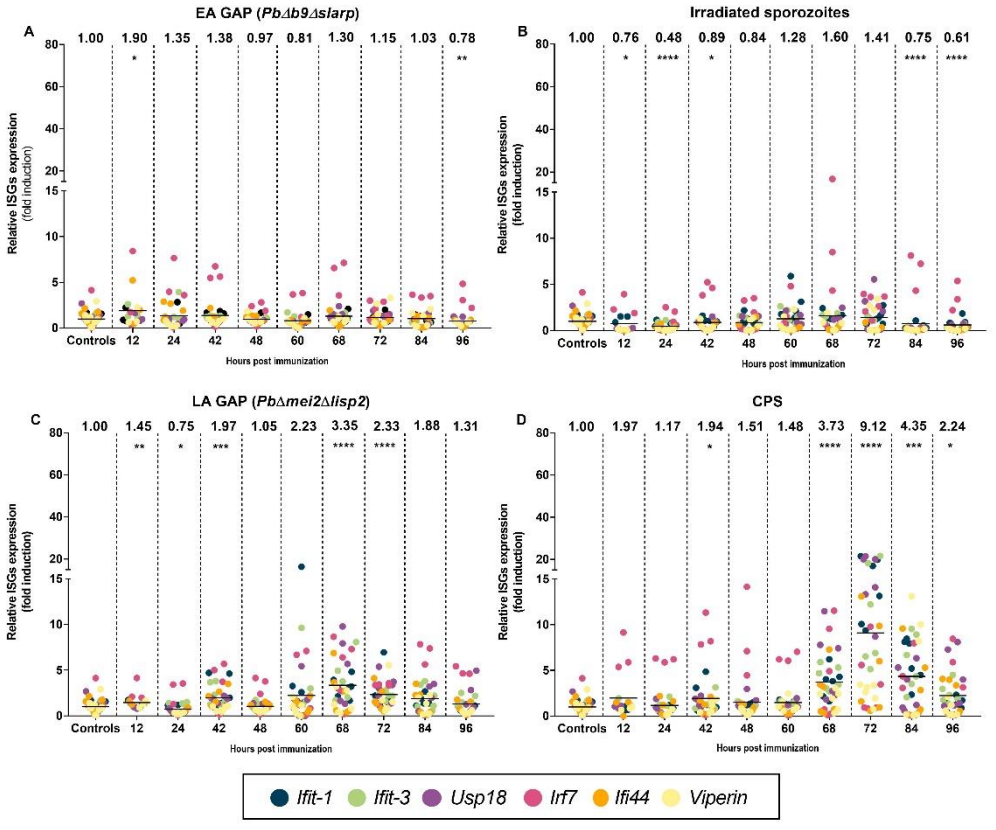

Figure 4.5. Different whole-sporozoite immunization approaches induce distinctive type I IFN response in the liver. ISGs (*Ifit-1, Ifit-3, Usp18, Irf7, Ifi44* and *Viperin)* expression was quantified in whole-liver extracts via qRT-PCR to determine the liver ISGs relative expression in mice immunized with 30 000 EA-GAP (*PbΔb9Δslarp)* sporozoites **(A)**, 30 000 Irradiated sporozoites **(B)**, 30 000 LA-GAP (*PbΔmei2Δlisp2*) sporozoites **(C)** and 30 000 *P. berghei* sporozoites concomitantly with the administration of chloroquine **(D)** at different times post immunization. Non-immunized mice were used as controls, data are expressed as individual values of expression of each ISG and means of the cumulative expression of all ISGs at each time-point, of two independent experiments (Controls, n=10; 12h, n=3; 24h, n=6; 42h, n=6; 48h, n=6; 60h, n=6; 68h, n=6; 72h, n=6; 84h, n=6; 96h, n=6).; 12h, n=3; 24h, n=6; 42h, n=6; 48h, n=6; 60h, n=6; 68h, n=6; 72h, n=6; 84h, n=6; 96h, n=6).

4.1.3. Liver immune cell analysis upon infection with wild-type *P. berghei* parasites

To assess the effect of the infection with wild-type *P. berghei* sporozoites and with each whole-sporozoite immunization approach on cellular immunity, liver leucocytes were isolated from mouse livers collected at various time-points after sporozoite inoculation and analysed by flow cytometry. Non-infected mice were used as controls, and analysis aimed to characterize not only the changing dynamics of immune cells in the liver, by evaluating relative frequencies of various sub-families of immune cells, but also their functional activation through the analysis of IFN-γ production.

It is important to note that the results presented in this dissertation are drawn from a single biological replicate, with 3 mice per experimental group, which limited the power of statistical analysis and the identification of significant differences between the various experimental groups. Therefore, conclusions drawn from the analysis of the following results should be reviewed with caution, as additional biological replicates are required to increase the confidence of the analysis and validation of the results. In this way, the following analysis not only focuses on statistically significant occurrences but also in clear trends in cell frequency observed, even if those do not reach statistical significance.

First, the simultaneous surface expression of the CD3 and CD8 or CD4 receptors was used to identify $CD8^+$ and $CD4^+$ T cells and determine their overall frequency within leukocytes collected from mice liver at various time-points post infection (Figure 4.6). Our results indicate that no major changes occur in the frequency of liver-isolated $CD4^+$ T or $CD8^+$ T cells (Figure 4.6 (A, C)) during the exo-erythrocytic development and exiting of wild-type parasites, with the exception of a small decrease in $CD4^+$ T cells frequency at 84 hpi. Interestingly, the frequency of tissue resident $CD4^+$ T cells and $CD8^+$ T cells (Figure 4.6 (B, D)), as identified by the concomitant expression of the receptor CD69, starts to increase at 62-68 hpi, upon the release of merosomes from the liver.

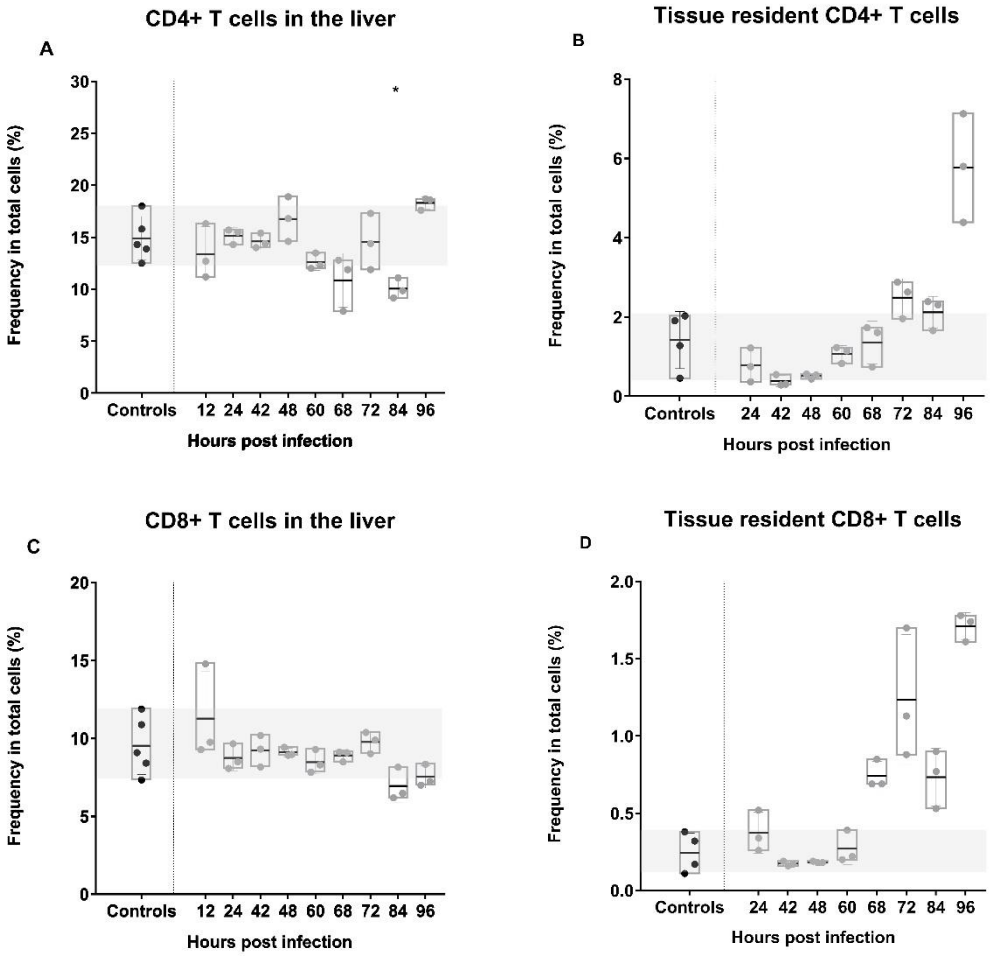

Figure 4.6 Frequency of CD4⁺ and CD8+ T cells in mice livers at different times after infection with wild-type *P. berghei* parasites. CD4⁺ T cells **(A)**, tissue resident CD4⁺ T cells **(B)**, CD8⁺ T cells **(C)** and tissue resident CD8⁺ T **(D)** frequency was quantified in isolated leucocytes from the liver of infected mice via flow cytometry. Mice were infected with 30 000 *P. berghei* wild-type sporozoites and non-infected mice were used as controls, data of one experiment are expressed as individual values of frequency of each cell type, mean and SD at each time-point. (Controls, n=5; 12h, n=3; 24h, n=3; 42h, n=3; 48h, n=3; 60h, n=3; 68h, n=3; 72h, n=3; 84h, n=3; 96h, n=3).

Subsequently, the frequency of NK, NKT, ILC1 and γδ T cells was also analysed, using an additional set of markers for specific cell receptors that included: a) the receptor NK1.1 for NK and NKT cells; b) the CD127 receptor for ILC1 cells; and c) simultaneous expression of CD3 and TCR γδ receptor for γδ T cells (Figure 4.7). Overall analysis of NK cell frequency in the liver shows no visible trend in the dynamics of these cells but significant variations across time-points. In fact, significant decreases are observed at both 60 and 84 hpi, followed by a significant increase at 96 hpi. However, the low magnitude of these changes, associated with the lack of biological replicates, and the low number of animals included in this analysis should be taken into account when interpreting their significance (Figure 4.7 (A)).

Conversely, no statistically significant differences could be observed for NKT cell frequency at any of the time-points analysed, but a clear trend for a continuous decrease in cell frequency can be observed starting at 24 hpi and ending in lower-than-basal frequency levels at 96 hpi (Figure 4.7 (B)). An identical trend for decreasing cell frequency in comparison to non-infected controls can be observed for the frequency of ILC1s in the liver (Figure 4.7 (C)), which reaches statistical significance from 60 hpi onwards. Finally, the analysis of γδ T cells frequency in the liver shows a single peak of increased cell frequency at 24 hpi, which is followed by lower-than-average frequency levels for all the remaining time-points analysed (Figure 4.7.(D)).

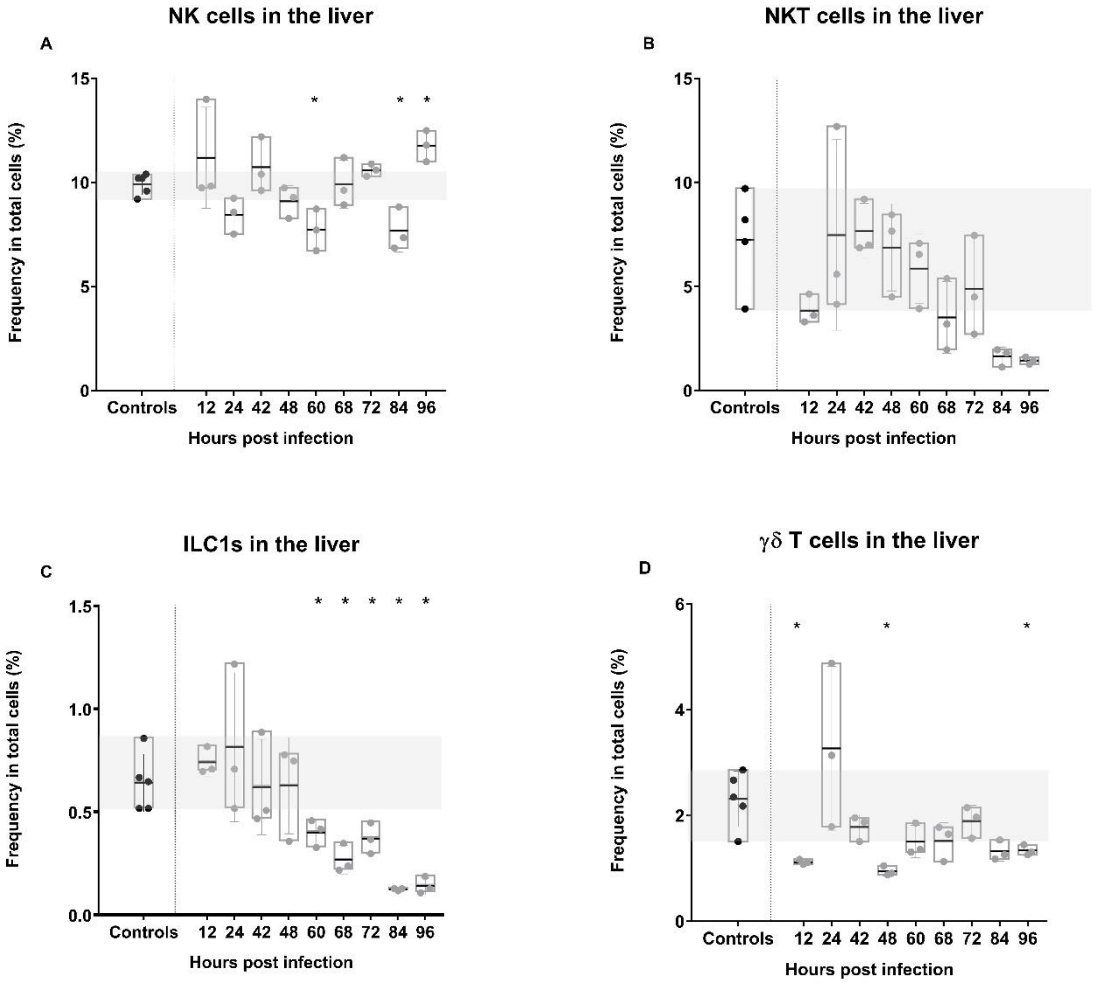

Figure 4.7 Frequency of NK, NKT, ILC1s and γδ cells in mice livers at different times after infection with wild-type *P. berghei* parasites. NK **(A),** NKT **(B),** ILC1s **(C)** and γδ cells **(D)** frequency was quantified in isolated leucocytes from the liver of infected mice via flow cytometry. Mice were infected with 30 000 *P. berghei* wild-type sporozoites and non-infected mice were used as controls, data of one experiment are expressed as individual values of frequency of each cell type, mean and SD at each time-point. (Controls, n=5; 12h, n=3; 24h, n=3; 42h, n=3; 48h, n=3; 60h, n=3; 68h, n=3; 72h, n=3; 84h, n=3; 96h, n=3).

The frequency and dynamics of myeloid cells in the liver of infected mice , in particular macrophages, monocytes and neutrophils, which are considered professional phagocytic cells, being capable of phagocytising and destroying infectious agents[65], during and immediately after exo-erythrocytic development was also assessed by flow cytometry (Figure 4.8).

The expression of the CD11b receptor was used to identify macrophages, while the expression of the receptors Ly6C or Ly6G allowed for separation of monocytes and neutrophils, respectively. Because the recruitment of monocytes is crucial for host defence[66], a more extensive analysis was performed for this sub-family of immune cells, which included their division into two distinct subsets based on the intensity of Ly6C expression, with different reported functions: pro-inflammatory and patrolling monocytes (high Ly6C receptor expression for pro-inflammatory monocytes; low Ly6C receptor expression for patrolling monocytes). Pro-inflammatory monocytes have antimicrobial functions during inflammation, being able to transport antigens to the lymph nodes and differentiate into macrophages or DCs that accumulate at the site of infection[65,66] Patrolling monocytes are in continuous contact with the endothelium, surveying the vasculature and being involved in the resolution of inflammation[69].

The results obtained indicate that monocytes, macrophages and neutrophils (Figure 4.8) are recruited to liver upon termination of *Plasmodium* liver development and merosome release, with an increase in cells' frequency from 60/68 hpi onwards. This increase probably results from the phagocytic activity of these cells, which are recruited to the site of infection to clear up infected and apoptotic hepatocytes[69].

The magnitude of the observed increase is more relevant for pro-inflammatory monocytes and macrophages, although similar trend can also be observed for patrolling monocytes (Figure 4.8 (A, B, C)). Less clear is the recruitment of neutrophils, as no clear trend could be detected. Nonetheless, our data does indicate a significant increase in neutrophils (Figure 4.8 (D)) at 84 hpi concomitantly with the peak in ISG induction.

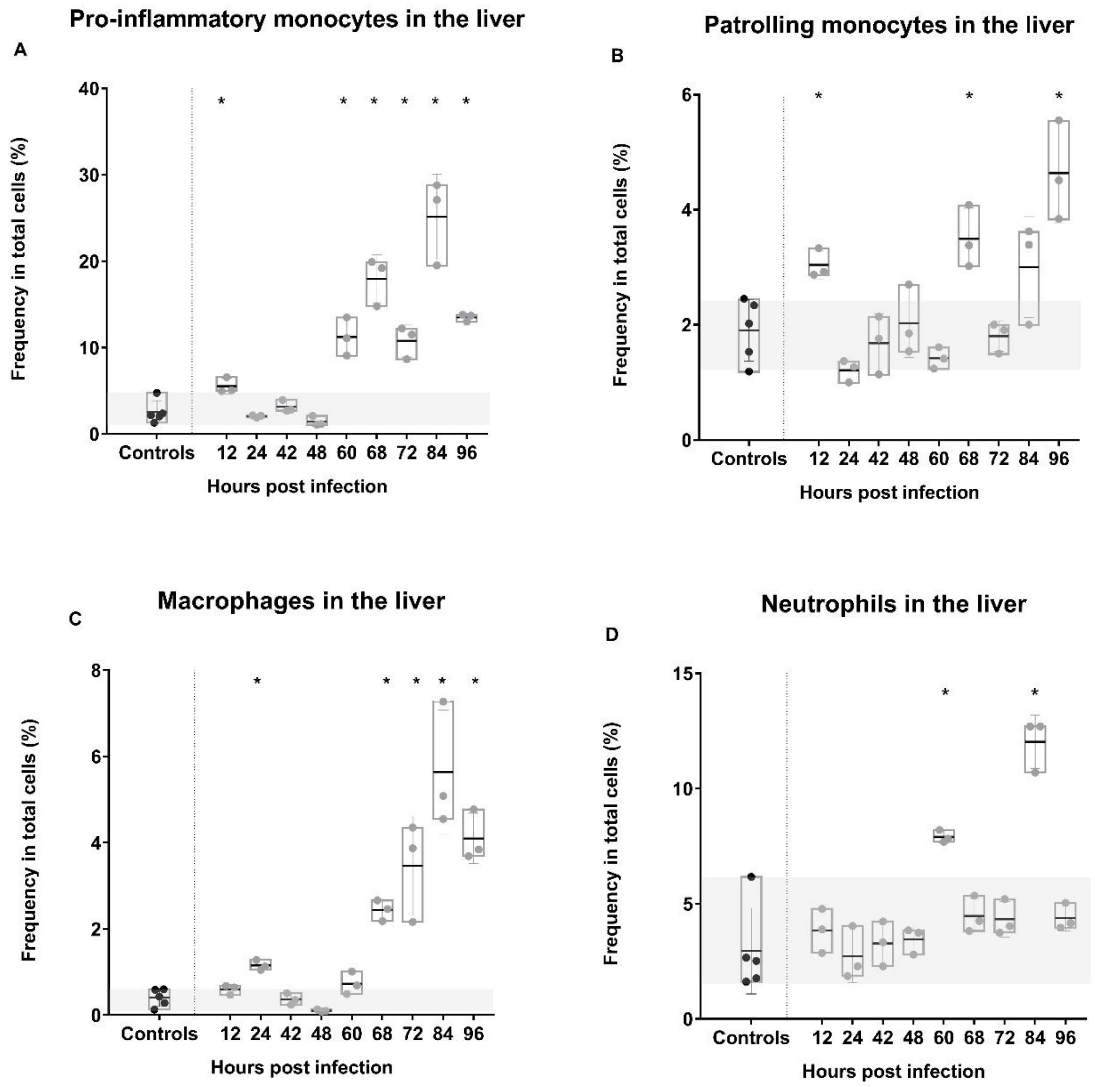

Figure 4.8 Frequency of myeloid cells in mice livers at different times after infection with wild-type *P. berghei* parasites. Pro-inflammatory monocytes **(A),** patrolling monocytes **(B),** macrophages **(C)** and neutrophils **(D)** frequency was quantified in isolated leucocytes from the liver of infected mice via flow cytometry. Mice were infected with 30 000 *P. berghei* wild-type sporozoites and non-infected mice were used as controls, data of one experiment are expressed as individual values of frequency of each cell type, mean and SD at each time-point. (Controls, n=5; 12h, n=3; 24h, n=3; 42h, n=3; 48h, n=3; 60h, n=3; 68h, n=3; 72h, n=3; 84h, n=3; 96h, n=3).

Finally, production of IFN-γ by immune cells was quantified by intracellular staining and flow cytometry analysis for the previously described cellular sub-families. IFN-γ secretion by lymphocytes such as $CD8^+$ T cells, NK and NKT cells may control the infection, as IFN-γ has several functions in the enhancement of the immune response such as increasing the phagocytic capacity of immune cells, inducing antibody production or potentiating the elimination of parasites by $CD8^+$ T cells[48].

As for type I IFN activation and ISG induction, IFN-γ production appears to present two distinct waves of increased production which include a first peak at 24 hpi followed by a decrease up to 60 hpi, increasing thereafter and achieving maximum production at 84 hpi (Figure 4.9). This pattern of IFN-γ production is clear for all cellular sub-families analysed, except for γδ T cells (Figure 4.9 (F)), for which induction at 24 hpi appears to be absent. Nonetheless, it is important to note the similarities between the patterns of expression observed for type I IFN activation and IFN-γ production by liver immune cells, both of which present a similar wave pattern of activation with an early peak at 24-42 hpi, followed by a depression and a high magnitude induction that peaks at 84 hpi, when parasite have already completed development in the liver and merosomes have been released into vasculature. As IFN-γ can have several tasks in the resolution of infection, its increased production is expected.

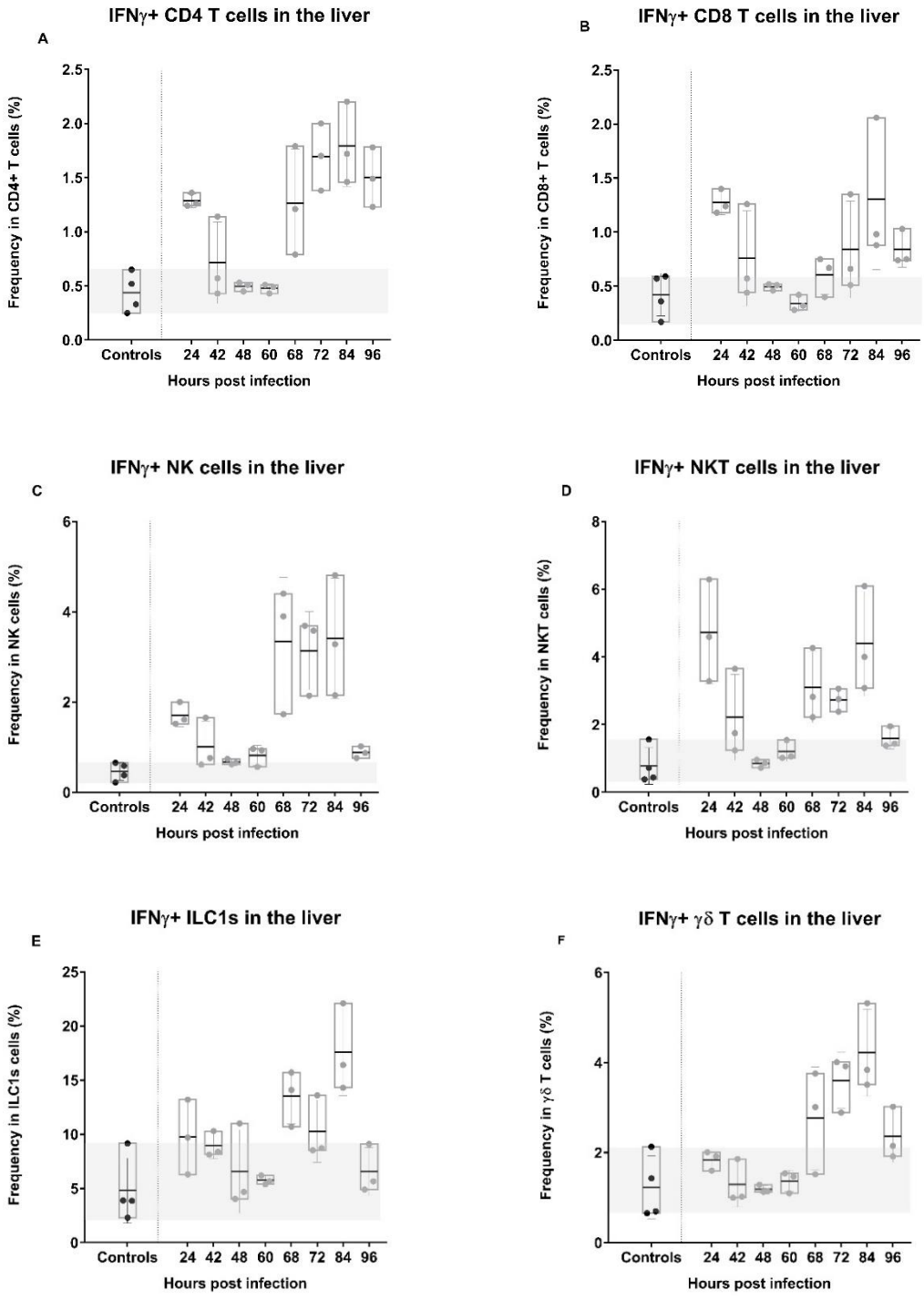

Figure 4.9 Frequency of IFN-γ+ cells in mice livers at different times infection with wild-type *P. berghei* parasites. The presence of IFNγ+ cells in certain cell populations was assessed by flow cytometry: CD4+ T cells **(A),** CD8+ T cells **(B),** NK cells **(C)**, NKT cells **(D)** ILC1s **(E)** and γδ T cells **(F)**. Mice were infected with 30 000 *P. berghei* wild-type sporozoites and non-infected mice were used as controls, data of one experiment are expressed as individual values of frequency of each cell type, mean and SD at each time-point. (Controls, n=5; 24h, n=3; 42h, n=3; 48h, n=3; 60h, n=3; 68h, n=3; 72h, n=3; 84h, n=3; 96h, n=3).

4.1.4. Liver immune cell analysis upon infection/immunization with different whole-sporozoite vaccination approaches

Similar liver immune cell dynamics and activation analyses as those performed for mice infected with wild-type *P. berghei* parasites were also performed for mice subjected to immunization with different whole-sporozoite vaccination approaches. A comparative analysis of the host cellular immune responses elicited during the exo-erythrocytic development of a fully infectious parasite and that elicited by infection/immunization with irradiated sporozoites, GAPs or under chloroquine cover is expected to highlight differences that may be at the basis of the different protective capabilities of such whole-sporozoite immunization approaches.

Our results for recruitment and dynamic changes in the liver frequency of CD4+ T cells (Figure 4.10A) indicate that no major changes can be observed during infection/immunization with either of the approaches for which the parasite arrest its development early in the liver stage, such as EA-GAP and irradiated sporozoites (Figure 4.10). Conversely, mice immunized with LA-GAP (*PbΔmei2Δlisp2*) and CPS reveal an increased frequency of $CD4^+$ T cells between 84 hpi and 96 hpi, with the LA-GAP group presenting a statistically significant maximum at 84 hpi and the CPS group at 96 hpi (Figure 4.10 (A)). It appears that the late interruption of parasite development either in the liver or just after merosome release, is a trigger for the increase in the liver of both $CD4^+$ T cells and tissue resident $CD4^+$ T cells (Figure 4.10 (B)), a phenomenon that was only observed for tissue resident $CD4^+$ T cells during a regular course of infection with wild-type *P. berghei* parasites (Figure 4.6 (A)).

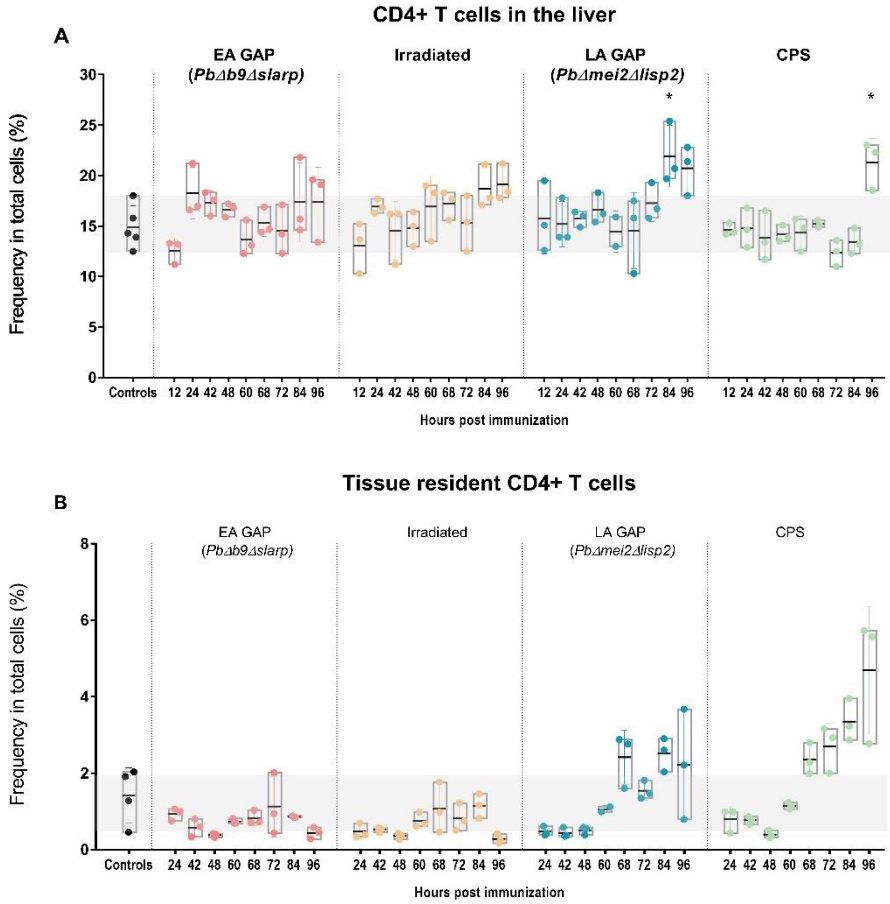

Figure 4.10 Dynamic frequency of CD4⁺ T cells and tissue resident CD4⁺ T cells in the liver of mice immunized with different whole-sporozoite immunization approaches. CD4⁺ T cells **(A)** and tissue resident CD4⁺ T cells **(B)** frequency was quantified in isolated leucocytes from the liver of immunized mice via flow cytometry at various time-points post infection. (Controls, n=5; 12h, n=3; 24h, n=3; 42h, n=3; 48h, n=3; 60h, n=3; 68h, n=3; 72h, n=3; 84h, n=3; 96h, n=3).

No relevant changes or tendencies are observed for overall CD8⁺ T cells (Figure 4.11 (A)) in any of the different experimental groups. However, the frequency of tissue-resident CD8⁺ T cells does appear to increase in the latest time-points, from 68/72 hpi to 96 hpi, as observed for mice infected wild-type *P. berghei* parasites (Figure 4.6 (D)).

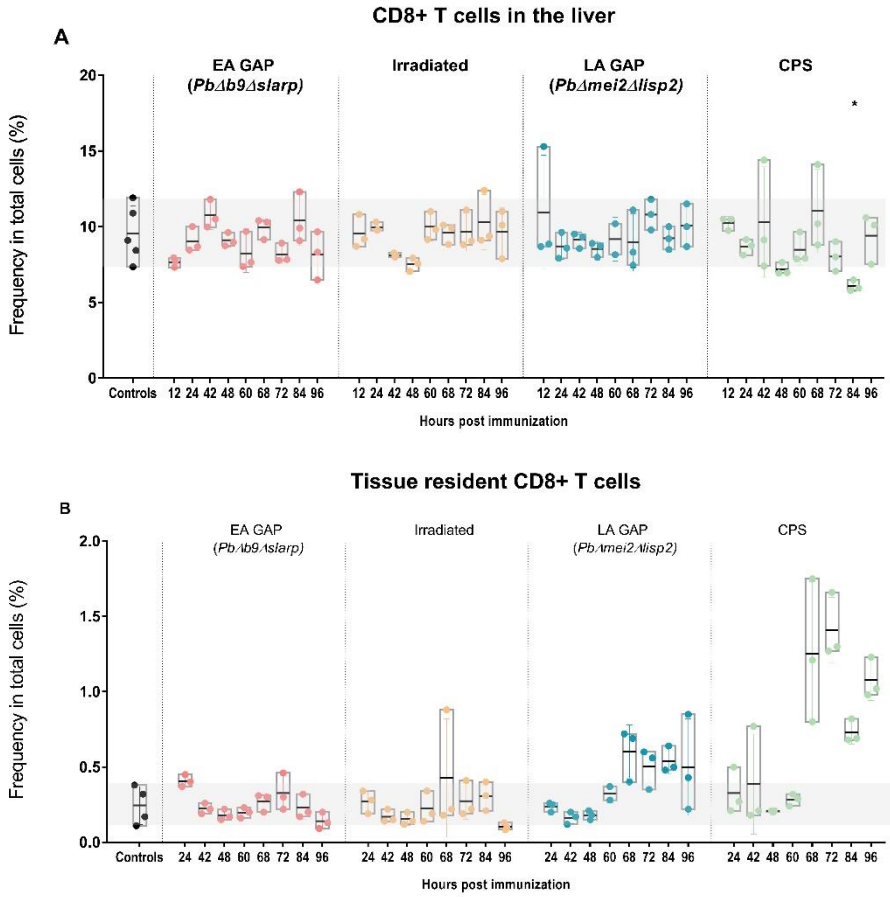

Figure 4.11. **Dynamic frequency of CD8⁺ T cells and tissue resident CD8⁺ T cells in the liver of mice immunized with different whole-sporozoite immunization approaches.** CD8⁺ T cells **(A)** and tissue resident CD8⁺ T cells **(B)** frequency was quantified in isolated leucocytes from the liver of immunized mice via flow cytometry. at various time-point post infection. Non-immunized mice were used as controls, data of one experiment are expressed as individual values o of each cell type, mean and SD at each time-point. (Controls, n=5; 24h, n=3; 42h, n=3; 48h, n=3; 60h, n=3; 68h, n=3; 72h, n=3; 84h, n=3; 96h, n=3).

A decrease in the frequency of NK cells is observed at 60 hpi for the LA-GAP and CPS groups (Figure 4.12 (A)), as observed for the WT group (Figure 4.7 (A)).

The frequency of NKT cells (Figure 4.12 (B)) seems to follow the same pattern in all experimental groups until 42 hpi, when an increase in the frequency of these cells is observed. After 42 hpi, the frequency of NKT cells in the irradiated and EA-GAP groups continues to increase until 84 hpi, followed by a sharp drop in frequency at 96 hpi. Conversely, LA-GAP and CPS infected/immunized mice show a continuous decrease in the frequency of NKT cells, starting at 48 hpi, until they reach levels below the basal frequency of NKT cells in the liver. It is interesting to note that the pattern identified for the early-arresting parasites (irradiated and EA-GAP (*PbΔb9Δslarp)*) and the late-arresting/fully infectious parasites (wild-type, *PbΔmei2Δlisp2*, CPS) is identical until 42 hpi, but the opposite from this time-point onward. The immunization with the

LA-GAP and CPS leads to a decrease in cell frequency identical to that observed during infection with wild-type *P. berghei* parasites.

Similarly, the frequency of ILC1s also shows a statistically significant decrease to levels lower than the basal levels in the LA-GAP and CPS groups, from 60 hpi onwards, which is also not observed in early-arresting parasites, such as EA-GAP or irradiated sporozoites (Figure 4.7 (C)). In fact, ILC1 frequency in the EA-GAP group seems to increase from 68 hpi to 96 hpi, as observed for NKT cells, reaching statistical significance at 72 hpi, but that increase is not observed for mice infected /immunized with irradiated sporozoites, for which no differences were found.

Analysis of γδ T cell frequency in the liver does not reveal major trends for altered cell frequency in the liver or differences between the various groups of infected/immunized mice (Figure 4.7 (D)). Nonetheless, it is important to note that a statistically significant decrease in the frequency of γδ T cells was consistently observed for all the groups at 48 hpi, independently of the time of developmental arrest of the parasite used in the infection/immunization.

Overall, of the major adaptive cellular sub-families analysed, NKT (Figure 4.7 (B)) and ILCs (Figure 4.7 (C)) were the ones where most differences were found, either when comparing mice immunized with the different parasites or when comparing to the cellular immune response induced by the regular exo-erythrocytic development of wild-type *P. berghei* parasites. Although repeating this experiment is crucial to confirm the results obtained, it seems that a focused analysis on these cell populations in the liver upon immunizations may be interesting to further explore the role of these cells in the outcome of the different whole-sporozoite immunization approaches.

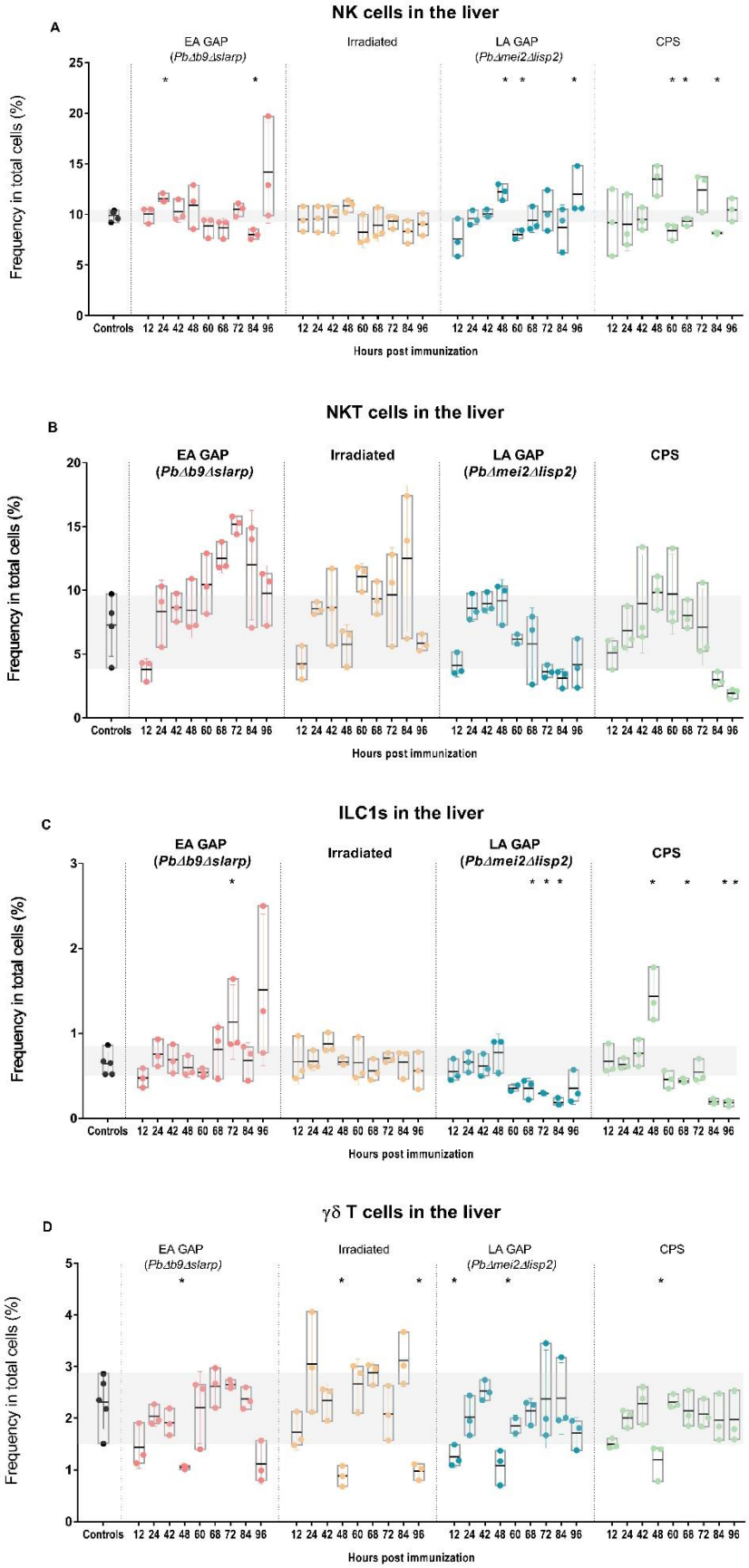

Figure 4.12 Dynamic frequency of NK, NKT, ILC1s and γδ cells in the liver of mice immunized with different whole-sporozoite immunization approaches. NK (A), NKT (B), ILC1s (C) and γδ cells (D) frequency was quantified in isolated leucocytes from the liver of immunized mice via flow cytometry at various time-points post infection. Non-immunized mice were used as controls, data of one experiment are expressed as individual values o of each cell type, mean and SD at each time-point. (Controls, n=5; 24h, n=3; 42h, n=3; 48h, n=3; 60h, n=3; 68h, n=3; 72h, n=3; 84h, n=3; 96h, n=3).

The presence of myeloid cells in the liver was also assessed by flow cytometry: macrophages, monocytes and neutrophils were quantified in the mice liver extracts collected at the various time-points post infection/immunization with the various attenuated parasites.

The results indicate an increase in the frequency of macrophages (Figure 4.13. (A)) and pro-inflammatory monocytes (Figure 4.13. (B)) from 68 hpi onwards. This is probably the result of the recruitment of phagocytic cells to the site of infection, the liver, to clear up infected and apoptotic hepatocytes, which does not occur in the EA-GAP or irradiated groups, as in those cases the parasites are no longer present in the liver of the mice at these time-points (Figure 4.1. (B), (C)). The same pattern is also observed for patrolling monocytes (Figure 4.13 (C)) and neutrophils (Figure 4.13 (D)), in the WT, LISP and CPS groups, with the increase of the frequency of these cells being more pronounced in liver of mice immunized with WT sporozoites and with CPS immunization.

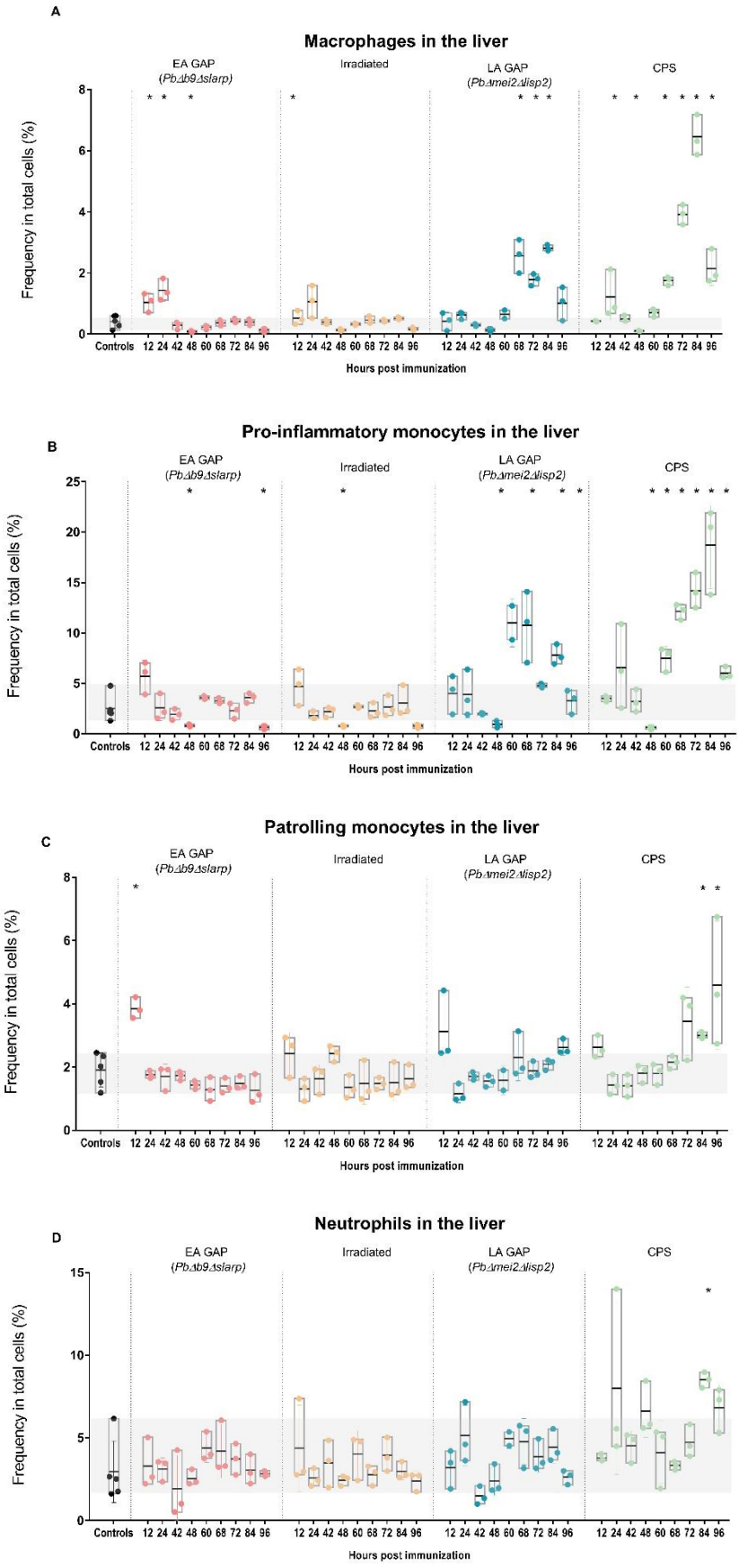

Figure 4.13 Dynamic frequency of myeloid cells in the liver of mice immunized with different whole-sporozoite immunization approaches. Macrophages **(A),** Pro-inflammatory monocytes **(B),** patrolling monocytes **(C)** and neutrophils **(D)** frequency was quantified in isolated leucocytes from the liver of immunized mice via flow cytometry at various time-points after infection. Non-immunized mice were used as controls, data of one experiment are expressed as individual values o of each cell type, mean and SD at each time-point. (Controls, n=5; 24h, n=3; 42h, n=3; 48h, n=3; 60h, n=3; 68h, n=3; 72h, n=3; 84h, n=3; 96h, n=3).

The quantification of IFN-γ production by the different sub-families of immune cells in the liver of whole-sporozoite-immunized mice was also assessed, starting with $CD4^+$ and $CD8^+$ T cells, using the same intracellular staining protocol as that used for mice infected with wild-type parasites (Figure 4.14).

Our results indicate that the overall temporal dynamics of IFN-γ production is similar for CD4+ and CD8+ T cells in the various immunization regimens analyzed. Production of IFN-γ appears to have a first peak between 12/24 hpi, followed by a return to basal levels for all immunizations, except in CPS-immunized mice, where IFN-γ production increases again from 68 hpi onwards, following a pattern similar to that observed in the liver of mice infected with wild-type parasites (Figure 4.9).

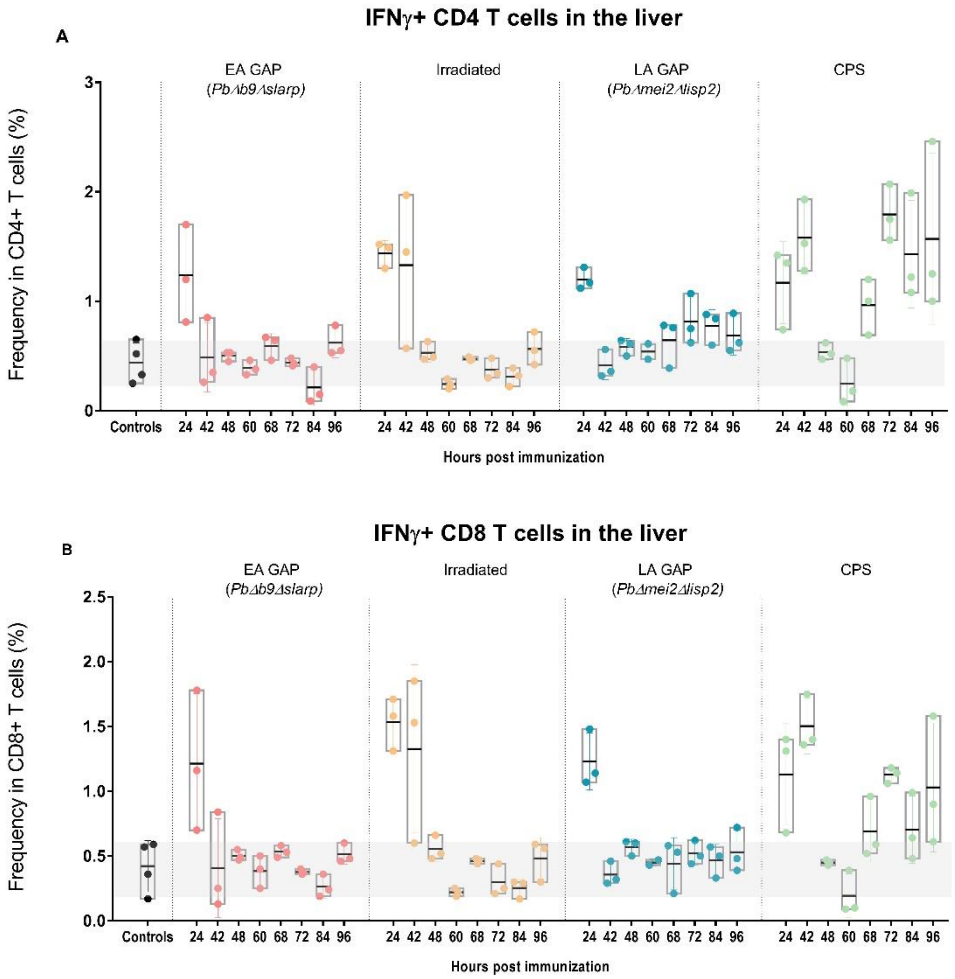

Figure 4.14 Dynamic frequency of IFN-γ production by CD4+ and CD8+ T cells in the liver of mice immunized with different whole-sporozoite vaccination approaches. The presence of IFNγ+ cells in certain cell populations was assessed by flow cytometry: CD4+ T cells **(A),** CD8+ T cells **(B).** Non-immunized mice were used as controls, data of one experiment are expressed as individual values o of each cell type, mean and SD at each time-point. (Controls, n=5; 24h, n=3; 42h, n=3; 48h, n=3; 60h, n=3; 68h, n=3; 72h, n=3; 84h, n=3; 96h, n=3).

A similar pattern of IFN-γ production was observed for the remaining cellular sub-families analysed, which included NK, NKT, ILC1s and γδ T cells (Figure 4.15). This appears to indicate that, after an initial peak of IFN-γ that is independent of the immunizing parasite used, the stage of parasite development dictates the increase in IFN-γ levels, with completion of liver stage development and release of parasite to circulation triggering a massive increase in IFN-γ production. Such an increase occurs independently of parasite replication in the blood, as it is observed even in CPS immunization, for which parasites are eliminated immediately after release from the liver.

Interestingly, the increase of IFN-γ production by ILC1s after 68 hpi occurs independently of merosome release from the liver and overall, this sub-family reveals the highest increase in the frequency of IFN-γ expressing cells from all the studied populations.

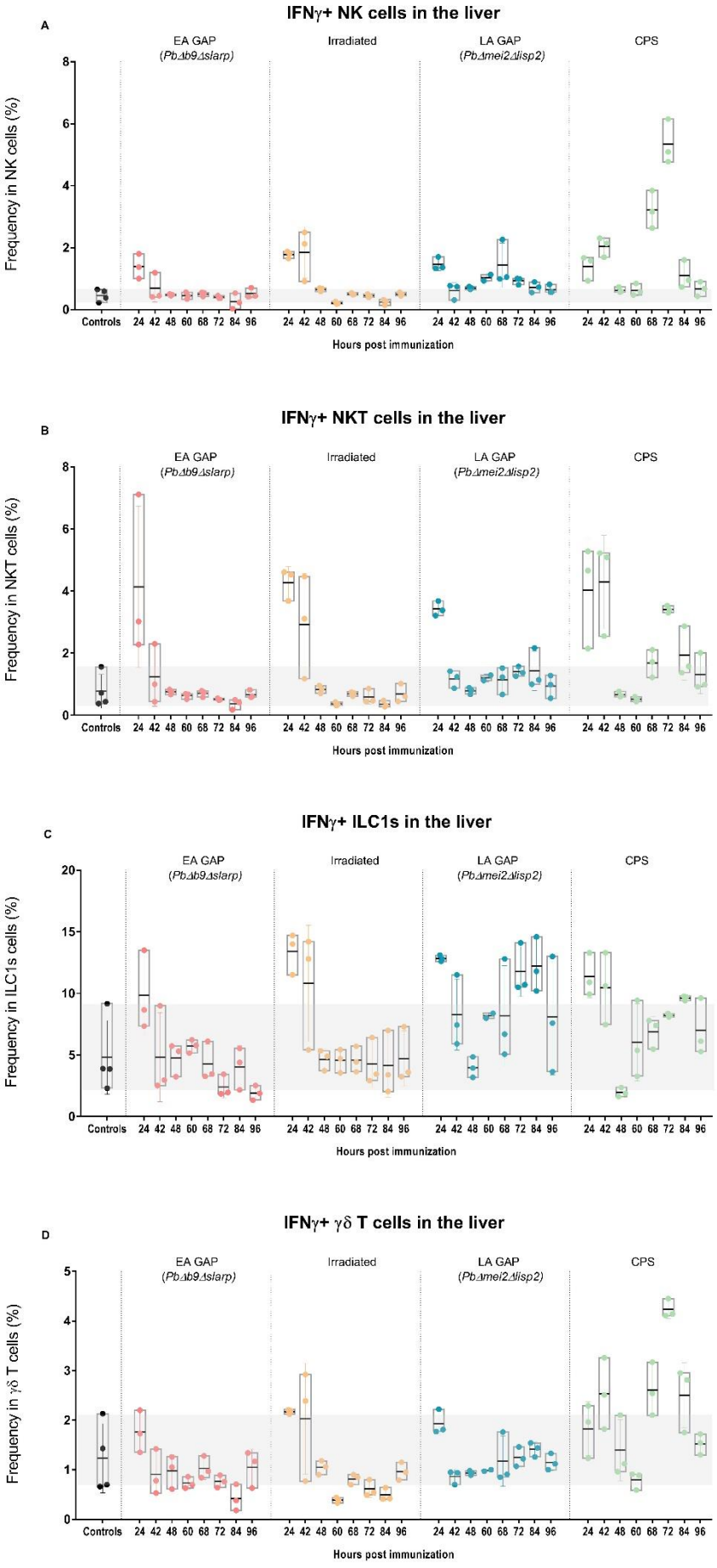

Figure 4.15 Dynamic frequency of IFNγ production by NK, NKT, ILC1s and γδ T cells and in the liver of mice immunized with different whole-sporozoite vaccination approaches. The presence of IFNγ+ cells in certain cell populations was assessed by flow cytometry: NK (A), NKT (B), ILC1s (C) and γδ T cells (D). Non-immunized mice were used as controls, data of one experiment are expressed as individual values of frequency of each cell type, mean and SD at each time-point. (Controls, n=5; 12h, n=3; 24h, n=3; 42h, n=3; 48h, n=3; 60h, n=3; 68h, n=3; 72h, n=3; 84h, n=3; 96h, n=3).

4.2. Protective efficacy of different types of whole-sporozoite vaccines

Protection conferred against a sporozoite challenge by different types of whole-sporozoite immunizations has been studied extensively. Recently, with the creation of a wide variety of EA or LA-GAP parasites, it was suggested that the capacity to induce protection against a new sporozoite challenge is directly related to the extent of the development of the immunizing parasite in the liver. This is justified by the fact that longer development in the liver would lead to a wider and more diverse antigen presentation to the immune system, resulting in a more efficacious method to protect against a sporozoite challenge[59,60]. However, detailed comparative experiments that include the various methods of parasite attenuation are sparse and several studies have put forward indication that the mechanism underlaying the induction of protection by the different methods may be complex. Therefore, upon analysing the liver development and the innate immune response induced by each parasite in the time-course experiments, we aimed to comparatively assess the functionality of these immunization approaches.

To address this issue, 10 independent experiments were performed, where mice were single immunized with a specific dosage of one of the different whole-sporozoite immunizations studied and a week later challenged with 30 000 wild-type *P. berghei* sporozoites.

Firstly, wild-type C57BL/6J mice were immunized with either irradiated sporozoites (irradiated group) or with wild-type sporozoites under daily coverage of chloroquine (CPS group) for the first 5 days post immunization (Figure 4.16). These two types of immunization were chosen as the parasites they employ represent the extremes in terms of parasite development in the liver: irradiated sporozoites can enter liver cells and undergo partial development but cannot undergo nuclear division, arresting their development early in the liver stage[30]; conversely, CPS immunization employs wild-type sporozoites, which develop fully in the liver, but are eliminated by a circulating drug (in this case, chloroquine) as soon as they reach the blood stream. Experimental groups not only differed in the type of immunization used, but also in the sporozoite dosages administered:1000 (1K), 3000 (3K), 5000 (5K), 10 000 (10K) and 30 000 (30K) sporozoites. In this way, we aimed at identifying a dosage conveying over 50% protection but not complete sterile protection for all immunized animals, in order to allow the identification of potential factors improving protection. One week after the immunization, mice were challenged with 30 000 wild-type sporozoites, and for the following 10 days, a sample of blood was collected daily. As the parasites used in this assay are genetically modified to constitutively express a luciferase reporter gene, we were able to analyse the collected blood samples by a bioluminescence assay[62], and determine the presence and quantity of parasites in the blood. Mice were considered sterily protected if no parasites could be detected in the blood until the end of the experiment – 10 days after challenge. Increase in pre-patency time, as conveyed by the time for detection of the first parasites in the blood was also taken into account as a measure of partial protection. Non-immunized but challenged C57BL/6J mice were used as controls and become

positive for blood stage parasites at day 3 post challenge, confirming the viability of the sporozoites used for challenge.

For mice immunized with irradiated sporozoites, we observed an increase in protection which was correlated with the increase in the immunizing dosage used, ranging from no mice protected when immunized with 1000 irradiated sporozoites to 75% of the mice protected when immunized with 30 000 irradiated sporozoites (Figure 4.16 (A, C, E)). Different results were obtained for the CPS group (Figure 4.16 (B, D, F)), in which most of the dosages tested did not confer sterile protection to any of the immunized mice. Furthermore, no correlation could be found between the sporozoite dosage used for immunization and protection, with a 10% protection rate observed for mice immunized with the lowest dosage (1000 sporozoites) and ~5% protection rate observed for the highest dosage tested (30 000 sporozoites).

Overall comparison indicates that immunization with irradiated sporozoites leads to a higher rate of protection than CPS immunization independently of the sporozoite dosage employed. These immunization approaches present substantial differences, specifically in the extent of parasite development in the liver (Figure 4.4 (B), (D)) and the type I IFN responses induced after the immunization (Figure 4.5 (B), (D)). As mentioned above, upon immunization with irradiated sporozoites, mice do not display a significant induction of any of the six ISGs assessed as a surrogate for type I IFN activation at any of the assayed time-points. Contrarily, CPS-immunized mice display a type I IFN response that is very similar to that observed in a wild-type infection, including a first wave of induction with ~2-fold increase of ISG expression at 42 hpi and a second wave of induction between 68 and 84 hpi, reaching a maximum of ~9-fold induction.

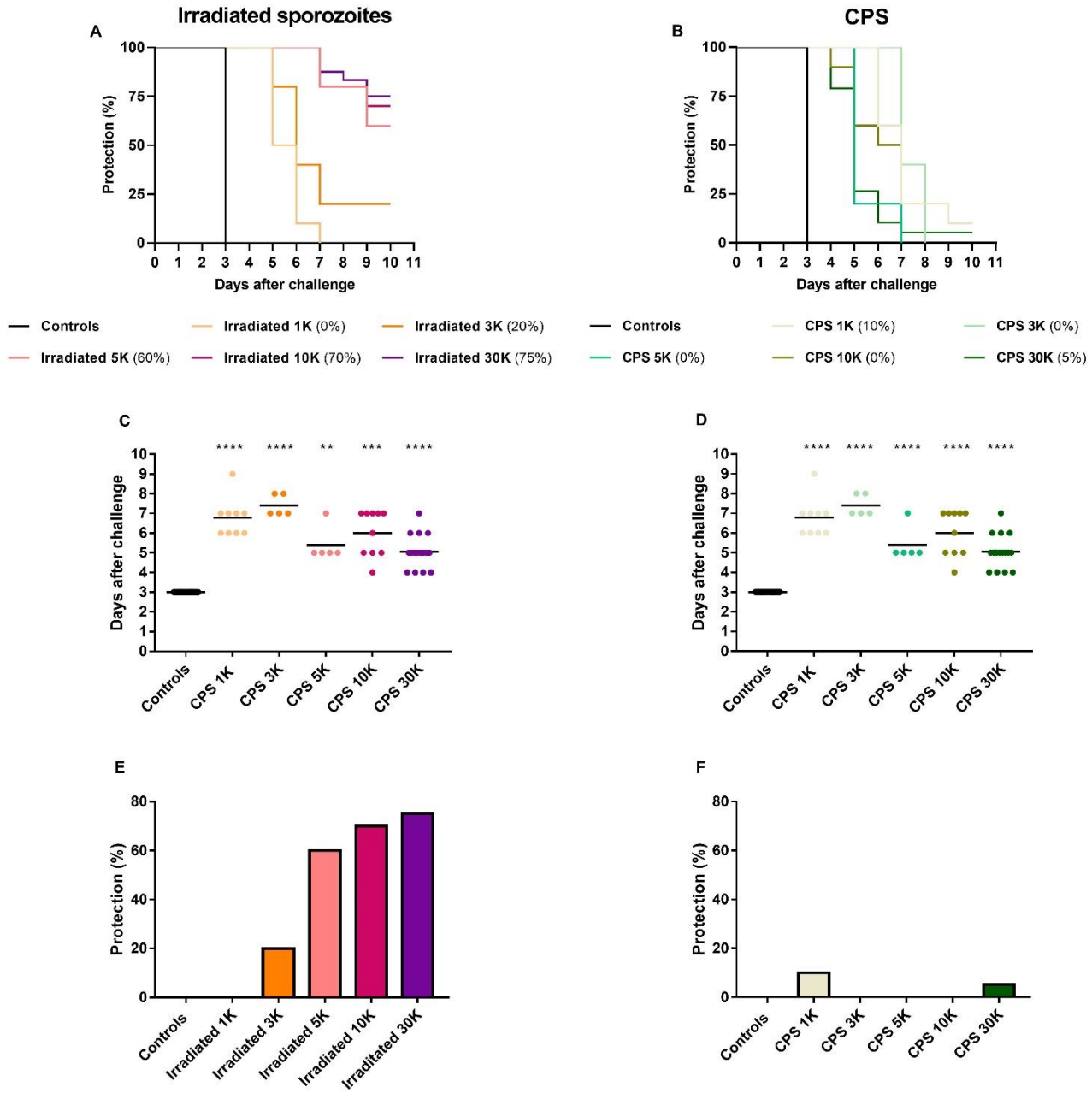

Figure 4.16 Protection curves after a sporozoite challenge of mice immunized with several doses of either Irradiated sporozoites or wild-type sporozoites under the administration of chloroquine. Mice were immunized with different dosages of either Irradiated sporozoites (A, C, E) or wild-type sporozoites under the administration of chloroquine (CPS) (B, D, F). A week after the immunization all mice were challenged with an injection of 30 000 wild-type *P. berghei* sporozoites and a blood bioluminescence assay was performed in blood samples collected daily until 10 days post challenge to assess the presence of parasites in the blood. Protection status of the immunized mice along the experiment (A,B); days at which non-protected became positive for parasites in their blood (C,D); protection conferred by each type of immunization according to the dosage employed (E,F). Mice were considered not protected when the bioluminescence assay was positive. Data are presented as the percentage of mice protected in each experimental group of ten independent experiments (A, B, E, F) or as the days at which individual mice became positive for parasites in the blood (C, D). (Controls, n=32; Irradiated 1K, n=10; Irradiated 3K, n=5; Irradiated 5K, n=5; Irradiated 10K, n=5; Irradiated 30K, n=24; CPS 1K, n=10; CPS 3K, n= 5; CPS 5K, n=5; CPS 10K, n=10; CPS 30K, n=19).

A dosage of 30 000 sporozoites per immunization was selected to compare the overall protective efficacy of different immunization approaches. At this stage, two groups were added to the experimental design: immunization with EA-GAP (*PbΔb9Δslarp*) and LA-GAP (*PbΔmei2Δlisp2*) parasites. (Figure 4.17 (A)). The experiments conducted revealed that with a dosage of 30 000 sporozoites/immunization, the irradiated group is, once again, the group that presents the highest rate of protection, with 75% of mice protected at day 10. The LA-GAP group follows closely with 73% of mice protected. Lastly, the EA-GAP and CPS groups are the ones with lower rates of protection, with 9% and 5% of mice protected, respectively.

Previously published literature indicates that the protective capacity of an immunization approach is directly related to the extent of parasite development in the liver, with parasites that complete their development and replication in the liver being significantly better at conferring protection against a sporozoite challenge, with either one or two immunizations employed[60]. Ultimately, the CPS immunization approach uses live non-attenuated parasites that exit the liver and only are eliminated in the blood, conferring the highest level of protection ever recorded, when in a regimen of three immunizations employed. According to our liver development analysis (Figure 4.4), the EA-GAP (*PbΔb9Δslarp*), is the parasite that arrests its development earliest in liver, followed by irradiated parasites and lastly by the LA-GAP (*PbΔmei2Δlisp2*). When comparing the protective efficacy of these three immunization approaches, using the experimental protocol previously mentioned (one single immunization followed by a challenge a week later), our results appear to be in partial agreement with what was previously observed, as EA-GAP parasites are the ones presenting the least liver development and protecting only 9% of the mice, while irradiated and LA-GAP parasite development is longer and their conferred protection is of 75% and 73% of mice, respectively. Nonetheless, it is interesting to note that although the massive difference in replication capacity between irradiated sporozoites and LA-GAP parasites, their overall protective capacity is similar. Furthermore, CPS immunization that should confer the highest level of protection in accordance to previous literature, only provides a small rate of protection (5%) that is comparable to that observed for the least developing parasites, the EA-GAP parasites.

Overall, analysis of the results presented in figure 4.17 taking into account specific parasite development as presented in figure 4.4, appears to indicate that: a) there is a fine threshold of minimal parasite development in the liver to generate an effective immune response, as immunization with EA-GAP (*PbΔb9Δslarp*) parasites and irradiated sporozoites show small differences in liver stage development but elicits distinct protection rates; b) parasite exit from the liver and exposure to parasite blood stages may have a negative impact on the induction of protection, as immunization with LA-GAP parasites confers higher protection rates than immunization with CPS.

Given that parasite exit of the liver leads to the induction of a massive type-I IFN response, which is not observed when parasites arrest their development in the liver (Figure 4.5), we hypothesized that such potential negative effect in the establishment of protection could be a

direct consequence of this induction, contributing to the decreased efficacy observed for the CPS immunization approach.

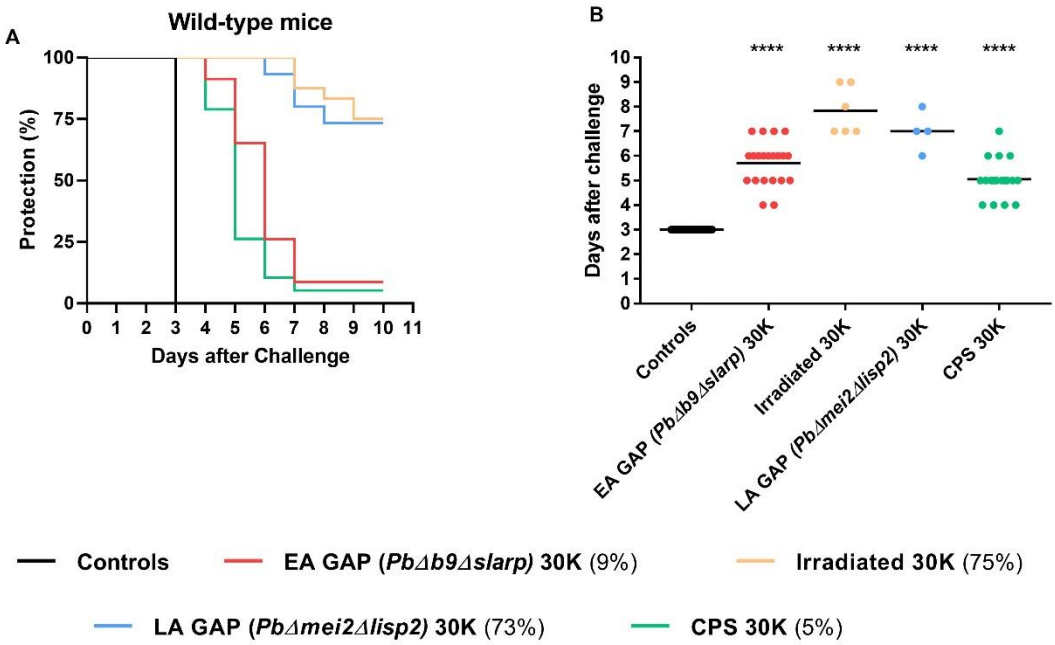

Figure 4.17. Protection curves for mice immunized with different whole-sporozoite immunization approaches. Wild-type C57BL/6J mice were immunized with different whole-sporozoite immunization approaches: Irradiated sporozoites, EA-GAP *PbΔb92Δslarp* sporozoites, LA-GAP *PbΔmei2Δlisp2* sporozoites, and CPS. All the experimental groups received the same dosage of immunization: 30 000 sporozoites. A week after the immunization all mice were challenged with an injection of 30 000 wild-type *P. berghei* sporozoites. A blood bioluminescence assay was performed in blood samples collected daily until 10 days post challenge to assess the presence of parasites in the blood. Protection status of the immunized mice along the experiment **(A)** and days at which non-protected became positive for parasites in their blood **(B).** Mice were considered not protected when the bioluminescence assay was positive. Data are presented as the percentage of mice protected in each experimental group of ten independent experiments. (Controls, n=32; EA-GAP, n=23; Irradiated 30K, n=24; LA-GAP 30K, n=15; CPS 30K, n=19)

To explore this hypothesis, *Ifnar1*$^{-/-}$ mice were employed in a similar immunization-challenge experimental design, receiving a dosage of 30 000 sporozoites, either irradiated, EA-GAP (*PbΔb9Δslarp*) or live non attenuated under chloroquine cover- CPS. These mice were challenged with 30 000 wild-type sporozoites one week after immunization and parasite appearance in the blood was monitored by luminescence. Unfortunately, due to technical issues, it was not possible to conduct the experiment using a group of *Ifnar1*$^{-/-}$ mice immunized with LA-GAP (*PbΔmei2Δlisp2*) parasites in this experiment (Figure 4.18).

A comparison of the results obtained using the same immunization approach and dosage for either wild-type (Figure 4.17) or *Ifnar1*$^{-/-}$ mice (Figure 4.18), shows that: (i) irradiated parasites completely lose their ability to protect against a sporozoite challenge in the absence of type I IFN, decreasing from 75% sterile protected wild-type mice to 0% protection in *Ifnar1*$^{-/-}$ mice; (ii) the EA-GAP also fails to provide any protection to *Ifnar1*$^{-/-}$ mice, decreasing from 9% protection in wild-type mice to 0% protection in *Ifnar1*$^{-/-}$ mice; and (iii) the CPS immunization approach is more

efficacious in the absence of a type I IFN response, protecting 25% of *Ifnar1*$^{-/-}$ mice from a challenge, compared to 5% of wild-type mice protected.

These results suggest a dual role for the type I IFN response. First, for immunization approaches with EA-GAP parasites or irradiated sporozoites, which do not induce a strong type I IFN response and where a second wave of type I IFN induction never occurs (Figure 4.5)), type I IFN response contributes positively for protection, since this immunization approaches fail in *Ifnar1*$^{-/-}$ mice. Second, for CPS immunization approach, which induces a strong type I IFN response occurs with two waves of induction (Figure 4.5), type I IFN response appears to negatively impact the outcome of the vaccination, which leads to better results *Ifnar1*$^{-/-}$ mice.

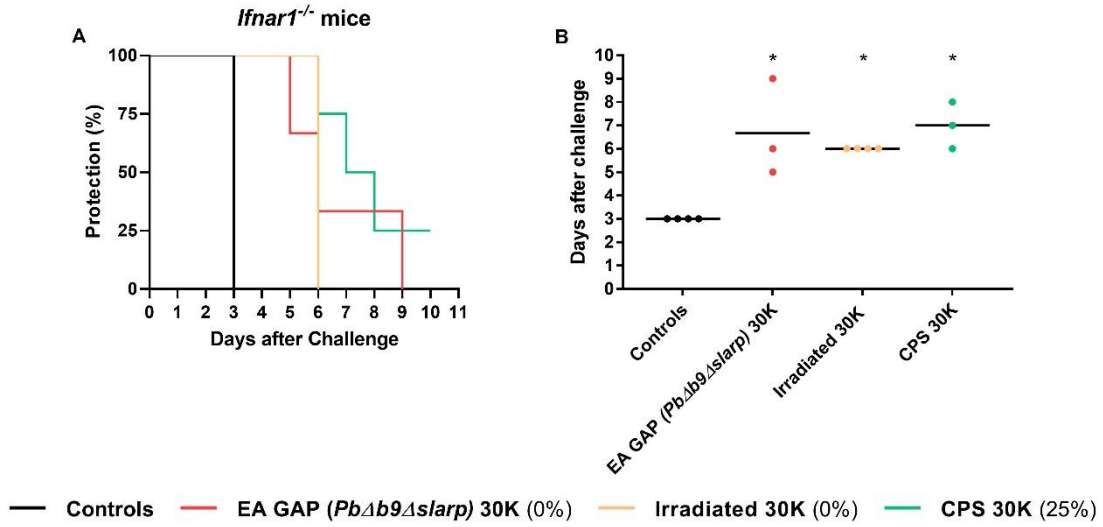

Figure 4.18 Protection curves for *Ifnar1*$^{-/-}$ mice immunized with different whole-sporozoite immunization approaches. *Ifnar1*$^{-/-}$ mice were immunized with different whole-sporozoite immunization approaches: Irradiated sporozoites, EA-GAP *PbΔb92Δslarp* sporozoites and CPS. All the experimental groups received the same dosage of immunization: 30 000 sporozoites. A week after the immunization all mice were challenged with an injection of 30 000 wild-type *P. berghei* sporozoites. A blood bioluminescence assay was performed in blood samples collected daily until 10 days post challenge to assess the presence of parasites in the blood. Protection status of the immunized mice along the experiment **(A)** and days at which non-protected became positive for parasites in their blood **(B).** Mice were considered not protected when the bioluminescence assay was positive. Data are presented as the percentage of mice protected in each experimental group of ten independent experiments. (Controls, n=4; EA-GAP, n=3; Irradiated 30K, n=4; CPS 30K, n=4)

Lastly, we aimed to improve the efficacy of whole-sporozoite malaria vaccines by inducing the specific activation of innate immune responses during immunization. We hypothesized that the expression of flagellin, a known vaccine adjuvant that activates pathways in the innate immune system of mice and humans [67] during *Plasmodium* liver stage development, could lead to the induction of a stronger immune response and consequently achieve higher protection rates. This would have a similar effect as the addition of an adjuvant during immunization but warrant that its presentation was directed to the correct target, the liver. To test

this hypothesis, we used a LA *P. berghei* GAP with a single knocked-out gene– *mei2, PbΔmei2.* In this LA-GAP parasite, the target KO gene, *mei2* was either replaced by a cassette encoding the expression of a GFP/luciferase gene or by a the flagellin gene, making two distinct parasite lines, both lacking the mei2 gene but expressing (FLAG) or not the flagellin gene (*PbΔmei2)*.

Mice were immunized with either 30 000 *PbΔmei2* or 30 000 FLAG sporozoites and, one week later, challenged with 30 000 wild-type *P. berghei* sporozoites, blood collection and evaluation of parasitaemia was done in a similar fashion of the previous experiments. Fifty % of the mice immunized the *PbΔmei2*and and 56% of the mice immunized with *PbΔmei2* FLAG were sterily protected, respectively. These results do not show a significant difference in the protection conferred by the two parasites. However, it is important to note that this is a single biological replicate and repetition of this experiment is essential to validate these results and confirm that expressing flagellin in the genome of GAPs can improve the efficacy of the immunization.

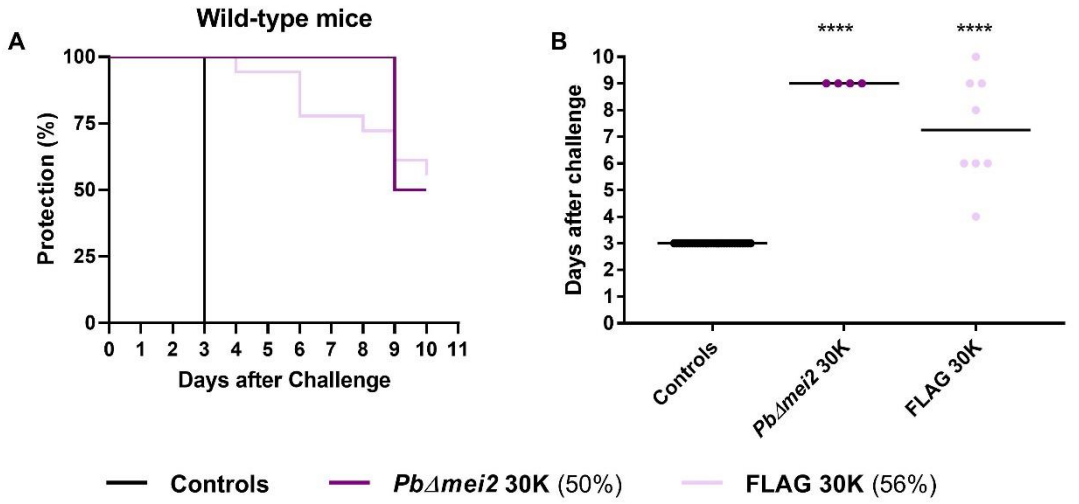

Figure 4.19 Protection curves for mice immunized with *PbΔmei2* or FLAG parasites. Wild-type C57BL/6J mice were immunized with either 30 000 MEI or 30 000 FLAG sporozoites. One week after the immunization all mice were challenged with an injection of 30 000 wild-type *P. berghei* sporozoites. A blood bioluminescence assay was performed in blood samples collected daily until 10 days post challenge to assess the presence of parasites in the blood. Protection status of the immunized mice along the experiment (A) and days at which non-protected became positive for parasites in their blood (B). Mice were considered not protected when the bioluminescence assay was positive. Data are presented as the percentage of mice protected in each experimental group of ten independent experiments. (Control, n=32; MEI 30K, n=8; FLAG 30K, n=18)

5. Conclusions and Future Work

The need for a reliable malaria vaccine is urgent as this infectious disease is a major health concern that affects hundreds of millions of people worldwide. Despite decades of efforts to find an efficacious vaccine conferring long lasting sterile immunity against malaria, such objective has yet to be accomplished. The most promising approach to immunize against malaria is to use whole-sporozoite vaccines. In order to create a successful whole-sporozoite vaccine it is essential to understand the immune responses that are at the basis of their action.

We proposed to study extensively the immune responses elicited upon immunization with various whole-sporozoite immunization approaches, using *P. berghei* parasites as a model of infection, and focusing specifically on: i) characterizing the extent of liver stage of development for each whole-sporozoite vaccination approach; ii) evaluating the dynamic activation of type I IFN innate immune responses in the liver upon immunization; iii) analysing the temporal dynamics of immune cellular recruitment and activation in the liver following an immunization and iv) assessing the level of protection conferred by each type of whole-sporozoite vaccine against a sporozoite challenge. To this end, several types of whole-sporozoite vaccines were employed in this work: irradiated sporozoites, genetically attenuated sporozoites that arrest early (EA-GAP) or late (LA-GAP) during the liver stage of development, and immunization with wild-type sporozoites under the administration of chemoprophylaxis (CPS). As control, mice were infected with wild-type *P. berghei* sporozoites.

Given its exploratory nature, the work in this dissertation did not aim to solve a specific problem or answer specific questions. Instead, it aimed to broaden the knowledge about the immune mechanisms behind whole-sporozoite vaccines. Hence, the conclusions presented here focus on the most relevant differences found between those immune responses and efficacy of the different whole-sporozoite immunizations approaches and on what can be done in the future to confirm such results or further explore interesting findings.

The results obtained for the characterization of the liver stage development for each whole-sporozoite vaccination approach tested are in accordance with what was expected. Wild-type *P. berghei* parasites replicate extensively in the liver until 48 hpi and a decrease in liver burden is subsequently observed, corresponding to the egress of parasites from the liver at approximately 56-58 hpi. Parasite liver burden increases again at ~96 hpi as parasites replicate abundantly in the blood. Parasites that arrest early in the liver stage of development such as irradiated and *PbΔb9Δslarp* parasites are only present in the liver of mice until 12/24 hpi. Parasites that arrest late in the liver stage, such as *PbΔmei2Δlisp2*, or those that fully develop in the liver and are then eliminated in the blood, such as the CPS approach, present a development similar to that of wild-type parasites until 72 hpi. After this time-point, the liver load in mice

immunized with such parasites decreases as a result of their developmental arrest or their elimination in the blood, respectively. Characterizing the liver stage development was essential to relate the extent to which the different parasites develop in the liver to the immunological effects of each type of whole-sporozoite vaccination approach.

When in the host's liver, malaria parasites, elicit a type I IFN immune response [47,48] that is capable of eliminating parasites and decrease re-infection. A characterization of type I IFN activation and of the magnitude of response upon immunization in mouse livers was performed for the various whole-sporozoite approaches tested, by evaluating the expression levels of six previously identified IFN-stimulated genes (ISGs). Results indicate that infection with wild-type *P. berghei* sporozoites leads to two waves of induction of ISGs, at 42 hpi (~2-fold induction) and at 84 hpi (~20-fold induction), as previously described by Liehl *et al*[47]. Immunization with EA-GAP parasites results in only a first induction at 42 hpi or none at all, in mice immunized with *PbΔb9Δslarp* and irradiated parasites, respectively. Immunization with LA-GAP (*PbΔmei2Δlisp2)* and CPS leads to two waves of induction, with the second one occurring earlier and at with a lower magnitude (~2-fold induction for *PbΔmei2Δlisp2* and ~9-fold induction for CPS immunized mice) compared to infection with wild-type parasites.

Analysis of the frequency of leucocyte populations in the liver of mice immunized with different whole-sporozoite vaccines revealed significant differences in the frequency of NKT cells. Until 42 hpi, all experimental groups showed a tendency for an increased frequency of these cells, which continues to increase even further in mice immunized with EA parasites, such as *PbΔb9Δslarp* and irradiated parasites, until 84 hpi. Conversely, the frequency of NKT cells in the livers of mice immunized with the LA parasite *PbΔmei2Δlisp2* or with parasites that fully develop in the liver (CPS) decreases after 42 hpi to values lower than basal levels at 96 hpi, similarly to what was observed for mice infected with wild-type *P. berghei* parasites. NKT cells have been shown to be relevant for type I IFN cell signalling, cell recruitment and clearance of liver stage *Plasmodium* parasites[48], particularly in the context of reinfection. Our results suggest that this cell subfamily may also be important during immunization and further experiment should be carried out to better characterize their role in relation to the establishment of protection.

Previous studies have established a direct correlation between the extent of liver development of parasites used for whole-sporozoite immunization and their capacity to protect against a subsequent sporozoite challenge. The reason proposed for this phenomenon is that the longer liver development associates with the presentation of a larger and more diverse set of antigens to the immune system, resulting in more efficacious vaccines[59]. We next proposed to compare and correlate the developmental and immunological data obtained for each type of whole-sporozoite immunizations with its protective capacity. For this, we set up immunization-challenge experiments were the schedule and dosage of immunization as well as challenge was similar for all the approaches.

First, we compared the protection conferred by immunizations with irradiated sporozoites or CPS in mice using an array of dosages between 1000 and 30 000 sporozoites in a single

immunization, followed one week later by a challenge with 30 000 wild-type sporozoites. It is clear that irradiated sporozoites confer better protection and are more efficacious than CPS in the experimental protocol employed. It is also clear that the protection conferred by irradiated sporozoites increases in accordance with the parasite dosage, achieving the highest protection rate at the highest dose tested (30 000 sporozoites). This dosage was then selected for further comparisons between other whole-sporozoite immunization approaches.

The data collected in these experiments revealed that, with a single immunization dosage of 30 000 sporozoites followed by a challenge of identical magnitude 7 days later, immunizations with irradiated parasites or with LA-GAP (*PbΔmei2Δlisp2)* are the most successful, conferring 75% and 73% of protection, respectively. Conversely, immunization with EA-GAP (*PbΔb9Δslarp)* or CPS resulted in lower protection rates, of 9% and 5%, respectively.

Taking into consideration the extent of liver stage development, from shorter which is *PbΔb9Δslarp*, followed by irradiated sporozoites with slightly longer development, to *PbΔmei2Δlisp2*, which complete their liver stage replication but do not exit from the liver, our results indicate that in these immunization approaches, the longer a parasite develops in the liver, the higher the protective rate observed. However, the results obtained for CPS immunization with the present protocol, in which parasites are eliminated after exiting the liver, appears to be in clear opposition to this correlation and in direct contrast to what has been previously reported.

We hypothesize that exiting of parasites to the blood negatively affects the outcome of the vaccination but further experiments are required to demonstrate this hypothesis. One proposed experiment to confirm this hypothesis could combine immunization with irradiated sporozoites and injection of *P.berghei* blood stages at the predicted time of merosome release to mimic parasite egress from the liver, while receiving a daily dose of chloroquine to prevent infection, mimicking CPS immunization conditions. Such an experiment would mimic parasite blood stage infection as observed in CPS immunization but using irradiated sporozoites. If the efficacy of the immunization with irradiated sporozoites plus the administration of blood stage parasites is lower than when mice are immunized with irradiated sporozoites only, and similar to when mice are immunized with CPS, it would be possible to ascertain whether the presence of blood stage parasites negatively impacts the efficacy of immunization.

Additionally, a correlation between the specific immune responses induced by immunization and their protective capacity, suggest that the strong induction of type I IFN response observed specifically for CPS-immunized mice late during liver stage development may also be at the basis of its lack of protective efficacy. To assess whether the type I IFN response was deleterious for the efficacy of the whole-sporozoite immunizations studied, a similar immunization and challenge experiment was conducted in *Ifnar1*$^{-/-}$ mice. The results obtained from this experiment indicated that CPS immunization resulted in higher protection rates in *Ifnar1*$^{-/-}$ mice, confirming that the type I IFN response has a negative impact on this type of immunization. On the other hand, *PbΔb9Δslarp* and irradiated sporozoites, when employed in *Ifnar1*$^{-/-}$ mice, completely lost their ability to sterile protect mice from a sporozoite challenge, suggesting that

type I IFN response is essential for the success of both immunizations. Because our ISG expression analysis revealed that both these immunizations failed to induce a strong expression of the panel of ISGs tested, we did not expect that the abrogation of type I IFN response affected the outcome of these immunizations. Therefore, we question the power of analysis of our assay to measure type I IFN activation, as the six ISGs chosen as a surrogate measure of the activation of type I IFN response may not be sufficient to evaluate the full activation of this pathway. To further examine the type I IFN response elicited by the various immunizations, techniques such as RNA sequencing or micro-arrays can be employed to analyse a broader set of genes that may better reflect the activation of the type I IFN response. Furthermore, a time-course experiment similar to the ones performed in this work can be conducted in *Ifnar1*$^{-/-}$ mice to reveal the differences between the cellular recruitment that occurs in the liver upon immunization with the different whole-sporozoite vaccinations in the absence of a type I IFN response.

Further exploring the effect of the expression of adjuvant proteins in malaria GAPs is also an important task, as adjuvants may strongly contribute for the improvement of vaccines' efficacy. In this work, we used a flagellin-expressing GAP to immunize mice but did not observe a significant increase in protection when comparing to mice immunized with the non-expressing flagellin GAP. However, these results were derived from a single biological replicate and repeating this experiment is essential to understand if an adjuvant presented directly to the liver can increase the efficacy of GAP immunizations, as expected.

Using other anti-malarial drugs that act against blood stage parasites instead of chloroquine in similar experiments as the ones performed can be useful to discard any secondary effects interfering in the immune response that might result from the drug itself rather than the CPS approach at whole-sporozoite immunizations.

Altogether, the results presented in this dissertation contribute for the understanding of the immunological responses elicited upon different whole-sporozoite immunizations and how these can contribute for their efficacy. The characterization of the parasite's liver development and of the immune responses elicited by the different parasites used in whole-sporozoite immunizations allowed for its correlation with the efficacy achieved by each approach, against a sporozoite challenge. This work is only the beginning of the characterization of complex immune mechanisms triggered by these vaccines and it must be considered as a gateway for raising new questions and pursuing novel interesting findings.

6. References

1. World Health Organization. *World Malaria Report 2018*. (2018).
2. Sachs, J. & Malaney, P. The economic and social burden of malaria. *Nature* **415**, 680–685 (2002).
3. Singh, M. P., Saha, K. B., Chand, S. K. & Sabin, L. L. The economic cost of malaria at the household level in high and low transmission areas of central India. *Acta Trop.* **190**, 344–349 (2019).
4. Amino, R., Thiberge, S., Shorte, S., Frischknecht, F. & Ménard, R. Quantitative imaging of Plasmodium sporozoites in the mammalian host. *C. R. Biol.* **329**, 858–62 (2006).
5. Cowman, A. F., Healer, J., Marapana, D. & Marsh, K. Malaria: Biology and Disease. *Cell* **167**, 610–624 (2016).
6. Amino, R. *et al.* Quantitative imaging of Plasmodium transmission from mosquito to mammal. *Nat Med* **12**, 220–224 (2006).
7. Pinzon-Ortiz, C., Friedman, J., Esko, J. & Sinnis, P. The Binding of the Circumsporozoite Protein to Cell Surface Heparan Sulfate Proteoglycans is Required for Plasmodium Sporozoite Attachment to Target Cells. *J. Biol. Chem.* **276**, 26784–26791 (2001).
8. Prudêncio, M., Rodriguez, A. & Mota, M. M. The silent path to thousands of merozoites: The Plasmodium liver stage. *Nat. Rev. Microbiol.* **4**, 849–856 (2006).
9. White, N. J. *et al.* Malaria. *Lancet* **383**, 723–735 (2014).
10. Zuzarte-Luis, V., Mota, M. M. & Vigário, A. M. Malaria infections: What and how can mice teach us. *J. Immunol. Methods* 1–10 (2014). doi:10.1016/j.jim.2014.05.001
11. Goh, Y. S., McGuire, D. & Rénia, L. Vaccination With Sporozoites: Models and Correlates of Protection. *Front. Immunol.* **10**, 1–18 (2019).
12. Cowman, A. F., Tonkin, C. J., Tham, W. H. & Duraisingh, M. T. The Molecular Basis of Erythrocyte Invasion by Malaria Parasites. *Cell Host Microbe* **22**, 232–245 (2017).
13. Ghosh, A., Edwards, M. J. & Jacobs-Lorena, M. The journey of the malaria parasite in the mosquito: Hopes for the new century. *Parasitol. Today* **16**, 196–201 (2000).
14. Wangai, L. N. *et al.* Sensitivity of microscopy compared to molecular diagnosis of p. Falciparum: implications on malaria treatment in epidemic areas in kenya. *African J. Infect. Dis.* **5**, 1–6 (2011).
15. Mouatcho, J. C. & Dean Goldring, J. P. Malaria rapid diagnostic tests: Challenges and prospects. *J. Med. Microbiol.* **62**, 1491–1505 (2013).
16. Krampa, F., Aniweh, Y., Awandare, G. & Kanyong, P. Recent Progress in the Development of Diagnostic Tests for Malaria. *Diagnostics* **7**, 54 (2017).
17. Miller, L. H., Good, M. F. & Milon, G. Malaria pathogenesis. *Cold Spring Harb. Perspect. Med.* **8**, a025569 (2017).
18. Ross, L. S. & Fidock, D. A. Elucidating Mechanisms of Drug-Resistant Plasmodium falciparum. *Cell Host Microbe* **26**, 35–47 (2019).
19. Flannery, E. L., Chatterjee, A. K. & Winzeler, E. a. Antimalarial drug discovery - approaches and progress towards new medicines. *Nat. Rev. Microbiol.* **11**, 849–62 (2013).

20. Lobo, N. F., Achee, N. L., Greico, J. & Collins, F. H. Modern vector control. *Cold Spring Harb. Perspect. Med.* **8**, (2018).

21. Ranson, H. Preventing Malaria Transmission via the Use of Insecticides. *Cold Spring Harb. Perspect. Med.* **7**, 1–12 (2017).

22. Beeson, J. G. *et al.* Challenges and strategies for developing efficacious and long-lasting malaria vaccines. *Sci. Transl. Med.* (2019). doi:10.1126/scitranslmed.aau1458

23. Wilson, K. L., Flanagan, K. L., Prakash, M. D. & Plebanski, M. Malaria vaccines in the eradication era: current status and future perspectives. *Expert Rev. Vaccines* **18**, 133–151 (2019).

24. Greenwood, B. M. Efficacy and safety of RTS,S/AS01 malaria vaccine with or without a booster dose in infants and children in Africa: Final results of a phase 3, individually randomised, controlled trial. *Lancet* **386**, 31–45 (2015).

25. Mendes, A. M. *et al.* Whole-Sporozoite Malaria Vaccines. in *Malaria Immune Response to Infection and Vaccination* (eds. Mota, M. M. & Rodriguez, A.) 99–137 (Springer, 2017).

26. Mendes, A. M. *et al.* A Plasmodium berghei sporozoite-based vaccination platform against human malaria. *npj Vaccines* **3**, (2018).

27. Nussenzweig, R. S., Vanderberg, J. P., Most, H. & Orton, C. Protective Immunity produced by the Injection of X-irradiated Sporozoites of Plasmodium Berghei. (1967).

28. Clyde, D. F., McCarthy, V. C., Miller, R. M. & Hornick, R. B. Specificity of protection of man immunized against sporozoite-induced falciparum malaria. *the American Journal of the Medical Sciences* **266**, 398–404 (1973).

29. Hoffman, S. L. *et al.* Protection of humans against malaria by immunization with radiation-attenuated Plasmodium falciparum sporozoites. *J. Infect. Dis.* **185**, 1155–1164 (2002).

30. Silvie, O. *et al.* Effects of irradiation on Plasmodium falciparum sporozoite hepatic development: implications for the design of pre-erythrocytic malaria vaccines. *Parasite Immunol.* **24**, 221–3 (2002).

31. Seder, R. a *et al.* Protection against malaria by intravenous immunization with a nonreplicating sporozoite vaccine. *Science* **341**, 1359–65 (2013).

32. Ishizuka, A. S. *et al.* Protection against malaria at 1 year and immune correlates following PfSPZ vaccination. *Nat. Med.* **22**, 614–623 (2016).

33. Jongo, S. A. *et al.* Safety, immunogenicity, and protective efficacy against controlled human malaria infection of plasmodium falciparum sporozoite vaccine in Tanzanian adults. *Am. J. Trop. Med. Hyg.* **99**, 338–349 (2018).

34. Vaughan, A. M., Wang, R. & Kappe, S. H. I. Genetically engineered, attenuated whole-cell vaccine approaches for malaria. *Hum. Vaccin.* **6**, (2010).

35. Mueller, A.-K., Labaied, M., Kappe, S. H. I. & Matuschewski, K. Genetically modified Plasmodium parasites as a protective experimental malaria vaccine. *Nature* **433**, 164–7 (2005).

36. Kublin, J. G. *et al.* Complete attenuation of genetically engineered Plasmodium falciparum sporozoites in human subjects. *Sci. Transl. Med.* **9**, 1–12 (2017).

37. Wiersma, J. *et al.* Protection against a malaria challenge by sporozoite inoculation. *N. Engl. J. Med.* **361**, 468–477 (2009).

38. Reuling, Isaie J. Mendes, A. M. *et al.* Clinical safety and protective efficacy after immunization with genetically modified Plasmodium berghei sporozoites expressing P. falciparum –circumsporozoite protein in a Phase 1/2a trial. *ASTMH 67th Annu. Meet. 28 Oct. - 1 Novemb. 2018 New Orleans, LA, USA*

39. Langhorne, J., Ndungu, F. M., Sponaas, A.-M. & Marsh, K. Immunity to malaria: more questions than answers. *Nat. Immunol.* **9**, 725–32 (2008).

40. Khan, Z. M. & Vanderberg, J. P. Specific inflammatory cell infiltration of hepatic schizonts in BALB/c mice immunized with attenuated plasmodium yoelii sporozoites. *Int. Immunol.* **4**, 711–718 (1992).

41. Riley, E. M. & Stewart, V. A. Immune mechanisms in malaria: new insights in vaccine development. *Nat. Med.* **19**, 168–78 (2013).

42. Isaacs, A. & Lindenmann, J. Virus Interference: I. The Interferon. *CA. Cancer J. Clin.* **38**, 280–290 (1988).

43. Pestka, S., Krause, C. D. & Walter, M. R. Interferons, interferon-like cytokines, and their receptors. (2004).

44. Ivashkiv, L. B. & Donlin, L. T. Regulation of type i interferon responses. *Nat. Rev. Immunol.* **14**, 36–49 (2014).

45. Schneider, W. M., Chevillotte, M. D. & Rice, C. M. Interferon-Stimulated Genes: A Complex Web of Host Defenses. *Annu. Rev. Immunol.* **32**, 513–545 (2014).

46. Jahiel, R. I., Vilcek, J. & Nussenzweig, R. S. Exogenous interferon protects mice against Plasmodium berghei malaria. *Nature* **227**, 1350–1351 (1970).

47. Liehl, P. *et al.* Host-cell sensors for Plasmodium activate innate immunity against liver-stage infection. *Nat. Med.* **20**, 47–53 (2014).

48. Miller, J. L., Sack, B. K., Baldwin, M., Vaughan, A. M. & Kappe, S. H. I. Interferon-Mediated Innate Immune Responses against Malaria Parasite Liver Stages. *Cell Rep.* **7**, 436–447 (2014).

49. Liehl, P. *et al.* Innate immunity induced by Plasmodium liver infection inhibits malaria reinfections. *Infect. Immun.* **83**, 1172–1180 (2015).

50. Zaidi, I. *et al.* γδ T Cells Are Required for the Induction of Sterile Immunity during Irradiated Sporozoite Vaccinations. *J. Immunol.* **199**, 3781–3788 (2017).

51. Silvie, O., Amino, R. & Hafalla, J. C. Tissue-specific cellular immune responses to malaria pre-erythrocytic stages. *Curr. Opin. Microbiol.* **40**, 160–167 (2017).

52. Schofield, L. *et al.* Gamma interferon, CD8+ T cells and antibodies required for immunity to malaria sporozoites. *Nature* **330**, 664–6

53. Schmidt, N. W. *et al.* Memory CD8 T cell responses exceeding a large but definable threshold provide long-term immunity to malaria. *Proc. Natl. Acad. Sci. U. S. A.* **105**, 14017–22 (2008).

54. Fernandez-Ruiz, D. *et al.* Liver-Resident Memory CD8+ T Cells Form a Front-Line Defense against Malaria Liver-Stage Infection. *Immunity* **45**, 889–902 (2016).

55. Gazzinelli, R. T., Kalantari, P., Fitzgerald, K. A. & Golenbock, D. T. Innate sensing of malaria parasites. *Nat. Rev. Immunol.* **14**, 744–757 (2014).

56. Yu, X. *et al.* Cross-Regulation of Two Type I Interferon Signaling Pathways in Plasmacytoid Dendritic Cells Controls Anti-malaria Immunity and Host Mortality. *Immunity* **45**, 1093–1107 (2016).

57. Spaulding, E. *et al.* STING-Licensed Macrophages Prime Type I IFN Production by Plasmacytoid Dendritic Cells in the Bone Marrow during Severe Plasmodium yoelii Malaria. *PLoS Pathog.* **12**, 1–29 (2016).

58. Matuschewski, K., Hafalla, J. C., Borrmann, S. & Friesen, J. Arrested Plasmodium liver stages as experimental anti-malaria vaccines. *Hum. Vaccin.* **7**, 16–21 (2011).

59. Friesen, J. & Matuschewski, K. Comparative efficacy of pre-erythrocytic whole organism

vaccine strategies against the malaria parasite. *Vaccine* **29**, 7002–7008 (2011).

60. Butler, N. S. *et al.* Superior antimalarial immunity after vaccination with late liver stage-arresting genetically attenuated parasites. *Cell Host Microbe* **9**, 451–62 (2011).

61. van Schaijk, B. C. L. *et al.* A genetically attenuated malaria vaccine candidate based on P. falciparum b9/slarp gene-deficient sporozoites. *Elife* **3**, 1–18 (2014).

62. Zuzarte-Luis, V., Sales-Dias, J. & Mota, M. M. Simple, sensitive and quantitative bioluminescence assay for determination of malaria pre-patent period. *Malar. J.* **13**, 15 (2014).

63. Schmittgen, T. D. & Livak, K. J. Analyzing real-time PCR data by the comparative CT method. *Nat. Protoc.* **3**, 1101–1108 (2008).

64. Ploemen, I. H. J. *et al.* Visualisation and quantitative analysis of the rodent malaria liver stage by real time imaging. *PLoS One* **4**, 1–12 (2009).

65. Kantari, C., Pederzoli-Ribeil, M. & Witko-Sarsat, V. The role of neutrophils and monocytes in innate immunity. *Contrib. Microbiol.* **15**, 118–146 (2008).

66. Kratofil, R. M., Kubes, P. & Deniset, J. F. Monocyte conversion during inflammation and injury. *Arterioscler. Thromb. Vasc. Biol.* **37**, 35–42 (2017).

67. Bargieri, D. Y. *et al.* Malaria Vaccine Development : Are Bacterial Flagellin Fusion Proteins the Bridge between Mouse and Humans ? *J. Parasitol. Res.* **2011**, (2011).

7. Appendices

Supplementary Table 1. Number of animals (n) and P-values for the data presented in each figure.

Fig.4.2		Liver load	Fig.4.4 (A)		Liver load	Fig.4.4 (B)		Liver load	Fig.4.4 (C)		Liver load	Fig.4.4 (D)		Liver load
WT	NI (n=10)	0,0070 **	*PbΔb9Δslarp*	NI (n=10)	0,0167 *	IRRADIATED	NI (n=10)	0,2937 ns	*PbΔmei2Δlisp2*	NI (n=10)	0,0070 **	CPS	NI (n=10)	0,0070 **
	12h (n=3)			12h (n=3)			12h (n=3)			12h (n=3)			12h (n=3)	
	NI (n=10)	0,0002 ***		NI (n=10)	0,7897 ns		NI (n=10)	0,0326 *		NI (n=10)	0,0002 ***		NI (n=10)	0,0002 ***
	24h (n=6)			24h (n=6)			24h (n=6)			24h (n=6)			24h (n=6)	
	NI (n=10)	0,0002 ***		NI (n=10)	0,4342 ns		NI (n=10)	0,0972 ns		NI (n=10)	0,0002 ***		NI (n=10)	0,0002 ***
	42h (n=6)			42h (n=6)			42h (n=6)			42h (n=6)			42h (n=6)	
	NI (n=10)	0,0002 ***		NI (n=10)	0,0719 ns		NI (n=10)	0,0754 ns		NI (n=10)	0,0002 ***		NI (n=10)	0,0002 ***
	48h (n=6)			48h (n=6)			48h (n=6)			48h (n=6)			48h (n=6)	
	NI (n=10)	0,0002 ***		NI (n=10)	0,4192 ns		NI (n=10)	0,1685 ns		NI (n=10)	0,0007 ***		NI (n=10)	0,0002 ***
	60h (n=6)			60h (n=6)			60h (n=6)			60h (n=6)			60h (n=6)	
	NI (n=10)	0,0002 ***		NI (n=10)	0,4850 ns		NI (n=10)	0,3598 ns		NI (n=10)	0,0002 ***		NI (n=10)	0,0002 ***
	68h (n=6)			68h (n=6)			68h (n=6)			68h (n=6)			68h (n=6)	
	NI (n=10)	0,0017 **		NI (n=10)	0,1523 ns		NI (n=10)	0,2122 ns		NI (n=10)	0,0167 *		NI (n=10)	0,0002 ***
	72h (n=6)			72h (n=6)			72h (n=6)			72h (n=6)			72h (n=6)	
	NI (n=10)	0,0002 ***		NI (n=10)	0,9784 ns		NI (n=10)	0,2621 ns		NI (n=10)	0,3111 ns		NI (n=10)	0,0002 ***
	84h (n=6)			84h (n=6)			84h (n=6)			84h (n=6)			84h (n=6)	
	NI (n=10)	0,0002 ***		NI (n=10)	0,0551 ns		NI (n=10)	0,0923 ns		NI (n=10)	0,5772 ns		NI (n=10)	0,0002 ***
	96h (n=6)			96h (n=6)			96h (n=6)			96h (n=6)			96h (n=6)	

Fig.4.2		ISGs	Fig.4.5 (A)		ISGs	Fig.4.5 (B)		ISGs	Fig. 4.5 (C)		ISGs	Fig. 4.5 (D)		ISGs
WT	NI (n=10)	0,5683 ns	*PbΔb9Δslarp*	NI (n=10)	0,0425 *	IRRADIATED	NI (n=10)	0,0195 *	*PbΔmei2Δlisp2*	NI (n=10)	0,0047 **	CPS	NI (n=10)	0,1283 ns
	12h (n=3)			12h (n=3)			12h (n=3)			12h (n=3)			12h (n=3)	
	NI (n=10)	0,5593 ns		NI (n=10)	>0,9999 ns		NI (n=10)	<0,0001 ****		NI (n=10)	0,0106 *		NI (n=10)	0,1611 ns
	24h (n=6)			24h (n=6)			24h (n=6)			24h (n=6)			24h (n=6)	
	NI (n=10)	0,0017 **		NI (n=10)	0,3363 ns		NI (n=10)	0,0179 *		NI (n=10)	0,0002 ***		NI (n=10)	0,0441 *
	42h (n=6)			42h (n=6)			42h (n=6)			42h (n=6)			42h (n=6)	
	NI (n=10)	0,9535 ns		NI (n=10)	0,7950 ns		NI (n=10)	0,0746 ns		NI (n=10)	0,7719 ns		NI (n=10)	0,9970 ns
	48h (n=6)			48h (n=6)			48h (n=6)			48h (n=6)			48h (n=6)	
	NI (n=10)	0,0021 **		NI (n=10)	0,0186 *		NI (n=10)	0,9034 ns		NI (n=10)	0,1144 ns		NI (n=10)	0,1680 ns
	60h (n=6)			60h (n=6)			60h (n=6)			60h (n=6)			60h (n=6)	
	NI (n=10)	<0,0001 ****		NI (n=10)	0,9970 ns		NI (n=10)	0,6006 ns		NI (n=10)	<0,0001 ****		NI (n=10)	<0,0001 ****
	68h (n=6)			68h (n=6)			68h (n=6)			68h (n=6)			68h (n=6)	
	NI (n=10)	<0,0001 ****		NI (n=10)	0,6164 ns		NI (n=10)	0,7661 ns		NI (n=10)	<0,0001 ****		NI (n=10)	<0,0001 ****
	72h (n=6)			72h (n=6)			72h (n=6)			72h (n=6)			72h (n=6)	
	NI (n=10)	<0,0001 ****		NI (n=10)	0,7206 ns		NI (n=10)	<0,0001 ****		NI (n=10)	0,1149 ns		NI (n=10)	0,0001 ***
	84h (n=6)			84h (n=6)			84h (n=6)			84h (n=6)			84h (n=6)	
	NI (n=10)	<0,0001 ****		NI (n=10)	0,0045 **		NI (n=10)	<0,0001 ****		NI (n=10)	0,7834 ns		NI (n=10)	0,0114 *
	96h (n=6)			96h (n=6)			96h (n=6)			96h (n=6)			96h (n=6)	

Fig. 4.6 (A)		CD4+ T cells	Fig. 4.10 (A)		CD4+ T cells	Fig. 4.10 (A)		CD4+ T cells	Fig. 4.10 (A)		CD4+ T cells	Figure 4.10 (A)		CD4+ T cells
WT	NI (n=5)	0,5714 ns	*PbΔb9Δslarp*	NI (n=5)	0,1429 ns	IRRADIATED	NI (n=5)	0,3929 ns	*PbΔmei2Δlisp2*	NI (n=5)	0,7857 ns	CPS	NI (n=5)	>0,9999 ns
	12h (n=3)			12h (n=3)			12h (n=3)			12h (n=3)			12h (n=3)	
	NI (n=5)	0,8393 ns		NI (n=5)	0,1429 ns		NI (n=5)	0,2500 ns		NI (n=5)	>0,9999 ns		NI (n=5)	>0,9999 ns
	24h (n=6)			24h (n=6)			24h (n=6)			24h (n=6)			24h (n=6)	
	NI (n=5)	>0,9999 ns		NI (n=5)	0,1429 ns		NI (n=5)	0,9286 ns		NI (n=5)	0,3929 ns		NI (n=5)	0,5174 ns
	42h (n=6)			42h (n=6)			42h (n=6)			42h (n=6)			42h (n=6)	
	NI (n=5)	0,2500 ns		NI (n=5)	0,2500 ns		NI (n=5)	>0,9999 ns		NI (n=5)	0,2500 ns		NI (n=5)	0,6250 ns
	48h (n=6)			48h (n=6)			48h (n=6)			48h (n=6)			48h (n=6)	
	NI (n=5)	0,0714 ns		NI (n=5)	0,3929 ns		NI (n=5)	0,3929 ns		NI (n=5)	>0,9999 ns		NI (n=5)	0,8750 ns
	60h (n=6)			60h (n=6)			60h (n=6)			60h (n=6)			60h (n=6)	
	NI (n=5)	0,0714 ns		NI (n=5)	0,5714 ns		NI (n=5)	0,2500 ns		NI (n=5)	>0,9999 ns		NI (n=5)	0,7857 ns
	68h (n=6)			68h (n=6)			68h (n=6)			68h (n=6)			68h (n=6)	
	NI (n=5)	>0,9999 ns		NI (n=5)	0,7857 ns		NI (n=5)	>0,9999 ns		NI (n=5)	0,1786 ns		NI (n=5)	0,0893 ns
	72h (n=6)			72h (n=6)			72h (n=6)			72h (n=6)			72h (n=6)	
	NI (n=5)	0,0357 *		NI (n=5)	0,3929 ns		NI (n=5)	0,1429 ns		NI (n=5)	0,0357 *		NI (n=5)	0,3929 ns
	84h (n=6)			84h (n=6)			84h (n=6)			84h (n=6)			84h (n=6)	
	NI (n=5)	0,0714 ns		NI (n=5)	0,3929 ns		NI (n=5)	0,0714 ns		NI (n=5)	0,0536 ns		NI (n=5)	0,0357 *
	96h (n=6)			96h (n=6)			96h (n=6)			96h (n=6)			96h (n=6)	

Fig. 4.6 (B)		Tissue resident CD4 T cells	Fig. 4.10 (B)		Tissue resident CD4 T cells	Fig. 4.10 (B)		Tissue resident CD4 T cells	Fig. 4.10 (B)		Tissue resident CD4 T cells	Fig. 4.10 (B)		Tissue resident CD4 T cells
WT	NI (n=5)	0,2286 ns	*PbΔb9Δslarp*	NI (n=5)	0,4000 ns	IRRADIATED	NI (n=5)	0,1143 ns	*PbΔmei2Δlisp2*	NI (n=5)	0,1143 ns	CPS	NI (n=5)	0,2286 ns
	24h (n=6)			24h (n=6)			24h (n=6)			24h (n=6)			24h (n=6)	
	NI (n=5)	0,1143 ns		NI (n=5)	0,2286 ns		NI (n=5)	0,2286 ns		NI (n=5)	0,1143 ns		NI (n=5)	0,4000 ns
	42h (n=6)			42h (n=6)			42h (n=6)			42h (n=6)			42h (n=6)	
	NI (n=5)	0,2286 ns		NI (n=5)	0,0571 ns		NI (n=5)	0,0571 ns		NI (n=5)	0,2286 ns		NI (n=5)	0,1143 ns
	48h (n=6)			48h (n=6)			48h (n=6)			48h (n=6)			48h (n=6)	
	NI (n=5)	0,4000 ns		NI (n=5)	0,3429 ns		NI (n=5)	0,4000 ns		NI (n=5)	0,5333 ns		NI (n=5)	0,4000 ns
	60h (n=6)			60h (n=6)			60h (n=6)			60h (n=6)			60h (n=6)	
	NI (n=5)	0,8571 ns		NI (n=5)	0,4000 ns		NI (n=5)	0,4571 ns		NI (n=5)	0,2286 ns		NI (n=5)	0,1143 ns
	68h (n=6)			68h (n=6)			68h (n=6)			68h (n=6)			68h (n=6)	
	NI (n=5)	0,1143 ns		NI (n=5)	0,6286 ns		NI (n=5)	0,4000 ns		NI (n=5)	>0,9999 ns		NI (n=5)	0,1143 ns
	72h (n=6)			72h (n=6)			72h (n=6)			72h (n=6)			72h (n=6)	
	NI (n=5)	0,2286 ns		NI (n=5)	0,4000 ns		NI (n=5)	0,6286 ns		NI (n=5)	0,0857 ns		NI (n=5)	0,0571 ns
	84h (n=6)			84h (n=6)			84h (n=6)			84h (n=6)			84h (n=6)	
	NI (n=5)	0,0571 ns		NI (n=5)	0,1143 ns		NI (n=5)	0,0571 ns		NI (n=5)	0,4000 ns		NI (n=5)	0,0571 ns
	96h (n=6)			96h (n=6)			96h (n=6)			96h (n=6)			96h (n=6)	

Fig. 4.6 (C)		CD8+ T cells	Fig. 4.11 (A)		CD8+ T cells	Fig. 4.11 (A)		CD8+ T cells	Fig. 4.11 (A)		CD8+ T cells	Fig. 4.11 (A)		CD8+ T cells
WT	NI (n=5)	0,3929 ns	PbΔb9Δslarp	NI (n=5)	0,1429 ns	IRRADIATED	NI (n=5)	>0,9999 ns	PbΔmei2Δlisp2	NI (n=5)	0,7857 ns	CPS	NI (n=5)	0,7321 ns
	12h (n=3)			12h (n=3)			12h (n=3)			12h (n=3)			12h (n=3)	
	NI (n=5)	0,7857 ns		NI (n=5)	>0,9999 ns		NI (n=5)	0,7857 ns		NI (n=5)	0,7857 ns		NI (n=5)	0,7857 ns
	24h (n=6)			24h (n=6)			24h (n=6)			24h (n=6)			24h (n=6)	
	NI (n=5)	>0,9999 ns		NI (n=5)	0,5714 ns		NI (n=5)	0,2500 ns		NI (n=5)	>0,9999 ns		NI (n=5)	0,7857 ns
	42h (n=6)			42h (n=6)			42h (n=6)			42h (n=6)			42h (n=6)	
	NI (n=5)	>0,9999 ns		NI (n=5)	>0,9999 ns		NI (n=5)	0,1429 ns		NI (n=5)	0,5714 ns		NI (n=5)	0,0714 ns
	48h (n=6)			48h (n=6)			48h (n=6)			48h (n=6)			48h (n=6)	
	NI (n=5)	0,5714 ns		NI (n=5)	0,5714 ns		NI (n=5)	0,5714 ns		NI (n=5)	0,8571 ns		NI (n=5)	0,5714 ns
	60h (n=6)			60h (n=6)			60h (n=6)			60h (n=6)			60h (n=6)	
	NI (n=5)	>0,9999 ns		NI (n=5)	0,7857 ns		NI (n=5)	>0,9999 ns		NI (n=5)	0,7857 ns		NI (n=5)	0,5714 ns
	68h (n=6)			68h (n=6)			68h (n=6)			68h (n=6)			68h (n=6)	
	NI (n=5)	>0,9999 ns		NI (n=5)	0,3929 ns		NI (n=5)	>0,9999 ns		NI (n=5)	0,5714 ns		NI (n=5)	0,2500 ns
	72h (n=6)			72h (n=6)			72h (n=6)			72h (n=6)			72h (n=6)	
	NI (n=5)	0,0714 ns		NI (n=5)	0,5714 ns		NI (n=5)	0,3929 ns		NI (n=5)	>0,9999 ns		NI (n=5)	0,0357 *
	84h (n=6)			84h (n=6)			84h (n=6)			84h (n=6)			84h (n=6)	
	NI (n=5)	0,0714 ns		NI (n=5)	0,3929 ns		NI (n=5)	>0,9999 ns		NI (n=5)	0,7857 ns		NI (n=5)	>0,9999 ns
	96h (n=6)			96h (n=6)			96h (n=6)			96h (n=6)			96h (n=6)	

Fig. 4.6 (D)		Tissue resident CD8 T cells	Fig. 4.11 (B)		Tissue resident CD8 T cells	Fig. 4.11 (B)		Tissue resident CD8 T cells	Fig. 4.11 (B)		Tissue resident CD8 T cells	Fig. 4.11 (B)		Tissue resident CD8 T cells
WT	NI (n=5)	0,4000 ns	*PbΔb9Δslarp*	NI (n=5)	0,1143 ns	IRRADIATED	NI (n=5)	0,8571 ns	*PbΔmei2Δlisp2*	NI (n=5)	>0,9999 ns	CPS	NI (n=5)	0,6286 ns
	24h (n=6)			24h (n=6)			24h (n=6)			24h (n=6)			24h (n=6)	
	NI (n=5)	0,6857 ns		NI (n=5)	>0,9999 ns		NI (n=5)	0,6286 ns		NI (n=5)	0,6857 ns		NI (n=5)	0,6286 ns
	42h (n=6)			42h (n=6)			42h (n=6)			42h (n=6)			42h (n=6)	
	NI (n=5)	>0,9999 ns		NI (n=5)	0,6857 ns		NI (n=5)	0,6286 ns		NI (n=5)	0,8571 ns		NI (n=5)	>0,9999 ns
	48h (n=6)			48h (n=6)			48h (n=6)			48h (n=6)			48h (n=6)	
	NI (n=5)	0,6286 ns		NI (n=5)	0,8571 ns		NI (n=5)	>0,9999 ns		NI (n=5)	0,8000 ns		NI (n=5)	0,9143 ns
	60h (n=6)			60h (n=6)			60h (n=6)			60h (n=6)			60h (n=6)	
	NI (n=5)	0,0571 ns		NI (n=5)	>0,9999 ns		NI (n=5)	0,6286 ns		NI (n=5)	0,0571 ns		NI (n=5)	0,0571 ns
	68h (n=6)			68h (n=6)			68h (n=6)			68h (n=6)			68h (n=6)	
	NI (n=5)	0,0571 ns		NI (n=5)	0,6286 ns		NI (n=5)	0,6286 ns		NI (n=5)	0,1143 ns		NI (n=5)	0,0571 ns
	72h (n=6)			72h (n=6)			72h (n=6)			72h (n=6)			72h (n=6)	
	NI (n=5)	0,0571 ns		NI (n=5)	>0,9999 ns		NI (n=5)	0,6286 ns		NI (n=5)	0,0571 ns		NI (n=5)	0,0571 ns
	84h (n=6)			84h (n=6)			84h (n=6)			84h (n=6)			84h (n=6)	
	NI (n=5)	0,0571 ns		NI (n=5)	0,4000 ns		NI (n=5)	0,1143 ns		NI (n=5)	0,2286 ns		NI (n=5)	0,0571 ns
	96h (n=6)			96h (n=6)			96h (n=6)			96h (n=6)			96h (n=6)	

Fig. 4.7 (A)		NK	Fig.4.12 (A)		NK	Fig.4.12 (A)		NK	Fig.4.12 (A)		NK	Fig.4.12 (A)		NK
WT	NI (n=5)	0,7321 ns	*PbΔb9Δslarp*	NI (n=5)	0,5000 ns	IRRADIATED	NI (n=5)	0,7321 ns	*PbΔmei2Δlisp2*	NI (n=5)	0,0714 ns	CPS	NI (n=5)	0,7321 ns
	12h (n=3)			12h (n=3)			12h (n=3)			12h (n=3)			12h (n=3)	
	NI (n=5)	0,0536 ns		NI (n=5)	0,0179 *		NI (n=5)	0,9643 ns		NI (n=5)	0,6071 ns		NI (n=5)	0,5179 ns
	24h (n=6)			24h (n=6)			24h (n=6)			24h (n=6)			24h (n=6)	
	NI (n=5)	0,3214 ns		NI (n=5)	0,9643 ns		NI (n=5)	0,7143 ns		NI (n=5)	0,6786 ns		NI (n=5)	0,7321 ns
	42h (n=6)			42h (n=6)			42h (n=6)			42h (n=6)			42h (n=6)	
	NI (n=5)	0,6429 ns		NI (n=5)	0,5357 ns		NI (n=5)	0,1250 ns		NI (n=5)	0,0179 *		NI (n=5)	0,0179 *
	48h (n=6)			48h (n=6)			48h (n=6)			48h (n=6)			48h (n=6)	
	NI (n=5)	0,0357 *		NI (n=5)	0,1250 ns		NI (n=5)	0,1250 ns		NI (n=5)	0,0476 *		NI (n=5)	0,0357 *
	60h (n=6)			60h (n=6)			60h (n=6)			60h (n=6)			60h (n=6)	
	NI (n=5)	0,9643 ns		NI (n=5)	0,1071 ns		NI (n=5)	0,5179 ns		NI (n=5)	0,5179 ns		NI (n=5)	0,3571 ns
	68h (n=6)			68h (n=6)			68h (n=6)			68h (n=6)			68h (n=6)	
	NI (n=5)	0,0714 ns		NI (n=5)	0,2143 ns		NI (n=5)	0,3571 ns		NI (n=5)	0,9643 ns		NI (n=5)	0,1250 ns
	72h (n=6)			72h (n=6)			72h (n=6)			72h (n=6)			72h (n=6)	
	NI (n=5)	0,0357 *		NI (n=5)	0,0357 *		NI (n=5)	0,0536 ns		NI (n=5)	0,7321 ns		NI (n=5)	0,0357 *
	84h (n=6)			84h (n=6)			84h (n=6)			84h (n=6)			84h (n=6)	
	NI (n=5)	0,0179 *		NI (n=5)	0,2143 ns		NI (n=5)	0,1250 ns		NI (n=5)	0,0179 *		NI (n=5)	0,3929 ns
	96h (n=6)			96h (n=6)			96h (n=6)			96h (n=6)			96h (n=6)	

Fig. 4.7 (B)		NKT cells	Fig.4.12 (B)		NKT cells	Fig.4.12 (A)		NKT cells	Fig.4.12 (B)		NKT cells	Fig.4.12 (B)		NKT cells
WT	NI (n=5)	0,1143 ns	*PbΔb9Δslarp*	NI (n=5)	0,2286 ns	IRRADIATED	NI (n=5)	0,2286 ns	*PbΔmei2Δlisp2*	NI (n=5)	0,1143 ns	CPS	NI (n=5)	0,2286 ns
	12h (n=3)			12h (n=3)			12h (n=3)			12h (n=3)			12h (n=3)	
	NI (n=5)	>0,9999 ns		NI (n=5)	0,6286 ns		NI (n=5)	0,6286 ns		NI (n=5)	0,4000 ns		NI (n=5)	0,8571 ns
	24h (n=6)			24h (n=6)			24h (n=6)			24h (n=6)			24h (n=6)	
	NI (n=5)	0,8571 ns		NI (n=5)	0,4000 ns		NI (n=5)	0,6286 ns		NI (n=5)	0,2286 ns		NI (n=5)	>0,9999 ns
	42h (n=6)			42h (n=6)			42h (n=6)			42h (n=6)			42h (n=6)	
	NI (n=5)	>0,9999 ns		NI (n=5)	0,8571 ns		NI (n=5)	0,4000 ns		NI (n=5)	0,2286 ns		NI (n=5)	0,1143 ns
	48h (n=6)			48h (n=6)			48h (n=6)			48h (n=6)			48h (n=6)	
	NI (n=5)	0,4000 ns		NI (n=5)	0,2286 ns		NI (n=5)	0,0571 ns		NI (n=5)	0,5333 ns		NI (n=5)	0,4000 ns
	60h (n=6)			60h (n=6)			60h (n=6)			60h (n=6)			60h (n=6)	
	NI (n=5)	0,1143 ns		NI (n=5)	0,0571 ns		NI (n=5)	0,4000 ns		NI (n=5)	0,4000 ns		NI (n=5)	>0,9999 ns
	68h (n=6)			68h (n=6)			68h (n=6)			68h (n=6)			68h (n=6)	
	NI (n=5)	0,4000 ns		NI (n=5)	0,0571 ns		NI (n=5)	0,4000 ns		NI (n=5)	0,1143 ns		NI (n=5)	>0,9999 ns
	72h (n=6)			72h (n=6)			72h (n=6)			72h (n=6)			72h (n=6)	
	NI (n=5)	0,0571 ns		NI (n=5)	0,4000 ns		NI (n=5)	0,4000 ns		NI (n=5)	0,0571 ns		NI (n=5)	0,0571 ns
	84h (n=6)			84h (n=6)			84h (n=6)			84h (n=6)			84h (n=6)	
	NI (n=5)	0,0571 ns		NI (n=5)	0,2286 ns		NI (n=5)	0,4000 ns		NI (n=5)	0,1143 ns		NI (n=5)	0,0571 ns
	96h (n=6)			96h (n=6)			96h (n=6)			96h (n=6)			96h (n=6)	

Fig. 4.7 (C)		ILC1s	Fig.4.12 (C)		ILC1s	Fig.4.12 (C)		ILC1s	Fig.4.12 (C)		ILC1s	Fig.4.12 (C)		ILC1s
WT	NI (n=5)	0,2321 ns	*PbΔb9Δslarp*	NI (n=5)	0,1250 ns	IRRADIATED	NI (n=5)	0,9286 ns	PbΔmei2Δlisp2	NI (n=5)	0,3214 ns	CPS	NI (n=5)	0,6964 ns
	12h (n=3)			12h (n=3)			12h (n=3)			12h (n=3)			12h (n=3)	
	NI (n=5)	0,5536 ns		NI (n=5)	0,3393 ns		NI (n=5)	0,9643 ns		NI (n=5)	0,6964 ns		NI (n=5)	0,9286 ns
	24h (n=6)			24h (n=6)			24h (n=6)			24h (n=6)			24h (n=6)	
	NI (n=5)	0,5179 ns		NI (n=5)	0,4464 ns		NI (n=5)	0,1250 ns		NI (n=5)	0,7321 ns		NI (n=5)	0,3393 ns
	42h (n=6)			42h (n=6)			42h (n=6)			42h (n=6)			42h (n=6)	
	NI (n=5)	0,9286 ns		NI (n=5)	>0,9999 ns		NI (n=5)	0,9643 ns		NI (n=5)	0,2143 ns		NI (n=5)	0,0357 *
	48h (n=6)			48h (n=6)			48h (n=6)			48h (n=6)			48h (n=6)	
	NI (n=5)	0,0357 *		NI (n=5)	0,3571 ns		NI (n=5)	0,9286 ns		NI (n=5)	0,0952 ns		NI (n=5)	0,1250 ns
	60h (n=6)			60h (n=6)			60h (n=6)			60h (n=6)			60h (n=6)	
	NI (n=5)	0,0357 *		NI (n=5)	0,5000 ns		NI (n=5)	0,7321 ns		NI (n=5)	0,0357 *		NI (n=5)	0,0357 *
	68h (n=6)			68h (n=6)			68h (n=6)			68h (n=6)			68h (n=6)	
	NI (n=5)	0,0357 *		NI (n=5)	0,0357 *		NI (n=5)	0,3393 ns		NI (n=5)	0,0357 *		NI (n=5)	0,3214 ns
	72h (n=6)			72h (n=6)			72h (n=6)			72h (n=6)			72h (n=6)	
	NI (n=5)	0,0357 *		NI (n=5)	0,9286 ns		NI (n=5)	0,9286 ns		NI (n=5)	0,0357 *		NI (n=5)	0,0357 *
	84h (n=6)			84h (n=6)			84h (n=6)			84h (n=6)			84h (n=6)	
	NI (n=5)	0,0357 *		NI (n=5)	0,0714 ns		NI (n=5)	0,7321 ns		NI (n=5)	0,1250 ns		NI (n=5)	0,0357 *
	96h (n=6)			96h (n=6)			96h (n=6)			96h (n=6)			96h (n=6)	

Fig. 4.7 (D)		γδ T cells	Fig. 4.12 (D)		γδ T cells	Fig. 4.12 (D)		γδ T cells	Fig. 4.12 (D)		γδ T cells	Fig. 4.12 (D)		γδ T cells
WT	NI (n=5)	0,0357 *	*PbΔb9Δslarp*	NI (n=5)	0,0714 ns	IRRADIATED	NI (n=5)	0,1429 ns	*PbΔmei2Δlisp2*	NI (n=5)	0,0357 *	CPS	NI (n=5)	0,0714 ns
	12h (n=3)			12h (n=3)			12h (n=3)			12h (n=3)			12h (n=3)	
	NI (n=5)	0,3929 ns		NI (n=5)	0,3929 ns		NI (n=5)	0,3929 ns		NI (n=5)	0,5714 ns		NI (n=5)	0,2500 ns
	24h (n=6)			24h (n=6)			24h (n=6)			24h (n=6)			24h (n=6)	
	NI (n=5)	0,1607 ns		NI (n=5)	0,3929 ns		NI (n=5)	>0,9999 ns		NI (n=5)	0,6250 ns		NI (n=5)	>0,9999 ns
	42h (n=6)			42h (n=6)			42h (n=6)			42h (n=6)			42h (n=6)	
	NI (n=5)	0,0357 *		NI (n=5)	0,0357 *		NI (n=5)	0,0357 *		NI (n=5)	0,0357 *		NI (n=5)	0,0357 *
	48h (n=6)			48h (n=6)			48h (n=6)			48h (n=6)			48h (n=6)	
	NI (n=5)	0,0714 ns		NI (n=5)	0,7857 ns		NI (n=5)	0,3929 ns		NI (n=5)	0,3810 ns		NI (n=5)	>0,9999 ns
	60h (n=6)			60h (n=6)			60h (n=6)			60h (n=6)			60h (n=6)	
	NI (n=5)	0,1429 ns		NI (n=5)	0,4643 ns		NI (n=5)	0,1429 ns		NI (n=5)	0,5714 ns		NI (n=5)	0,5714 ns
	68h (n=6)			68h (n=6)			68h (n=6)			68h (n=6)			68h (n=6)	
	NI (n=5)	0,2500 ns		NI (n=5)	0,5714 ns		NI (n=5)	0,5714 ns		NI (n=5)	>0,9999 ns		NI (n=5)	0,5714 ns
	72h (n=6)			72h (n=6)			72h (n=6)			72h (n=6)			72h (n=6)	
	NI (n=5)	0,0714 ns		NI (n=5)	0,8393 ns		NI (n=5)	0,1071 ns		NI (n=5)	>0,9999 ns		NI (n=5)	0,5714 ns
	84h (n=6)			84h (n=6)			84h (n=6)			84h (n=6)			84h (n=6)	
	NI (n=5)	0,0357 *		NI (n=5)	0,0714 ns		NI (n=5)	0,0357 *		NI (n=5)	0,1429 ns		NI (n=5)	0,5714 ns
	96h (n=6)			96h (n=6)			96h (n=6)			96h (n=6)			96h (n=6)	

Fig. 4.8 (A)		Pro-inflammatory monocytes	Fig. 4.13 (A)		Pro-inflammatory monocytes	Fig. 4.13 (A)		Pro-inflammatory monocytes	Fig. 4.13 (A)		Pro-inflammatory monocytes	Fig. 4.13 (A)		Pro-inflammatory monocytes
WT	NI (n=5)	0,0357 *	*PbΔb9Δslarp*	NI (n=5)	0,0714 s	IRRADIATED	NI (n=5)	0,0714 s	*PbΔmei2Δlisp2*	NI (n=5)	0,5714 ns	CPS	NI (n=5)	0,2500 ns
	12h (n=3)			12h (n=3)			12h (n=3)			12h (n=3)			12h (n=3)	
	NI (n=5)	0,5714 ns		NI (n=5)	>0,9999 ns		NI (n=5)	0,5714 ns		NI (n=5)	0,5714 ns		NI (n=5)	0,0714 ns
	24h (n=6)			24h (n=6)			24h (n=6)			24h (n=6)			24h (n=6)	
	NI (n=5)	0,2500 ns		NI (n=5)	0,7857 ns		NI (n=5)	0,7857 ns		NI (n=5)	0,3929 ns		NI (n=5)	0,3929 ns
	42h (n=6)			42h (n=6)			42h (n=6)			42h (n=6)			42h (n=6)	
	NI (n=5)	0,1429 ns		NI (n=5)	0,0357 *		NI (n=5)	0,0357 *		NI (n=5)	0,0357 *		NI (n=5)	0,0357 *
	48h (n=6)			48h (n=6)			48h (n=6)			48h (n=6)			48h (n=6)	
	NI (n=5)	0,0357 *		NI (n=5)	0,2500 ns		NI (n=5)	0,2500 ns		NI (n=5)	0,0952 ns		NI (n=5)	0,0357 *
	60h (n=6)			60h (n=6)			60h (n=6)			60h (n=6)			60h (n=6)	
	NI (n=5)	0,0357 *		NI (n=5)	0,2500 ns		NI (n=5)	0,8393 ns		NI (n=5)	0,0357 *		NI (n=5)	0,0357 *
	68h (n=6)			68h (n=6)			68h (n=6)			68h (n=6)			68h (n=6)	
	NI (n=5)	0,0357 *		NI (n=5)	0,7857 ns		NI (n=5)	>0,9999 ns		NI (n=5)	0,1429 ns		NI (n=5)	0,0357 *
	72h (n=6)			72h (n=6)			72h (n=6)			72h (n=6)			72h (n=6)	
	NI (n=5)	0,0357 *		NI (n=5)	0,2500 ns		NI (n=5)	0,5714 ns		NI (n=5)	0,0357 *		NI (n=5)	0,0357 *
	84h (n=6)			84h (n=6)			84h (n=6)			84h (n=6)			84h (n=6)	
	NI (n=5)	0,0357 *		NI (n=5)	0,0357 *		NI (n=5)	0,0357 *		NI (n=5)	0,7857 ns		NI (n=5)	0,0357 *
	96h (n=6)			96h (n=6)			96h (n=6)			96h (n=6)			96h (n=6)	

Fig. 4.8 (B)		Patrolling monocytes	Fig. 4.13 (B)		Patrolling monocytes	Fig. 4.13 (B)		Patrolling monocytes	Fig. 4.13 (B)		Patrolling monocytes	Fig. 4.13 (B)		Patrolling monocytes
WT	NI (n=5)		*PbΔb9Δslarp*	NI (n=5)		IRRADIATED	NI (n=5)		*PbΔmei2Δlisp2*	NI (n=5)		CPS	NI (n=5)	
	12h (n=3)	0,1429 ns		12h (n=3)	0,0357 *		12h (n=3)	0,5714 ns		12h (n=3)	>0,9999 ns		12h (n=3)	0,9643 ns
	NI (n=5)			NI (n=5)			NI (n=5)			NI (n=5)			NI (n=5)	
	24h (n=6)	0,0357 *		24h (n=6)	0,0357 *		24h (n=6)	0,1429 ns		24h (n=6)	0,1429 ns		24h (n=6)	0,0357 *
	NI (n=5)			NI (n=5)			NI (n=5)			NI (n=5)			NI (n=5)	
	42h (n=6)	0,0536 ns		42h (n=6)	0,5714 ns		42h (n=6)	>0,9999 ns		42h (n=6)	0,4643 ns		42h (n=6)	0,5536 ns
	NI (n=5)			NI (n=5)			NI (n=5)			NI (n=5)			NI (n=5)	
	48h (n=6)	0,7857 ns		48h (n=6)	0,0357 *		48h (n=6)	0,0714 ns		48h (n=6)	0,1429 ns		48h (n=6)	0,0357 *
	NI (n=5)			NI (n=5)			NI (n=5)			NI (n=5)			NI (n=5)	
	60h (n=6)	0,1429 ns		60h (n=6)	0,2500 ns		60h (n=6)	0,7857 ns		60h (n=6)	0,3810 ns		60h (n=6)	0,1429 ns
	NI (n=5)			NI (n=5)			NI (n=5)			NI (n=5)			NI (n=5)	
	68h (n=6)	0,0357 *		68h (n=6)	0,7857 ns		68h (n=6)	0,9643 ns		68h (n=6)	0,0357 *		68h (n=6)	0,0357 *
	NI (n=5)			NI (n=5)			NI (n=5)			NI (n=5)			NI (n=5)	
	72h (n=6)	0,0357 *		72h (n=6)	>0,9999 ns		72h (n=6)	>0,9999 ns		72h (n=6)	0,0357 *		72h (n=6)	0,0357 *
	NI (n=5)			NI (n=5)			NI (n=5)			NI (n=5)			NI (n=5)	
	84h (n=6)	0,0357 *		84h (n=6)	>0,9999 ns		84h (n=6)	0,7857 ns		84h (n=6)	0,0357 *		84h (n=6)	0,0357 *
	NI (n=5)			NI (n=5)			NI (n=5)			NI (n=5)			NI (n=5)	
	96h (n=6)	0,0357 *		96h (n=6)	0,1250 ns		96h (n=6)	0,1607 ns		96h (n=6)	0,1429 ns		96h (n=6)	0,0357 *

Fig. 4.8 (C)		Macrophages	Fig. 4.13 (C)		Macrophages	Fig. 4.13 (C)		Macrophages	Fig. 4.13 (C)		Macrophages	Fig. 4.13 (C)		Macrophages
WT	NI (n=5)	0,1429 ns	*PbΔb9Δslarp*	NI (n=5)	0,0357 *	IRRADIATED	NI (n=5)	0,5714 ns	*PbΔmei2Δlisp2*	NI (n=5)	>0,9999 ns	CPS	NI (n=5)	0,9643 ns
	12h (n=3)			12h (n=3)			12h (n=3)			12h (n=3)			12h (n=3)	
	NI (n=5)	0,0357 *		NI (n=5)	0,0357 *		NI (n=5)	0,1429 ns		NI (n=5)	0,1429 ns		NI (n=5)	0,0357 *
	24h (n=6)			24h (n=6)			24h (n=6)			24h (n=6)			24h (n=6)	
	NI (n=5)	0,0536 ns		NI (n=5)	0,5714 ns		NI (n=5)	>0,9999 ns		NI (n=5)	0,4643 ns		NI (n=5)	0,5536 ns
	42h (n=6)			42h (n=6)			42h (n=6)			42h (n=6)			42h (n=6)	
	NI (n=5)	0,7857 ns		NI (n=5)	0,0357 *		NI (n=5)	0,0714 ns		NI (n=5)	0,1429 ns		NI (n=5)	0,0357 *
	48h (n=6)			48h (n=6)			48h (n=6)			48h (n=6)			48h (n=6)	
	NI (n=5)	0,1429 ns		NI (n=5)	0,2500 ns		NI (n=5)	0,7857 ns		NI (n=5)	0,3810 ns		NI (n=5)	0,1429 ns
	60h (n=6)			60h (n=6)			60h (n=6)			60h (n=6)			60h (n=6)	
	NI (n=5)	0,0357 *		NI (n=5)	0,7857 ns		NI (n=5)	0,9643 ns		NI (n=5)	0,0357 *		NI (n=5)	0,0357 *
	68h (n=6)			68h (n=6)			68h (n=6)			68h (n=6)			68h (n=6)	
	NI (n=5)	0,0357 *		NI (n=5)	>0,9999 ns		NI (n=5)	>0,9999 ns		NI (n=5)	0,0357 *		NI (n=5)	0,0357 *
	72h (n=6)			72h (n=6)			72h (n=6)			72h (n=6)			72h (n=6)	
	NI (n=5)	0,0357 *		NI (n=5)	>0,9999 ns		NI (n=5)	0,7857 ns		NI (n=5)	0,0357 *		NI (n=5)	0,0357 *
	84h (n=6)			84h (n=6)			84h (n=6)			84h (n=6)			84h (n=6)	
	NI (n=5)	0,0357 *		NI (n=5)	0,1250 ns		NI (n=5)	0,1607 ns		NI (n=5)	0,1429 ns		NI (n=5)	0,0357 *
	96h (n=6)			96h (n=6)			96h (n=6)			96h (n=6)			96h (n=6)	

Fig. 4.8 (D)		Neutrophils	Fig. 4.13 (D)		Neutrophils	Fig. 4.13 (D)		Neutrophils	Fig. 4.13 (D)		Neutrophils	Fig. 4.13 (D)		Neutrophils
WT	NI (n=5)	0,2500 ns	*PbΔb9Δslarp*	NI (n=5)	0,7857 ns	IRRADIATED	NI (n=5)	0,1429 ns	*PbΔmei2Δlisp2*	NI (n=5)	0,5714 ns	CPS	NI (n=5)	0,2500 ns
	12h (n=3)			12h (n=3)			12h (n=3)			12h (n=3)			12h (n=3)	
	NI (n=5)	>0,9999 ns		NI (n=5)	0,5714 ns		NI (n=5)	>0,9999 ns		NI (n=5)	0,1429 ns		NI (n=5)	0,1429 ns
	24h (n=6)			24h (n=6)			24h (n=6)			24h (n=6)			24h (n=6)	
	NI (n=5)	0,5714 ns		NI (n=5)	0,3929 ns		NI (n=5)	0,5714 ns		NI (n=5)	0,1429 ns		NI (n=5)	0,2500 ns
	42h (n=6)			42h (n=6)			42h (n=6)			42h (n=6)			42h (n=6)	
	NI (n=5)	0,2500 ns		NI (n=5)	>0,9999 ns		NI (n=5)	0,7857 ns		NI (n=5)	>0,9999 ns		NI (n=5)	0,1429 ns
	48h (n=6)			48h (n=6)			48h (n=6)			48h (n=6)			48h (n=6)	
	NI (n=5)	0,0357 *		NI (n=5)	0,2500 ns		NI (n=5)	0,5714 ns		NI (n=5)	0,3810 ns		NI (n=5)	0,5714 ns
	60h (n=6)			60h (n=6)			60h (n=6)			60h (n=6)			60h (n=6)	
	NI (n=5)	0,2500 ns		NI (n=5)	0,2500 ns		NI (n=5)	0,5714 ns		NI (n=5)	0,2500 ns		NI (n=5)	0,2500 ns
	68h (n=6)			68h (n=6)			68h (n=6)			68h (n=6)			68h (n=6)	
	NI (n=5)	0,2500 ns		NI (n=5)	0,2500 ns		NI (n=5)	0,2500 ns		NI (n=5)	0,2500 ns		NI (n=5)	0,2500 ns
	72h (n=6)			72h (n=6)			72h (n=6)			72h (n=6)			72h (n=6)	
	NI (n=5)	0,0357 *		NI (n=5)	0,5714 ns		NI (n=5)	0,3929 ns		NI (n=5)	0,2500 ns		NI (n=5)	0,0357 *
	84h (n=6)			84h (n=6)			84h (n=6)			84h (n=6)			84h (n=6)	
	NI (n=5)	0,2500 ns		NI (n=5)	0,2500 ns		NI (n=5)	0,7857 ns		NI (n=5)	0,5714 ns		NI (n=5)	0,0714 ns
	96h (n=6)			96h (n=6)			96h (n=6)			96h (n=6)			96h (n=6)	

Fig. 4.9 (A)		IFN-γ CD4 T cells	Fig. 4.14 (A)		IFN-γ CD4 T cells	Fig. 4.14 (A)		IFN-γ CD4 T cells	Fig. 4.14 (A)		IFN-γ CD4 T cells	Fig. 4.14 (A)		IFN-γ CD4 T cells
WT	NI (n=5)	0,0571 ns	*PbΔb9Δslarp*	NI (n=5)	0,0571 ns	IRRADIATED	NI (n=5)	0,0571 ns	*PbΔmei2Δlisp2*	NI (n=5)	0,0571 ns	CPS	NI (n=10)	0,0571 ns
	24h (n=6)			24h (n=6)			24h (n=6)			24h (n=6)			24h (n=6)	
	NI (n=5)	0,4000 ns		NI (n=5)	0,8571 ns		NI (n=5)	0,1143 ns		NI (n=5)	>0,999 9 ns		NI (n=10)	0,0571 ns
	42h (n=6)			42h (n=6)			42h (n=6)			42h (n=6)			42h (n=6)	
	NI (n=5)	0,8571 ns		NI (n=5)	0,5429 ns		NI (n=5)	0,8571 ns		NI (n=5)	0,6286 ns		NI (n=10)	0,6857 ns
	48h (n=6)			48h (n=6)			48h (n=6)			48h (n=6)			48h (n=6)	
	NI (n=5)	>0,999 9 ns		NI (n=5)	0,9143 ns		NI (n=5)	0,1143 ns		NI (n=5)	0,8000 ns		NI (n=10)	0,2286 ns
	60h (n=6)			60h (n=6)			60h (n=6)			60h (n=6)			60h (n=6)	
	NI (n=5)	0,0571 ns		NI (n=5)	0,4000 ns		NI (n=5)	>0,999 9 ns		NI (n=5)	0,2286 ns		NI (n=10)	0,0571 ns
	68h (n=6)			68h (n=6)			68h (n=6)			68h (n=6)			68h (n=6)	
	NI (n=5)	0,0571 ns		NI (n=5)	>0,999 9 ns		NI (n=5)	0,8571 ns		NI (n=5)	0,1143 ns		NI (n=10)	0,0571 ns
	72h (n=6)			72h (n=6)			72h (n=6)			72h (n=6)			72h (n=6)	
	NI (n=5)	0,0571 ns		NI (n=5)	0,2286 ns		NI (n=5)	0,4000 ns		NI (n=5)	0,1143 ns		NI (n=10)	0,0571 ns
	84h (n=6)			84h (n=6)			84h (n=6)			84h (n=6)			84h (n=6)	
	NI (n=5)	0,0571 ns		NI (n=5)	0,2286 ns		NI (n=5)	0,4000 ns		NI (n=5)	0,2286 ns		NI (n=10)	0,0571 ns
	96h (n=6)			96h (n=6)			96h (n=6)			96h (n=6)			96h (n=6)	

Fig. 4.9 (B)		IFN-γ CD8 T cells	Fig. 4.14 (B)		IFN-γ CD8 T cells	Fig. 4.14 (B)		IFN-γ CD8 T cells	Fig. 4.14 (B)		IFN-γ CD8 T cells	Fig. 4.14 (B)		IFN-γ CD8 T cells
WT	NI (n=5)	0,4571 ns	*PbΔb9Δslarp*	NI (n=5)	0,0571 ns	IRRADIATED	NI (n=5)	0,0571 ns	*PbΔmei2Δlisp2*	NI (n=5)	0,0571 ns	CPS	NI (n=10)	0,0571 ns
	24h (n=6)			24h (n=6)			24h (n=6)			24h (n=6)			24h (n=6)	
	NI (n=5)	>0,999 9 ns		NI (n=5)	0,8571 ns		NI (n=5)	0,0571 ns		NI (n=5)	0,6286 ns		NI (n=10)	0,0571 ns
	42h (n=6)			42h (n=6)			42h (n=6)			42h (n=6)			42h (n=6)	
	NI (n=5)	>0,999 9 ns		NI (n=5)	>0,999 9 ns		NI (n=5)	0,6286 ns		NI (n=5)	0,2286 ns		NI (n=10)	>0,999 9 ns
	48h (n=6)			48h (n=6)			48h (n=6)			48h (n=6)			48h (n=6)	
	NI (n=5)	0,6286 ns		NI (n=5)	0,8571 ns		NI (n=5)	0,4000 ns		NI (n=5)	>0,999 9 ns		NI (n=10)	0,2286 ns
	60h (n=6)			60h (n=6)			60h (n=6)			60h (n=6)			60h (n=6)	
	NI (n=5)	0,2286 ns		NI (n=5)	0,8571 ns		NI (n=5)	>0,999 9 ns		NI (n=5)	>0,999 9 ns		NI (n=10)	0,2857 ns
	68h (n=6)			68h (n=6)			68h (n=6)			68h (n=6)			68h (n=6)	
	NI (n=5)	0,2286 ns		NI (n=5)	0,9143 ns		NI (n=5)	0,6286 ns		NI (n=5)	0,6286 ns		NI (n=10)	0,0571 ns
	72h (n=6)			72h (n=6)			72h (n=6)			72h (n=6)			72h (n=6)	
	NI (n=5)	0,0571 ns		NI (n=5)	0,4571 ns		NI (n=5)	0,2571 ns		NI (n=5)	0,9143 ns		NI (n=10)	0,2286 ns
	84h (n=6)			84h (n=6)			84h (n=6)			84h (n=6)			84h (n=6)	
	NI (n=5)	0,0571 ns		NI (n=5)	0,6286 ns		NI (n=5)	0,9714 ns		NI (n=5)	0,6286 ns		NI (n=10)	0,0571 ns
	96h (n=6)			96h (n=6)			96h (n=6)			96h (n=6)			96h (n=6)	

Fig. 4.9 (C)		IFN-γ NK cells	Fig. 4.15 (A)		IFN-γ NK cells	Fig. 4.15 (A)		IFN-γ NK cells	Fig. 4.15 (A)		IFN-γ NK cells	Fig. 4.15 (A)		IFN-γ NK cells
WT	NI (n=5)	0,0571 ns	*PbΔb9Δslarp*	NI (n=5)	0,0571 ns	IRRADIATED	NI (n=5)	0,0571 ns	*PbΔmei2Δlisp2*	NI (n=5)	0,0571 ns	CPS	NI (n=5)	0,0571 ns
	24h (n=6)			24h (n=6)			24h (n=6)			24h (n=6)			24h (n=6)	
	NI (n=5)	0,1143 ns		NI (n=5)	0,6286 ns		NI (n=5)	0,0571 ns		NI (n=5)	0,4000 ns		NI (n=5)	0,0571 ns
	42h (n=6)			42h (n=6)			42h (n=6)			42h (n=6)			42h (n=6)	
	NI (n=5)	0,1429 ns		NI (n=5)	>0,9999 ns		NI (n=5)	0,2286 ns		NI (n=5)	0,0857 ns		NI (n=5)	0,4571 ns
	48h (n=6)			48h (n=6)			48h (n=6)			48h (n=6)			48h (n=6)	
	NI (n=5)	0,2286 ns		NI (n=5)	0,8571 ns		NI (n=5)	0,1143 ns		NI (n=5)	0,1333 ns		NI (n=5)	0,6286 ns
	60h (n=6)			60h (n=6)			60h (n=6)			60h (n=6)			60h (n=6)	
	NI (n=5)	0,0571 ns		NI (n=5)	>0,9999 ns		NI (n=5)	>0,9999 ns		NI (n=5)	0,0571 ns		NI (n=5)	0,0571 ns
	68h (n=6)			68h (n=6)			68h (n=6)			68h (n=6)			68h (n=6)	
	NI (n=5)	0,0571 ns		NI (n=5)	0,5429 ns		NI (n=5)	>0,9999 ns		NI (n=5)	0,0571 ns		NI (n=5)	0,0571 ns
	72h (n=6)			72h (n=6)			72h (n=6)			72h (n=6)			72h (n=6)	
	NI (n=5)	0,0571 ns		NI (n=5)	0,4000 ns		NI (n=5)	0,2286 ns		NI (n=5)	0,2286 ns		NI (n=5)	0,0571 ns
	84h (n=6)			84h (n=6)			84h (n=6)			84h (n=6)			84h (n=6)	
	NI (n=5)	0,0571 ns		NI (n=5)	0,6286 ns		NI (n=5)	>0,9999 ns		NI (n=5)	0,6286 ns		NI (n=5)	0,2286 ns
	96h (n=6)			96h (n=6)			96h (n=6)			96h (n=6)			96h (n=6)	

Fig. 4.9 (D)		IFN-γ NKT cells	Fig. 4.15 (B)		IFN-γ NKT cells	Fig. 4.15 (B)		IFN-γ NKT cells	Fig. 4.15 (B)		IFN-γ NKT cells	Fig. 4.15 (B)		IFN-γ NKT cells
WT	NI (n=5)	0,0571 ns	*PbΔb9Δslarp*	NI (n=5)	0,0571 ns	IRRADIATED	NI (n=5)	0,0571 ns	*PbΔmei2Δlisp2*	NI (n=5)	0,0571 ns	CPS	NI (n=5)	0,0571 ns
	24h (n=6)			24h (n=6)			24h (n=6)			24h (n=6)			24h (n=6)	
	NI (n=5)	0,1143 ns		NI (n=5)	0,4571 ns		NI (n=5)	0,1143 ns		NI (n=5)	0,4000 ns		NI (n=5)	0,0571 ns
	42h (n=6)			42h (n=6)			42h (n=6)			42h (n=6)			42h (n=6)	
	NI (n=5)	0,4571 ns		NI (n=5)	0,6286 ns		NI (n=5)	0,6286 ns		NI (n=5)	0,6286 ns		NI (n=5)	0,8571 ns
	48h (n=6)			48h (n=6)			48h (n=6)			48h (n=6)			48h (n=6)	
	NI (n=5)	0,400 ns		NI (n=5)	>0,9999 ns		NI (n=5)	0,1143 ns		NI (n=5)	0,5333 ns		NI (n=5)	0,9143 ns
	60h (n=6)			60h (n=6)			60h (n=6)			60h (n=6)			60h (n=6)	
	NI (n=5)	0,0571 ns		NI (n=5)	0,6286 ns		NI (n=5)	0,6857 ns		NI (n=5)	0,6286 ns		NI (n=5)	0,1143 ns
	68h (n=6)			68h (n=6)			68h (n=6)			68h (n=6)			68h (n=6)	
	NI (n=5)	0,0571 ns		NI (n=5)	>0,9999 ns		NI (n=5)	0,8571 ns		NI (n=5)	0,2286 ns		NI (n=5)	0,0571 ns
	72h (n=6)			72h (n=6)			72h (n=6)			72h (n=6)			72h (n=6)	
	NI (n=5)	0,0571 ns		NI (n=5)	0,4000 ns		NI (n=5)	0,2286 ns		NI (n=5)	0,2286 ns		NI (n=5)	0,1143 ns
	84h (n=6)			84h (n=6)			84h (n=6)			84h (n=6)			84h (n=6)	
	NI (n=5)	0,2286 ns		NI (n=5)	0,8571 ns		NI (n=5)	0,8571 ns		NI (n=5)	0,6286 ns		NI (n=5)	0,2286 ns
	96h (n=6)			96h (n=6)			96h (n=6)			96h (n=6)			96h (n=6)	

Fig. 4.9 (E)		IFN-γ ILC1s	Fig. 4.15 (C)		IFN-γ ILC1s	Fig. 4.15 (C)		IFN-γ ILC1s	Fig. 4.15 (C)		IFN-γ ILC1s	Fig. 4.15 (C)		IFN-γ ILC1s
WT	NI (n=5)	0,1143 ns	*PbΔb9Δslarp*	NI (n=5)	0,2286 ns	IRRADIATED	NI (n=5)	0,0571 ns	*PbΔmei2Δlisp2*	NI (n=5)	0,0571 ns	CPS	NI (n=5)	0,0571 ns
	24h (n=6)			24h (n=6)			24h (n=6)			24h (n=6)			24h (n=6)	
	NI (n=5)	0,2286 ns		NI (n=5)	0,8571 ns		NI (n=5)	0,1143 ns		NI (n=5)	0,2286 ns		NI (n=5)	0,1143 ns
	42h (n=6)			42h (n=6)			42h (n=6)			42h (n=6)			42h (n=6)	
	NI (n=5)	0,2286 ns		NI (n=5)	0,8571 ns		NI (n=5)	0,8571 ns		NI (n=5)	0,8571 ns		NI (n=5)	0,1143 ns
	48h (n=6)			48h (n=6)			48h (n=6)			48h (n=6)			48h (n=6)	
	NI (n=5)	0,4000 ns		NI (n=5)	0,4000 ns		NI (n=5)	0,8571 ns		NI (n=5)	0,5333 ns		NI (n=5)	0,6286 ns
	60h (n=6)			60h (n=6)			60h (n=6)			60h (n=6)			60h (n=6)	
	NI (n=5)	0,0571 ns		NI (n=5)	0,8571 ns		NI (n=5)	0,8571 ns		NI (n=5)	0,2286 ns		NI (n=5)	0,4000 ns
	68h (n=6)			68h (n=6)			68h (n=6)			68h (n=6)			68h (n=6)	
	NI (n=5)	0,2286 ns		NI (n=5)	0,1143 ns		NI (n=5)	0,8571 ns		NI (n=5)	0,0571 ns		NI (n=5)	0,4000 ns
	72h (n=6)			72h (n=6)			72h (n=6)			72h (n=6)			72h (n=6)	
	NI (n=5)	0,0571 ns		NI (n=5)	>0,9999 ns		NI (n=5)	0,6286 ns		NI (n=5)	0,0571 ns		NI (n=5)	0,0571 ns
	84h (n=6)			84h (n=6)			84h (n=6)			84h (n=6)			84h (n=6)	
	NI (n=5)	0,4000 ns		NI (n=5)	0,1143 ns		NI (n=5)	0,8571 ns		NI (n=5)	0,6286 ns		NI (n=5)	0,2286 ns
	96h (n=6)			96h (n=6)			96h (n=6)			96h (n=6)			96h (n=6)	

Fig. 4.9 (F)		IFN-γ γδ T cells	Fig. 4.15 (D)		IFN-γ γδ T cells	Fig. 4.15 (D)		IFN-γ γδ T cells	Fig. 4.15 (D)		IFN-γ γδ T cells	Fig. 4.15 (D)		IFN-γ γδ T cells
WT	NI (n=5)	0,4000 ns	*PbΔb9Δslarp*	NI (n=5)	0,4000 ns	IRRADIATED	NI (n=5)	0,1143 ns	*PbΔmei2Δlisp2*	NI (n=5)	0,2286 ns	CPS	NI (n=5)	0,4000 ns
	24h (n=6)			24h (n=6)			24h (n=6)			24h (n=6)			24h (n=6)	
	NI (n=5)	0,8571 ns		NI (n=5)	0,6286 ns		NI (n=5)	0,2286 ns		NI (n=5)	0,9143 ns		NI (n=5)	0,1143 ns
	42h (n=6)			42h (n=6)			42h (n=6)			42h (n=6)			42h (n=6)	
	NI (n=5)	>0,9999 ns		NI (n=5)	0,6286 ns		NI (n=5)	>0,9999 ns		NI (n=5)	>0,9999 ns		NI (n=5)	0,8571 ns
	48h (n=6)			48h (n=6)			48h (n=6)			48h (n=6)			48h (n=6)	
	NI (n=5)	0,6286 ns		NI (n=5)	0,4571 ns		NI (n=5)	0,0571 ns		NI (n=5)	>0,9999 ns		NI (n=5)	0,6286 ns
	60h (n=6)			60h (n=6)			60h (n=6)			60h (n=6)			60h (n=6)	
	NI (n=5)	0,1143 ns		NI (n=5)	>0,9999 ns		NI (n=5)	0,9143 ns		NI (n=5)	0,8571 ns		NI (n=5)	0,1143 ns
	68h (n=6)			68h (n=6)			68h (n=6)			68h (n=6)			68h (n=6)	
	NI (n=5)	0,0571 ns		NI (n=5)	0,6286 ns		NI (n=5)	0,2286 ns		NI (n=5)	0,8571 ns		NI (n=5)	0,0571 ns
	72h (n=6)			72h (n=6)			72h (n=6)			72h (n=6)			72h (n=6)	
	NI (n=5)	0,0571 ns		NI (n=5)	0,6286 ns		NI (n=5)	0,0571 ns		NI (n=5)	0,6286 ns		NI (n=5)	0,1143 ns
	84h (n=6)			84h (n=6)			84h (n=6)			84h (n=6)			84h (n=6)	
	NI (n=5)	0,1143 ns		NI (n=5)	0,6286 ns		NI (n=5)	>0,9999 ns		NI (n=5)	>0,9999 ns		NI (n=5)	0,6286 ns
	96h (n=6)			96h (n=6)			96h (n=6)			96h (n=6)			96h (n=6)	

Figure 4.16 (C)			Figure 4.16 (D)		
IRRADIATED	Controls (n=32)		CPS	Controls (n=32)	
	Irradiated 1K (n=10)	<0,0001 ****		CPS 1K (n=10)	<0,0001 ****
	Controls (n=32)			Controls (n=32)	
	Irradiated 3 K (n=5)	<0,0001 ****		CPS 3 K (n=5)	<0,0001 ****
	Controls (n=32)			Controls (n=32)	
	Irradiated 5 K (n=5)	0,0018 **		CPS 5 K (n=5)	<0,0001 ****
	Controls (n=32)			Controls (n=32)	
	Irradiated 10 K (n=5)	0,0002 ***		CPS 10 K (n=10)	<0,0001 ****
	Controls (n=32)			Controls (n=32)	
	Irradiated 30 K (n=24)	<0,0001 ****		CPS 30 K (n=19)	<0,0001 ****

Figure 4.17 (B)			Figure 4.18 (B)		
Wild-type mice	Controls (n=32)		IFNAR-KO mice	Controls (n=4)	
	PbΔb9Δslarp 30 K (n=23)	<0,0001 ****		*PbΔb9Δslarp* 30 K (n=3)	0,0286 *
	Controls (n=32)			Controls (n=4)	
	Irradiated 30 K (n=24)	<0,0001 ****		Irradiated 30 K (n=4)	0,0286 *
	Controls (n=32)			Controls (n=4)	
	PbΔmei2Δlisp2 30K (n=15)	<0,0001 ****		CPS 30K (n=4)	0,0159 *
	Controls (n=32)				
	CPS 30K (n=19)	<0,0001 ****			

Figure 4.19 (B)	
Controls (n=31)	
PbΔmei2 30K K (n=4)	<0,0001 ****
Controls (n=32)	
FLAG 30 K (n=8)	<0,0001 ****